UNIVERSIDADE FEDERAL DE SANTA CATARINA

CENTRO TECNOLÓGICO

PROGRAMA DE PÓS-GRADUAÇÃO EM ENGENHARIA DE ALIMENTOS

Jônatas Lopes Dias

**PRODUCTION OF QUERCETIN COCRYSTALS BY GAS ANTISOLVENT METHOD (GAS)**

FLORIANÓPOLIS

2022

Jônatas Lopes Dias

# PRODUÇÃO DE COCRISTAIS DE QUERCETINA PELO MÉTODO ANTISSOLVENTE GASOSO (GAS)

Tese de Doutoramento submetida ao Programa Pós-graduação em Engenharia Alimentos da Universidade Federal de Santa Catarina para a obtenção do título de Doutor em Engenharia de Alimentos
Orientadora: Profª. Drª. Sandra R.S. Ferreira
Coorientador: Prof. Dr. Marcelo Lanza

FLORIANÓPOLIS

2022

Jônatas Lopes Dias

**PRODUCTION OF QUERCETIN COCRYSTALS BY GAS ANTISOLVENT METHOD (GAS)**

O presente trabalho em nível de doutorado foi avaliado e aprovado por banca examinadora composta pelos seguintes membros:

Profª. Drª. Sandra Regina Salvador Ferreira - Presidente - UFSC

Prof. Dr. Alcidênio Soares Pessoa - Membro Externo - IFSertãoPE

Prof. Dr. Adailton João Bortoluzzi - Membro Externo - UFSC

Prof. Dr. Acácio Antônio Ferreira Zielinski - Membro Interno - UFSC

Profª. Drª. Cláudia Sayer - Suplente - UFSC

Prof. Dr. Germán Ayala Valencia - Suplente - UFSC

Certificamos que esta é a **versão original e final** do trabalho de conclusão que foi julgado adequado para obtenção do título de doutor em Engenharia de Alimentos.

_____

Profa. Dra. Sandra Regina Salvador Ferreira

Coordenadora do Programa

_____

Profa. Dra. Sandra Regina Salvador Ferreira

Orientadora

Florianópolis, 23 de setembro de 2022.

**AGRADECIMENTOS**

Aos Professores Sandra R.S. Ferreira e Marcelo Lanza pela orientação, apoio, dedicação e paciência que foram fundamentais para o desenvolvimento deste trabalho.

À CAPES pela bolsa de estudos concedida.

Aos Professores Adailton Bortoluzzi e Dachamir Hotza que possibilitaram a utilização de suas instalações para a realização de várias análises.

Aos amigos que fiz durante o curso de doutorado, Eto, Kátia, Simone, Ade, Bruno, Ferro, Camila M., Camilinha, Aline, Laís, Talyta e tantos outros que passaram pelo LATESC no período que conduzi minha pesquisa.

Aos meus amigos nordestinos do coração, Alcidênio, Sandra, Páulia, Jeferson, Vini, Júlia e Peuzinho.

À Laís, minha namorada, amiga e companheira.

Aos meus tios, Eleusa, Dito e Nida pela força, carinho e apoio.

À minha mãe, que mesmo à distância me deu todo o apoio

# RESUMO

A quercetina é um polifenol de origem alimentar que possui diversas atividades biológicas. No entanto, devido à sua baixa solubilidade em água e estabilidade em fluidos gastrointestinais, é pouco explorada. A cocristalização é uma técnica emergente baseada na recristalização de duas ou mais moléculas numa mesma rede cristalina para melhorar as propriedades físico-químicas de compostos ativos como a quercetina (QUE). Neste trabalho, o método do antissolvente gasoso (GAS), baseado nas propriedades do $CO_2$ supercrítico, foi explorado pela primeira vez para obter cocristais de QUE. Nicotinamida (NIC) e L-prolina (PRO) foram escolhidos como coformadores para ontenção de cocristais de QUE porque são considerados GRAS, possuindo propriedades biológicas benéficas adicionais às da QUE. Cocristais de QUE foram preparados por GAS empregando acetona (QUE/NIC) ou etanol (QUE/PRO) como solventes, respectivamente. Os cocristais foram basicamente caracterizados por difratometria de raios-X de pó (PXRD), calorimetria exploratória diferencial (DSC), espectroscopia Raman, e microscopia eletrônica de varredura (SEM). No caso dos cocristais de QUE/NIC, análise termogravimetrica (TGA), cromatografia liquida de alta performance (HPLC) e analise elementar foram também utilizadas. Os cocristais de QUE/NIC e QUE/PRO foram obtidos com sucesso pelo método GAS, no qual foram avaliadas as seguintes variáveis de processo: pressão, temperatura e razão molar entre QUE e coformador (NIC ou PRO). Este último foi o parâmetro que mais afetou o rendimento em cocristais e suas caracteristicas, como tamanho de partícula. O perfil de dissolução dos cocristais produzidos por GAS apresentaram bom desempenho de dissolução em pH 1,2 e 6,8 onde a liberação de QUE dos cocristais, em relação a QUE pura, foi aumentada em aproximadamente 2 vezes para (QUE/NIC) e em 1,5 vezes para (QUE/PRO). Os achados reportados nesta tese são inovadores pois propõem uma rota alternativa para obtenção de cocristais de QUE pelo método GAS e contribuem para o entendimento dos fatores operacionais que afetam a produção de cocristais pelo método GAS. Estes resultados motram que cocristais de QUE assim produzidos são formulações sólidas promissoras para melhorar a dissolução e a biodisponibilidade da QUE, indicando que possiveis problemas práticos do uso da QUE pura poderiam ser contornados pelo uso da QUE na forma cocristalizada. Finalmente, os resultados sugerem que QUE cocristalizada pode ser futuramente explorada na formulação de produtos nutracêuticos baseados em polifenóis.

**Palavras-chave:** Flavonóide, $CO_2$ antisolvente, vitamina B3, Prolina, dissolução

**RESUMO EXPADIDO**

**Introdução**

A quercetina (QUE) é um flavonóide com importantes propriedades biológicas (por exemplo, antioxidante, anticancerígeno, anti-inflamatório e anti-obesidade), e devido à sua baixa solubilidade em água, apresenta baixa biodisponibilidade. ara superar esse problema, várias abordagens de formulação foram projetadas, como nanopartículas lipídicas sólidas, nanoemulsões, partículas de biopolímero e outras. No entanto, essas estratégias de formulação apresentam desvantagens como baixa carga de encapsulamento, liberação rápida, baixa estabilidade, sabor indesejável. Então, a cocristalização surgiu como uma metodologia alternativa para aumentar a solubilidade aparente em água e a dissolução de moléculas com baixa biodisponibilidade como o QUE, além disso, este método geralmente supera os problemas enfrentados pelas formulações típicas, proporcionando também efeito benéfico na biodisponibilidade. Os métodos baseados em $CO_2$ supercrítico, como. *Gaseous antisolvent* GAS, *Supercritical antisolvent* (SAS), *Rapid Expansion of Supercritical Solutions* (RESS), *Cocrystallization with supercritical solvent* (CSS) apresentam apelo ambiental, devido ao uso de solventes verdes, reciclagem de solventes e baixo consumo de solventes e energia. GAS é um método de cocristalização com baseado em $CO_2$ supercrítico que usa a capacidade de fluidos supercríticos em causar expansão de líquidos, diminuindo a capacidade de solvência de solventes orgânicos e levando à cristalização de solutos. Essa abordagem proporciona um processo rápido de etapa única e melhora o controle da morfologia do cocristal e do tamanho das partículas por meio do ajuste dos parâmetros de processamento (por exemplo, pressão, temperatura, taxa de fluxo). O método GAS tem sido empregado com sucesso para a micronização de fármacos, pigmentos, coprecipitação de materiais bioativos-poliméricos entre outros, porém o uso do método GAS para cocristalização é bastante recente. Estudos envolvendo o papel das variáveis do processo no resultado das cocristalizações de GAS são escassos, portanto, generalizações sobre o efeito dos parâmetros do processo não são diretas. No entanto, e considerando a escassa literatura disponível, parece que o efeito dos parâmetros do processo depende fortemente das propriedades químicas e físico-químicas das moléculas de origem. Até onde sabemos, cocristais com QUE ainda não foram produzidos pelo método GAS.

**Objetivos**

Nosso objetivo foi desenvolver um processo alternativo de cocristalização para produção de cocristais de quercetina utilizando o método antissolvente gasoso (GAS), visando melhorar o tamanho das partículas, a área superficial e o desempenho de dissolução em fluidos biológicos simulados.

**Metodologia**

Cocristais de QUE com os coformadores nicotinamida (NIC) e L-prolina (PRO) foram produzidos pelo método GAS. Em cada sistema QUE-coformador foram estudados os efeitos das varáveis: pressão (8-10 MPa), temperatura (35-45 °C), e razão molar entre QUE e os coformadores (1:1-1:2) no rendimento, pureza, tamanho de partículas e área superficial. Adicionalmente, os materiais foram caracterizados por difração de raios-x de pó (PXRD), calorimetria diferencial de varredura (DSC), análise termogravimétrica (TGA), microscopia eletrônica de varredura (SEM), cromatografia líquida de alta eficiência (HPLC) e análise

elementar. Materiais também foram caracterizados em relação à distribuição de tamanho de partículas e área superficial.

**Resultados e discussão**

Os ensaios conduzidos com relação QUE-para-NIC 1:1 (#1- #4) mostraram que a pressão e a temperatura quase não tiveram efeito sobre o rendimento, apenas o ensaio #4 (10 MPa/45°C) mostrou um rendimento estatisticamente diferente de outros ensaios (p<0,05). O rendimento mais baixo do ensaio #4, em comparação com os outros ensaios com proporção 1:1 QUE-para-NIC, pode ser provavelmente devido a: (1) maior solubilização de QUE e/ou NIC na mistura supercrítica $CO_2$ + acetona em temperaturas mais altas, o que reduz a quantidade de material precipitado; (2) ressolubilização do cocristal em $CO_2$ + acetona e/ou em $CO_2$ puro durante a etapa de pressurização e/ou secagem, respectivamente.

Considerando a relação QUE-NIC, o rendimento diminui pela redução da quantidade de QUE, ou seja, ensaios realizados com relação 1:1 (#1-#4) apresentaram maior rendimento do que com relação 1:2. Provavelmente, porque a solução inicial é mais diluída na proporção 1:2, em comparação com a proporção 1:1, o que reduz a supersaturação inicial, para a mesma quantidade de $CO_2$, portanto, espera-se menor precipitação de cocristais. Além disso, o crescimento de partículas menores é favorecido. As soluções diluídas também podem promover o crescimento de partículas pequenas, ainda menores que o tamanho de corte do filtro da unidade (220 nm), devido ao aumento da nucleação ao invés do crescimento do cristal, resultando em perda de partículas e consequentemente diminuindo o rendimento. A pressão e a temperatura apresentaram um efeito considerável no tamanho das partículas principalmente em 1:1 QUE:NIC. Nessa relação, o incremento da temperatura a pressão constante produziu partículas menores, contrastando com alguns relatos anteriores relacionados a partículas produzidas por GAS. O aumento da pressão, a temperatura constante, por outro lado, reduziu o tamanho das partículas. O aumento da pressão aumenta a densidade do $CO_2$, o que aumenta a solubilidade do $CO_2$ em solventes orgânicos, como a acetona. Consequentemente, a expansão do líquido é maior e o estado de supersaturação necessário para iniciar a precipitação das partículas ocorre mais rapidamente, favorecendo o mecanismo de nucleação e o crescimento de partículas menores. A razão molar entre QUE e NIC afetou mais significativamente o tamanho de partícula dos cocristais produzidos em comparação com a variação de pressão e temperatura. Geralmente, na proporção de 1:1, os tamanhos das partículas e a variabilidade entre as amostras foram maiores em comparação com a proporção de 1:2. Usando a proporção de 1:1, os tamanhos das partículas ($d_{50}$) variaram de 112,1 a 280,3 nm. Caso contrário, para a razão 1:2, foram produzidas partículas menores (87,8-114,1 nm), e isso pode estar relacionado ao fato de a solução inicial ser mais diluída, o que aumenta a nucleação ao invés do crescimento do cristal. Coletivamente, os dados de difração de raios X, calorimétricos e espectroscópicos indicam que os parâmetros de processamento, dentro da faixa avaliada, não desempenham um papel significativo nas características do cocristal, ou seja, o mesmo produto cristalino é produzido independentemente da pressão ou temperatura utilizada para sua produção. Comparando a proporção de QUE para NIC alimentada com a das amostras processadas, após o processamento de GAS, os dados de HPLC sugerem que todas as amostras mudaram sua proporção para 1:1 QUE-NIC. Além disso, os valores de porcentagem de carbono, hidrogênio e nitrogênio determinados para todas as amostras são consistentes com os valores calculados para 1:1 QUE/NIC (considerando $C_{21}H_{16}N_2O_8$: C: 59,43%; H: 3,80%; N: 6,60%). Esses resultados sugerem que o cocristal formado possui uma estequiometria de 1:1.

A estabilidade da quercetina na forma de cocristal e a capacidade do cocristal em manter alta concentração de quercetina no ambiente gastrointestinal foram avaliadas por meio de ensaios de dissolução conduzidos em diferentes valores de pH. As amostras de cocristais apresentaram maiores taxas de dissolução, para ambos os valores de pH, em comparação com QUE puro. Por exemplo, em meio ácido (pH 1,2), as amostras #1 (8 MPa/35°C/1:1) e #5 (8 MPa/35°C/1:2) liberaram uma quantidade cerca de 2 vezes maior de QUE do que o pó QUE bruto em 180 min. Em pH 6,8, um perfil de liberação semelhante também foi observado para a amostra #1, que promoveu um aumento de 2,3 vezes no teor de QUE em comparação com o QUE puro em 180 min, enquanto a amostra #5 apresentou um incremento relativamente alto nos primeiros 20 min (1,7 vezes), mas seguido de sucessivas diminuições ligeiras da concentração até atingir uma concentração correspondente a um incremento de cerca de 1,3 vezes (180 min).

Pequenas diferenças na taxa de dissolução e na quantidade de QUE liberada pelas amostras #1 e #5 podem ser atribuídas a diferenças entre as distribuições de tamanho de partícula. Em geral, partículas menores promovem maior quantidade de soluto dissolvido. Pelo contrário, a amostra #5 teve um desempenho de dissolução inferior em comparação com a amostra #1, mesmo com partículas menores ($d_{50}$ 96,3 vs 280,3 nm). Infelizmente, a redução excessiva de tamanho não só aumenta a quantidade de soluto dissolvido, mas também aumenta o grau de supersaturação, a força motriz para a precipitação do soluto, reduzindo a dissolução.

Em relação aos cocristais QUE/PRO, na proporção 1:1 QUE/PRO mol (ensaios #1-#4) os parâmetros pressão e temperatura não apresentam efeito significativo sobre os rendimentos de precipitação dos cocristais. Caso contrário, usando a razão molar de 1:2 QUE/PRO (ensaios #5-#8), o efeito significativo da pressão e da temperatura no rendimento de cocristal pode estar relacionado à densidade de $CO_2$, ou seja, o menor rendimento foi obtido com a maior densidade de $CO_2$ (0,7128 g·mL-1), ensaio #7, com rendimento de 51,7%. Além disso, as densidades do $CO_2$ nas corridas #5, #6 e #8 provavelmente não são tão diferentes umas das outras para causar uma diferença significativa no rendimento.

Os rendimentos das amostras processadas com GAS foram tipicamente superiores aos obtidos por cocristalização *slurry* (51,7 – 80,8 vs 58,4%, respectivamente). O rendimento das amostras produzidas pelo método *slurry* pode variar amplamente, com base nas condições de operação. Embora a cocristalização da pasta normalmente opere com maior massa inicial de materiais de partida em comparação com o processamento de GAS, pode ocorrer perda significativa de material devido à solubilidade residual no solvente, reduzindo o rendimento. O parâmetro de razão molar QUE/PRO desempenha um papel significativo no resultado da cocristalização por GAS. O uso de uma proporção de 1:2 de componentes originais forneceu amostras compostas por cocristal 1:2 QUE/PRO com alta pureza. Caso contrário, usando uma proporção de 1:1, ou seja, aumentando a quantidade de QUE em relação ao PRO, nenhum novo polimorfo cocristal pôde ser obtido, mas pós compostos por uma mistura de QUE/PRO cocristal 1:2 e QUE não cocristalizada (anidra). Em relação aos PSDs, a relação QUE-to-PRO teve um efeito significativo no tamanho das partículas. Em geral, na proporção de 1:2, os tamanhos das partículas dos cocristais formados foram menores em comparação com as amostras processadas usando a proporção de 1:1 (0,171-0,265 μm vs 0,264-2,593 μm, respectivamente). Na razão 1:2, a solução inicial é mais diluída em relação à solução inicial na razão 1:1, portanto a razão de supersaturação inicial é menor, o que favorece a nucleação ao invés do crescimento do cristal, resultando em partículas menores. Por outro lado, as variações de pressão e temperatura não mostraram um efeito claro no tamanho das partículas dos cocristais produzidos. De fato, o efeito dessas variáveis pode ser difícil de avaliar, devido à sua influência em diferentes aspectos da cristalização, muitas vezes de forma antagônica. Por exemplo, um aumento de temperatura

aumenta a supersaturação devido ao seu efeito positivo na transferência de massa devido à melhor dissolução do $CO_2$ em solução causada pela melhoria da difusão e redução da tensão interfacial do líquido. Ao contrário, um aumento na temperatura reduz a solubilidade do soluto na solução, diminuindo o grau de supersaturação. Em relação à área de superfície do cocristal, a amostra #5 apresentou a maior área de superfície (8.881 m2·g-1), o que pode estar relacionado ao seu menor tamanho médio de partícula em comparação com outras amostras de GAS. No entanto, comparando a amostra #5 com a amostra LAS, a relação inversa entre a área de superfície e o tamanho da partícula não é clara, ou seja, a amostra LAS tem maior área de superfície em relação à amostra #5 (10,370 vs 8,881 $m^2 \cdot g^{-1}$, respectivamente), mesmo tendo um tamanho médio de partícula maior (1,18 vs 0,171 μm, respectivamente). Este comportamento está possivelmente relacionado a diferenças na morfologia das amostras de GAS e LAS (semelhante a agulha vs floculada, respectivamente).

O cocristal produzido pelo GAS (amostra #5) foi superior em desempenho de dissolução do que a amostra LAS, em ambos os meios de dissolução utilizados (pH 1,2 e 6,8). Isso significa que, um nível supersaturado de QUE foi alcançado se comparado ao pó de QUE puro. Isso significa que, um nível supersaturado mais alto de QUE foi alcançado se comparado ao pó de QUE puro. Em pH 1,2, o cocristal produzido por GAS atingiu a concentração máxima (~8,5 μg·mL$^{-1}$) em cerca de 20 min e pôde sustentar valores supersaturados (de 8,5 a 4 μg·mL$^{-1}$) por 180 min, enquanto LAS atingiu um valor máximo significativamente menor (~3,6 μg·mL$^{-1}$) no mesmo período de tempo, mantendo um nível de supersaturação inferior em comparação com a amostra GAS. Em outras palavras, o cocristal produzido pelo GAS teve melhor desempenho de dissolução e foi mais estável que o cocristal obtido pelo LAS. Da mesma forma, em pH 6,8, o cocristal obtido pelo GAS foi capaz de gerar e sustentar por um período significativo (180 min), níveis de supersaturação de QUE superiores aos alcançados pelo cocristal LAS. Por exemplo, o cocristal produzido com GAS atingiu a concentração máxima (~9,7 μg·mL$^{-1}$) em cerca de 60 min, mantendo uma concentração pelo menos 1,5 vezes maior em relação à amostra de cocristal LAS.

**Considerações finais**
Ambos os cocristais de QUE formados foram preparados usando tecnologia supercrítica (método GAS). No entanto, o papel dos parâmetros do processo em algumas características do cocristal foi bastante distinto dependendo do cocristal de quercetina. Para o cocristal QUE/NIC, independente do nível dos parâmetros do processo, foram produzidos cocristais QUE/NIC de alta pureza. Enquanto para o cocristal QUE/PRO, amostras com alta pureza de cocristal foram obtidas apenas usando uma relação QUE/PRO igual a 1:2. As rotas de produção aqui propostas proporcionaram altos rendimentos para ambos os sistemas de cocristais. Para ambos, a relação QUE-coformador foi o parâmetro que mais influenciou o rendimento, proporcionando maiores rendimentos aumentando a razão molar, ou em essência, reduzindo a concentração global. Como rendimento, o tamanho das partículas também foi fortemente afetado pela razão entre os componentes originais. Para ambos os sistemas de cocristais, o aumento na razão QUE-coformador (ou seja, diminuição na concentração global) forneceu cocristais com menor tamanho de partícula.

Além disso, ambos os cocristais de QUE produzidos por GAS apresentaram desempenho de dissolução adequado em ambiente gastrointestinal simulado (pH 1,2 e pH 6,8), sendo capazes de atingir e manter altos níveis supersaturados de QUE por intervalo de tempo significativo. Este estudo consistiu em uma investigação inédita, focada no desenvolvimento de uma plataforma alternativa para a produção de cocristais de quercetina usando tecnologias ecologicamente amigáveis envolvendo $CO_2$. Foi possível analisar o papel das variáveis de

processo relacionadas à cocristalização GAS e compreender seu efeito nas propriedades finais dos cocristais QUE.

O pioneirismo deste trabalho pode ser utilizado para ampliar a possibilidade de obtenção de outros cocristais QUE com outros coformadores de solubilidade moderada a desprezível em fase supercrítica. Além disso, nossos achados podem ser úteis para o desenvolvimento de novos procedimentos de cocristalização de outros polifenóis por processamento de GAS, fornecendo conhecimento fundamental para o sucesso desses procedimentos adicionais. Finalmente, nossas descobertas podem ajudar a impulsionar o uso de $CO_2$ e a tecnologia de fluido supercrítico para aplicações mais nobres, expandindo o espectro de aplicações para

# ABSTRACT

Quercetin is a food-borne polyphenol that has several biological activities. However, due to its low solubility in water and stability in gastrointestinal fluids, it is poorly explored. Cocrystallization is an emerging technique based on the recrystallization of two or more molecules in the same crystal lattice to improve the physicochemical properties of active compounds such as quercetin (QUE). In this work, the gaseous antisolvent (GAS) method based on the antisolvent characteristic of supercritical $CO_2$ was explored for the first time to obtain QUE cocrystals. Nicotinamide (NIC) and L-proline (PRO) were selected as coformers to obtain QUE cocrystals because they are regarded as GRAS molecules, exhibiting beneficial biological properties which can be added to those of QUE. QUE cocrystals were prepared by GAS employing acetone (QUE/NIC) or ethanol (QUE/PRO) as solvents, respectively. The cocrystals were basically characterized by powder X-ray diffractometry (PXRD), differential scanning calorimetry (DSC), Raman spectroscopy, and scanning electron microscopy (SEM). In the case of the QUE/NIC cocrystals, thermogravimetric analysis (TGA), high performance liquid chromatography (HPLC) and elemental analysis were also used. The QUE/NIC and QUE/PRO cocrystals were successfully obtained by the GAS method, in which were evaluated the process variables: pressure,temperature, and the molar ratio between QUE and the coformer (NIC or PRO). The later was the parameter that most affected the cocrystal yield and its characteristics, such as particle size. The dissolution profile of the cocrystals produced by GAS showed good dissolution performance at pH 1.2 and 6.8 where the release of QUE in relation to pure QUE could be increased by approximately 2-times (QUE/NIC) and 1.5-times (QUE/PRO ). The findings reported here are a novelty thus they propose an alternative route to obtain QUE cocrystals by the GAS method. These results show that the QUE cocrystals thus produced are promising solid formulations to improve the dissolution and bioavailability of QUE, indicating that possible practical problems of the use of pure QUE could be circumvented by the use of QUE in cocrystallized form. Finally, the results suggest that cocrystallized QUE can be further explored in the formulation of polyphenol-based nutraceuticals.

**Keywords:** Flavonoid, $CO_2$-antisolvent, Vitamin B3, Proline, Dissolution

# LIST OF FIGURES

# LIST OF TABLES

# TABLE OF CONTENTS

**CHAPTER 1 INTRODUCTION**

Currently, there has been a growing concern of the world population about healthy habits, especially related to food consumption. Numerous scientific evidences have attested a close relation between the consum of healthy foods and the prevention of several chronic degenerative diseases, such as cancer and heart diseases.

In this context, the food industries have avoided the use of synthetic ingredients, focusing their efforts to develop food products containing health-promoting compounds (DIAS; FERREIRA; BARREIRO, 2015). Functional foods and nutraceuticals are the two main classes of food-related products that have been developed to promote health benefits. A 'functional food' is a type of food that provides health benefits beyond basic nutrition, as it contains components that have the potential to improve health or reduce the risk of certain diseases. They include foods that have been enriched or fortified to restore nutrient levels lost during processing, (for instance, flour enriched with folic acid), to improve the nutritional quality of foods deficient in nutrients (calcium in orange juice), or to solve health public problems (vitamin D in milk, iodized table salt). Otherwise, a nutraceutical product is a type of dietary supplement that provides a concentrated form of a biologically active component of a food, presented in a non-food matrix, and in dosages that exceed those that could be obtained from regular foods (NOOMHORM; AHMAD; ANAL, 2014; PHILLIPS; RIMMER, 2013).

Phenolic compounds are a class of bioactive molecules that have been extensively studied because of their diverse health benefits. Among these, quercetin, a molecule of the flavonoid group, has several important properties, such as antioxidant, anticancer, cardioprotective, bacteriostatic and antiviral activity (SMITH et al., 2011).

Therefore, the intake of a diet rich in quercetin is recommended, and it is positively correlated with health promotion. Quercetin ingestion can also be accomplished through dietary supplementation, with recommended daily doses of 200-1200 mg, as well as through the ingestion of nutraceuticals and/or functional foods with a concentration of 10 to 125 mg per serving. Dietary supplementation with quercetin and its addition to food is highly supported by its toxicity data, which prove the safety of its use (LESJAK *et al.*, 2018).

However, studies have shown that quercetin has low bioavailability, mainly due to its very low water solubility, which limits its therapeutic use (VEVERKA *et al.*, 2015). In humans, it was found that less than 1% of quercetin was absorbed when a single dose of 4 g was ingested (GUGLER; LESCHIK; DENGLER, 1975).

Recently, cocrystal synthesis has emerged as an approach to modulate physicochemical properties of active compounds, such as physical and chemical stability, solubility, dissolution rate, and consequently, their bioavailability. The formation of cocrystals is particularly relevant for poorly soluble active compounds such as quercetin, without altering their molecular structure and/or biological interactions (MALAMATARI et al., 2017).

Cocrystals are homogeneous crystalline materials, solid under ambient conditions, formed by two or more compounds in the same crystal lattice, and in a defined stoichiometric proportion (KARAGIANNI; MALAMATARI; KACHRIMANIS, 2018; PI et al., 2019a). They are formed by non-covalent interactions, mainly hydrogen bonds, pi-stack interactions and Van der Waals forces, where a molecule containing an active principle binds to another molecule, called a coformer, which generally should be GRAS (Generally Recognized as Safe) (PANG et al., 2019). In recent decades, the interest in obtaining cocrystals for pharmaceutical use has increased, because cocrystals have characteristics such as increased solubility, and high dissolution rate and bioavailability, compared to single component (LUO et al., 2019a).

Although it has been gaining special attention from researchers in the pharmaceutical field, the synthesis of cocrystals can also be used to modulate the properties of molecules for other purposes. Studies on the production of cocrystals with potential for food uses, such as nutraceutical, functional or additive uses are scarce. The few researches about cocrystals with food relevant molecules are focused on obtaining cocrystals of phenolic compounds. This scenario motivates scientific investigation about the potential of this technique to obtain polyphenol-based cocrystals for the food industry, specially combining polyphenols with GRAS coformers that present additional biological properties. In this context, coformers such as nicotinamide (NIC) and L-proline (PRO) are intersting, because NIC is a vitamin, being important in metabolic pathways, and PRO is a amino acid with significant role in protein synthesis (NIKAS; PASCHOU; RYU, 2020; NUGRAHANI; JESSICA, 2021).

Cocrystals can be produced by several traditional low-pressure techniques, such as milling, solvent-assisted milling, slow evaporation, liquid antisolvent, and slurry. However, these techniques have some drawbacks, including the generation of amorphous material, formation of hydrates/solvates, and production of homocrystals (PANDO; CABAÑAS; CUADRA, 2016).

The main disadvantage related to some of the well-known methods is related to the excessive use of hazardous organic solvents. Some organic solvents used in these processes

have enormous environmental and economic costs, contributing to health problems, affecting negatively the environment, and are flammable, toxic, and difficult to treat. The elimination of hazardous organic solvents and the search for sustainable solvents is the main goal of "green chemistry", and in this context, methods using supercritical carbon dioxide (SC-$CO_2$) have been proposed to overcome some disadvantages of conventional methods (BRUNNER, 2010).

The use of SC-$CO_2$ presents a new and interesting path for the formation of cocrystals, having as main advantages its low toxicity, chemical stability, high availability and ease of reuse. The high purity of the products obtained, the control of crystalline polymorphism, the possibility of processing thermolabile molecules, and the control of the particle size distribution are notable advantages of these methods, mostly due to the adjust of the $CO_2$ characteristics by tuning the process variables (PANDO; CABAÑAS; CUADRA, 2016).

For the synthesis of cocrystals from molecules poorly soluble in SC-$CO_2$, such as quercetin, antisolvent methods with SC-$CO_2$ have been used. In this approach, SC-$CO_2$ acts reducing the solvating power of the solvent, reducing the solubility of the active ingredient and coformer, allowing them to precipitate together in the same crystalline structure. The most promising antisolvent $CO_2$-based method is called gas antisolvent (GAS), which involves saturating a solution containing the active ingredient/coformer inside a high pressure vessel with SC-$CO_2$ until cocrystallization occurs (KARIMI-JAFARI *et al.*, 2018a).

GAS cocrystallization offers some advantages compared to conventional methods. It offers a rapid single-step process and provides a tunable and versatile approach to produce cocrystals with different morphologies and particle sizes by adjusting operating parameters. Also, the thermal and mechanical stresses of the products are reduced, compared to mechanochemical processes. Furthermore, it decreases organic solvent use and minimizes residual solvent in the cocrystal, unlike solution-based methods (WICHIANPHONG; CHAROENCHAITRAKOOL, 2018b).

Quercetin cocrystals were reported by Vasisht et al. (2016) Wu et al. (2020), (SMITH *et al.*, 2011), and (HE *et al.*, 2016), who explored conventional cocrystallization methods and GRAS coformers (nicotinamide, caffeine, and proline, respectively) to obtain quercetin cocrystals with improved dissolution profile, bioavailability, antihaemolytic and antioxidant activities. In this scenario, the studies mentioned above support the idea that improved quercetin dissolution and bioavailability could be achieved by cocrystallization, particularly by

supercritical processes. However, as far as we know, no previous studies have investigated the GAS process as an alternative route for quercetin cocrystals production.

The investigation of alternative routes for cocrystallization is a vital research topic on crystal engineering because it may lead to a greater variety of cocrystals with better attributes and properties for specific applications. Variables of the cocrystallization synthesis, such as the pressure, temperature, ratio between quercetin/coformer, and the type of coformer to be incorporated into the crystal lattice can be changed to obtain materials with different modulated properties. In other words, by varying these parameters, a wide range of engineered materials, with different characteristics and high potential for food and pharmaceutical applications, can be produced. In this sense, we consider that our study is a pioneer in developing new quercetin solid-forms, especially in cocrystallized form and using high-pressure antisolvent methods such as GAS. Quercetin has a broad scope of applications and by cocrystallization through herein proposed method, its properties could be improved and the possibility of practical uses could be widened.

## 1.1 OBJECTIVES

To develop an alternative cocrystallization process for production of quercetin cocrystals using the gas antisolvent method (GAS), aiming the improvement of paticle size, surface area, and dissolution performance in simulated biological fluids. In this way, the specific goals of this work are:

- *Evaluate* the role of the process parameters pressure, temperature, and quercetin-to-nicotinamide (used as GRAS coformer) ratio on yield, morphology, paticle size, and stoichiometry of the quercetin/nicotinamide cocrystal (QUE/NIC);
- *Confirm and characterize* the quercetin/nicotinamide cocrystals formed by powder X-ray diffractometry (PXRD), differential scanning calorimetry (DSC), thermogravimetric analysis (TGA), Raman spectroscopy, scanning electron microscopy (SEM), high performance liquid chromatography (HPLC), and elemental analysis;
- *Evaluate* the dissolution profile of the quercetin/nicotinamide cocrystals produced in a simulated gastrointestinal environment (pH 1.2 and pH 6.8);
- *Evaluate* the role of process parameters pressure, temperature, and quercetin-to-proline (used as GRAS coformer) ratio on yield, purity, morphology, paticle size, stoichiometry, and surface area of the quercetin/proline cocrystal (QUE/PRO);

- *Confirm and characterize* the quercetin/proline cocrystals formed by powder X-ray diffractometry (PXRD), differential scanning calorimetry (DSC), Raman spectroscopy, and scanning electron microscopy (SEM);

- *Evaluate* the dissolution profile of the quercetin/proline cocrystals produced in a simulated gastrointestinal environment (pH 1.2 and pH 6.8);

- *Compare* the routes of cocrystallization of QUE/NIC and QUE/PRO.

**CHAPTER 2 LITERATURE REVIEW**

This chapter presents a compilation of the available literature on the subjects of this work. The fundamental aspects of cocrystals are introduced, and some screening methods for coformer selection are presented. Also, the principal methods of synthesis and characterization are presented and addressed. Finally, the current state of the art concerning the cocrystallization of food-relevant polyphenols focusing on modulation of physicochemical and biological properties is summarized and discussed.

This chapter was published as a review article in the peer-reviewed journal *Trends in Food Science & Technology*. Impact factor (2022): 16.002. According to Elsevier subscription rules, the authors retain the right to include the article in a thesis.

(https://doi.org/10.1016/j.tifs.2021.01.035)

**Graphical abstract**
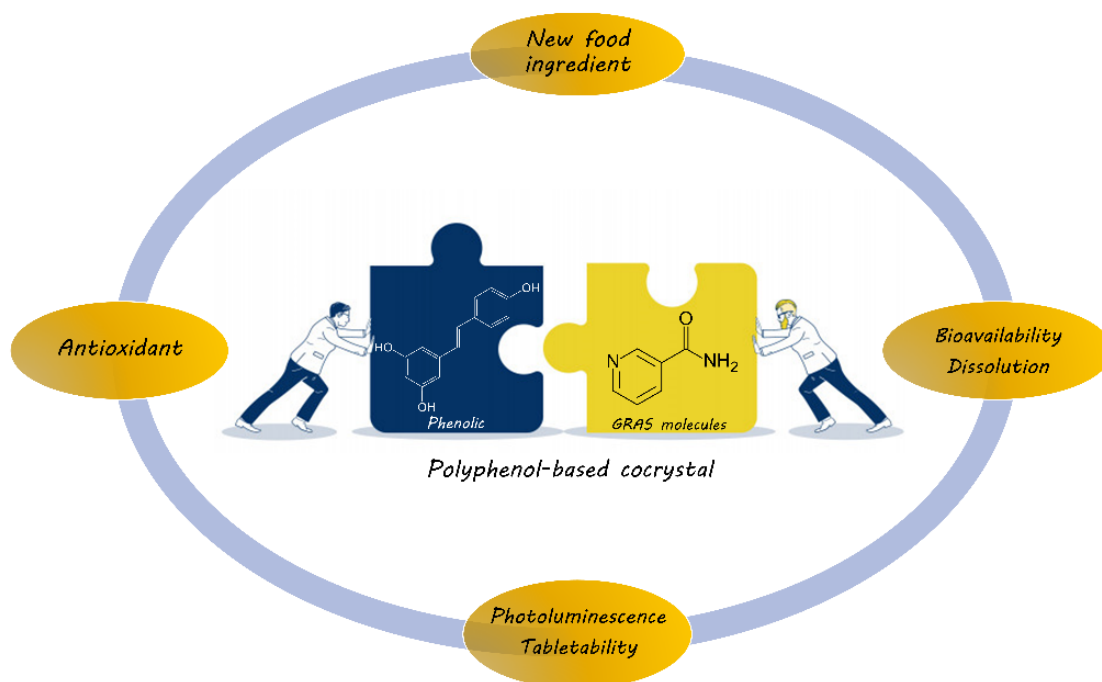
**Abstract**

*Background:* Polyphenols are an important group of bioactive compounds used as food ingredients and supplements. However, its application is limited because they have low water-solubility, bioavailability and stability in gastrointestinal fluids, aspects that can be modulated by polyphenols cocrystallization. Nevertheless, cocrystals have been mostly used in pharmaceutical field, with only few recent uses for food-related polyphenols.

*Scope and approach:* Cocrystallization is addressed as a powerful tool to modulate the properties of food-relevant polyphenols. As the first review concerning food related cocrystals, this review emphasizes cocrystals from food-grade coformers, summarizing production routes, solvents used, and safety-related problems.

*Key findings and conclusions:* Polyphenol-based cocrystals can be produced by slurry, liquid-assisted grinding and slow evaporation, and most recently by microwave assisted and supercritical solvent. The cocrystallization can modulate polyphenol properties such as dissolution, bioavailability, photoluminescence and tensile strength. The bioactivity can also be tuned, providing cocrystals with better antioxidant, antihemolytic, and anti-inflammatory properties. These combined attributes widespread the possible applications of these new materials.

## 2.1 INTRODUCTION

Currently, there is a growing interest in new materials with unique properties and applications, designed for particular uses. This is most relevant for food area, where several attempts have been directed to develop materials for food-related purposes. For instance, colloidal systems developed to modify food microstructure, functionality, quality and sensorial attributes (MARTINS *et al.*, 2018) Development of biobased packaging materials is also relevant for food industries, with focus on special features such as enhancements in antimicrobial activity, mechanical attributes, barrier properties and biodegradability (ZINOVIADOU; GOUGOULI; BILIADERIS, 2016).

A trendy topic in food research is focus on developing functional ingredients. Although, some potential functional ingredients are underexploited due to physical-chemical properties' limitations, restricting its uses. For instance, bioactive essential oils and most polyphenols have low water solubility and are easily oxidized, reducing their application in various food products (AGUILAR-VELOZ *et al.*, 2020). In this context, cocrystallization can be a valuable tool for designing new solid materials with desired physical and chemical properties for specific applications.

The history of cocrystals is intertwined with the history of chemistry itself. The German chemist Friedrich Wöhler, the pioneer of organic chemistry, was the first researcher to obtain, in 1844, a cocrystal formed by quinone/hydroquinone. It took a long time for the academic community to chemically elucidate the cocrystals formation and its rational production. And it was only in the 1990s that cocrystals could be rationally designed, using the idea that supramolecular-bonded units would be responsible for the cocrystals cohesion. Relevant improvements in clarifying the cocrystals synthesis were reached after availability of a search tool for crystal structures from the Cambridge Structural Database. This scientific effort from a journey of almost 200 years culminated with the first commercial product in cocrystallized form. It was the Entresto®, a valsartan-sacubitril cocrystal drug, launched in 2015 by Novartis for the treatment of chronic heart failure (BOLLA; NANGIA, 2016).

Most cocrystal researches are related to improving drug properties because the pharmaceutical area involves large amounts of money. However, in recent years, there has been an increasing interest in the cocrystallization of different compounds, such as polyphenols, known for their biological relevance for food products. Since the cocristalization is an interdisciplinary topic, on the knowledge frontier of food area, this review aims to present fundamentals, synthesis methods, and cocrystals characterization. Food-related properties were addresses through polyphenol based cocrystals, enabling to discuss future perspectives for food applications of cocrystals.

## 2.2 FUNDAMENTAL ASPECTS

Historically, the term 'cocrystal' has been used to describe crystalline materials with two or more different molecules in the same crystal lattice (i.e. multicomponent molecular crystals). In other words, cocrystals are highly orientated three-dimensional assemblage of molecules in solid-state. These periodic organized structures are controlled by symmetry and long-range intermolecular interactions that ultimately determine several fundamental physical properties (GUNAWARDANA; AAKERÖY, 2018).

Diverse intermolecular interactions, such as van der Waals forces, $\pi$-stacking, hydrogen bonding, electrostatic interactions, and halogen bonding, are involved in cocrystals cohesion. Spatial arrangements of those intermolecular interactions are defined as 'supramolecular synthons'. They combine chemical elements of molecular recognition with the geometrical requirements of crystal packing (BOND, 2012).

In short, it means that the molecules are recognized via noncovalent interactions, in guest-host association, where certain groups "see" others as complementary. These molecular

recognition can be used to define specific 'coformers' for tuning physical-chemical properties of the synthetized cocrystals (DAI; CHEN; LU, 2018). Particularly regarding polyphenol-based cocrystals, molecular recognition between hydroxyl groups and hydrogen-bond donating groups such as carboxyl, carbonyl, amide, and pyridyl has been reported as the main synthon beyond these cocrystals formation (SINHA; MAGUIRE; LAWRENCE, 2015). And, with the large number of compounds with these groups, the amount of theorically potential coformers is unlimited.

Nevertheless, accidental cocrystal productions, without rational protocols for coformers selection, are potentially low (GUNAWARDANA; AAKERÖY, 2018). Therefore, how does potential coformers may be reliably and logicaly selected to form polyphenol-based cocrystals? To help with this, some screening strategies for coformers selection are followed discussed.

## 2.2.1 Coformer screening applied to polyphenol-based cocrystals

Polyphenols are an outstanding group of bioactive molecules with several food- related applications. Consequently, selection of coformers to modify polyphenol-based cocrystals for food purposes depends strongly on human been safety issues. Then, harmlessness coformers should be selected from trustfull data. A useful database is the *Substances Added to Food* (formerly EAFUS), which includes food additives, colorants, and the substances "*Generally Recognized as Safe*" (GRAS), regulated by U.S. Food and Drug Administration (US FDA, 2020). The EAFUS inventory currently contains almost 4000 entries, with near 50% listed as GRAS materials, while others have some toxicity.

Alongside with safety aspects, the analysis of target molecular structures and the identification of potential binding sites are fundamental. For polyphenols, hydrogen bond interactions are expected due to the hydroxyl groups in their structure, which places them as potential building-blocks to form supramolecular synthons. Thus, a rational attempt behind selecting coformers for polyphenol-based cocrystals should be based on indicators for hydrogen bond formation (KRAWCZUK; GRYL, 2018).

The well-known intermolecular hydrogen bond concept starts by assuming that the binding site is formed by two motifs, one as hydrogen donor, and other as hydrogen acceptor. Consequently, a useful tool to examine hydrogen bond feasibility between cocrystal constituents is the *motif search* module within *Mercury* software (MACRAE *et al.*, 2020), which searches, on the *Cambridge Structural Database* (CSD), the frequency of any interaction between two specific functional groups.

A typical result from the *motif search* (*Mercury* software version 4.3.0) is shown in **Figure 2.1**, where a polyphenol is represented by a molecule with at least one phenol group. This search engine investigates functional groups capable of forming hydrogen bonds with polyphenol molecules. The example from Figure 2.1 compares the frequency of intermolecular hydrogen bonds between a phenolic group with common organic functions, i.e., pyridine, primary amides, carboxylic acids and carbonyl. The frequency of a particular hydrogen bond represents the number of entries divided by the number of deposited structures containing the two functional groups (phenol and organic function). Based on these statistics, intermolecular hydrogen bonds are more likely to form between polyphenols and the functional molecules in this order: pyridine, primary amides, carboxylic acids, and carbonyl. Consequently, molecules containing aromatic nitrogen represent potential coformers for polyphenol-based cocrystals. The groups carboxylic-OH and amide-$NH_2$ barely act as hydrogen acceptors in hydrogen bonding linkages, with very low interactions frequency. Then, for simplicity, these linkage types are not represented in **Figure 2.1.**
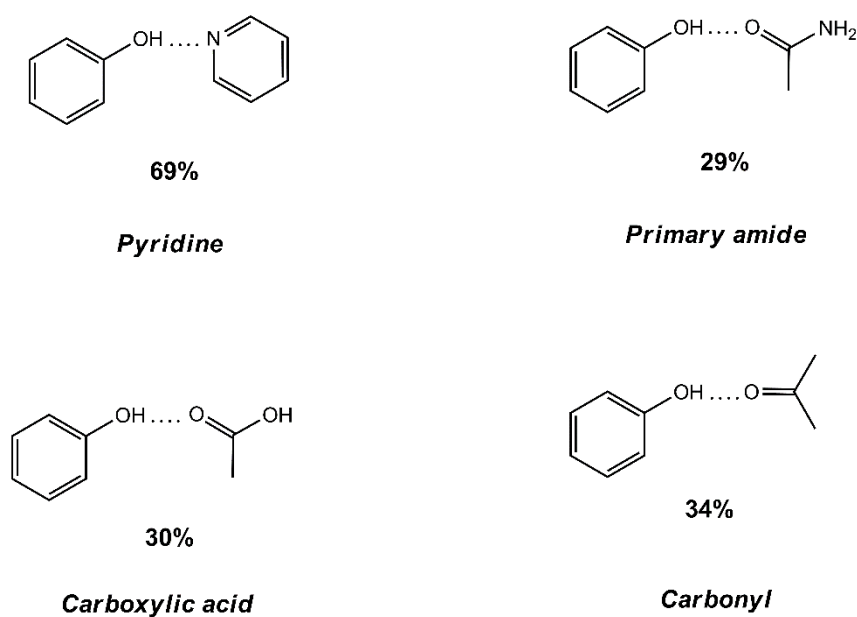


**Figure 2.1** - Frequency of hydrogen bond occurrence between a polyphenol and other functional groups. Constraints: no ions, only organic functions, R-factor: ≤7.5% and structures with 3D coordinates.

Another helpful tool from Mercury software is the molecular complementarity. This functionality evaluates the likelihood of two molecules to form a cocrystal, based on molecular descriptor comparison. The method, created and validated by Fábián (2009), considers a Quantitative-structure-activity relationship (QSAR) model to predict the cocrystal formation

using molecular descriptors data (e.g. dipole moment, shape, size) from the constituent molecules. For a suitable cocrystallization, the molecular descriptors difference, between the two former components, should be small. The Mercury database provides calculated molecular descriptors and characteristic parameters for each molecular pair of target-compound/coformer. The differences between molecular descriptors are compared to pre-established cut-off values (calculated by QSAR model), until acceptable differences are achieved for all descriptors. The calculations are carried out for all combinations of target-compound/coformer, and succeeded comparisons are expressed by Hit Rate (%), which values above 70% indicate cocrystal likelihood (KRAWCZUK; GRYL, 2018).

Examples of this method from the perspective of food-related polyphenols have not been found in literature. Nevertheless, to illustrate this approach, an *in silico* coformer evaluation was performed for the polyphenol "quercetin". The results for best quercetin coformers (Hit rate from 80% to 100%) show different classes of possible coformes. From amino acids like L-tryptophan, L-tyrosine and L-arginine; to flavonoid such as hesperidin; to biotin (complex B vitamin); to organic acids, like sorbic acid, adipic acid, 4-aminobenzoic acid, 4-hydroxybenzoic acid, benzoic acid, fumaric acid, and hydrocinnamic acid, with allowed use in food. Xanthines are also good coformers candidates, like theophylline, with 100% hit rate, whith unfurtunatelly does not attend safety issues, although it may indicate that other xanthines, like caffeine and theobromine, food grade substances, are useful coformers for quercetin cocrystallization.

Alternatively, Loschen & Klamt (2015) presented another *in silico* method to evaluate the cocrystallization tendency of two substances based on estimated mixing enthalpy of parent components. Enthalpy values are determined by theory COSMO-RS (COnductor-like Screening MOdel for Real Solvents), conducted by the *COSMOtherm* software and considering crystal interactions similar to hypothetical supercooled liquid under ambient conditions. In this physical state, the mixture enthalpy is a rough approximation of Gibbs energy of cocrystal formation, enabling the screening for possible coformers because negative values of mixing enthalpy indicate that cocrystals are spontaneously formed.

Coformer screening can also be evaluated from electrostatic and energetic viewpoint. Musumeci et al. (2011) proposed a methodology to evaluate cocrystal formation by comparing cocrystal energy with pure compound's energy. Calculated values of molecular electrostatic potential surfaces are used to identify possible donor and acceptor hydrogen-bond sites. The hydrogen-bond donation and acceptance tendencies are quantitatively expressed by calculated parameters used to estimate interaction site pairing energies. Energy differences between

homomeric (target–target and coformer–coformer) and heteromeric (target–coformer) interactions provide a parameter to energetically rank the coformers. Positive energy differences mean that heteromeric interactions are dominant, enabling cocrystallization, while negative energy differences favor homomeric interactions, without cocrystal formation.

In general, *in silico* methods provide straightforward guidelines for coformer screening, in an inexpensive and fast way. Disregarding the practical and economical aspects, these methods should be used with caution and should not replace experimental screens. Only few studies have evaluated these method robustness (ABRAMOV; LOSCHEN; KLAMT, 2012; MUSUMECI *et al.*, 2011; SARKAR; AAKERÖY, 2020). It seems that the screening performance of those approaches diverges considerably, and depend on the molecules nature. Also, virtual screenings may result in different raking of possible coformers, which may be justified due to different scientific theories behind the calculations, and possible methodological limitations.

For instance, the above mentioned methods are partly based on known crystal structures deposited at CSD. Once negative cocrystallization results are less consistently reported in literature, this lack of information may lead to wrong cocrystallization predictions. Finally, because of the intrinsic limitations of *in silico* methods, we strongly recommend the use of more than one computational screening procedure along with few experimental data, in early stages of research, to establishes potential coformers for cocrystal formation.

An interesting alternative, proposed by Yamamoto, Tsutsumi, Ikeda (2012), was based on five 'cocktails' of coformer candidates, containing four components from the same functional group (*e.g.* citric, fumaric, succinic, and L-tartaric acid). Each mixture, with equimolar quantities of the coformers, were tested to form cocrystals with a target model molecule. The coformer mixture strategy improved data collection by 50%, compared to conventional one-to-one coformer evaluation. Besides, this is an attractive approach for food-related cocrystals once various 'cocktail' coformers are food grade compounds (*e.g.* citric acid, nicotinamide, L-lysine, saccharin). Therefore, expanding the "cocktails", by adding food-safe coformers with high hydrogen-bonding potential with polyphenols (*e.g.* caffeine), could improve this methodology to form polyphenol-based cocrystals.

## 2.3 COCRYSTALLIZATION METHODS

The cocrystallization method deeply affects the final cocrystal characteristics such as purity, particle size and size distribution, morphology, and biological and mechanical properties. Therefore, the procedure selection plays a fundamental role in cocrystal formation.

According to Rodrigues et al. (2018), cocrystallization methods can be broadly classified in two groups, (i) solid-state methods, which use very little or no solvent and (ii) solvent-based methods, involving large amounts of solvent in the production routes. Another classification, also proposed by Rodrigues et al. (2018), takes into account the cocrystallization driving-force. Kinetic methods involve non-equilibrium conditions and are energy- and time-dependent, mostly resulting in metastable cocrystal forms, with higher Gibbs energy compared to stable forms. Grinding, slurry sonication, spray-drying, and supercritical fluid techniques are some kinetic methods. Alternatively, thermodynamic methods take place at equilibrium conditions and are typically carried for long periods. Some examples are slow solvent evaporation and melt cocrystallization. The following sections describe briefly the main cocrystallization methods. These methods are summarized in Table 2.1, containing processing principles, advantages and issues.

**Table 2.1** - Summary of common methods for cocrystal preparation.

| Cocrystallization methods | Working principle | Main advantages | Main issues |
|---|---|---|---|
| *Solid-state methods* | | | |
| **Neat grinding** | Cocrystallization by impact particle size reduction | Cheap, simple process, solvent-free, avoid solvate/hydrate formation, solubility-independent, Suitable for screening essays | Incomplete conversion, Undesirable amorphization, Time-consuming process |
| **Liquid assisted grinding** *(LAG)* | Cocrystallization by material's comminution with addition of small quantities of solvent as catalyst. | Affordable, Easy process, Low solvent usage, Environmentally-friendly (using green-solvents), Versatile, Suitable for screening essays | Solvate formation, Time-consuming process |
| **Hot melt extrusion** *(HME)* | Cocrystallization involving melting and extrusion of mixture of the starting materials. | Solvent-free, Fast operating times, High cocrystal conversion, Low waste, Continuous process, Scalable, Avoid solvate/hydrate formation | Thermal degradation of labile molecules Complex process |
| *Solvent-based methods* | | | |
| **Slow evaporation** *(SE)* | Cocrystallization is triggered through supersaturation provided by solvent evaporation. | Simple process, Simple equipment, Easy to process | High propensity of single component formation, Impure cocrystals, Low cocrystal conversion, High tendency to form solvates/hydrates, Environmentally hazardous, Limited by thermodynamic equilibrium, Slow process |
| **Isothermal Slurry Conversion (ISC)** | Cocrystallization by solution-mediated phase transformation from suspension/slurry of parent materials in a liquid solvent. | Simple process, Simple equipment, Easy to process, High efficiency | Material loss due to residual solubility in the solvent, Solvate formation, Environmentally hazardous, Difficult to scale-up |
| **Supercritical fluid techniques (*CSS, RESS, GAS, SAS*)** | *CSS:* cocrystallization by solution-mediated phase transformation from suspension/slurry of parent materials in supercritical $CO_2$. *RESS:* cocrystallization from the expansion of a supercritical solution of the starting materials. *GAS* and *SAS:* cocrystallization induced by $CO_2$ antisolvent in a solute/solution mixture. *GAS* working in batchwise while *SAS* works continuously. | Versatile, Single step process, Avoids solvates/hydrates (manly *CSS*), Solvent/antisolvent re-use, Low waste, Environmentally-friendly, Scalable | Certain number of prerequisites about solvents (*GAS* and *SAS*), Limited by materials solubility in $CO_2$ (*RESS* and *CSS*). |

### 2.3.1 Solid-state methods

Solid-state methods are based on mechanochemical principles by coupling mechanical and chemical phenomena on molecular scale. Cocrystals are produced by direct mechanical energy absorption, which promotes solid fractures on the starting materials, increasing surface area, facilitating interpenetration and the molecular contact. In some cases, small amounts of solvent can accelerate the process due to an increase in molecular mobility (KARIMI-JAFARI *et al.*, 2018b; RODRIGUES *et al.*, 2018). The common solid-state methods are as follows.

*Neat grinding*: also called dry grinding or solid-state grinding, is one of the most important cocrystallization methods. It consists of grind the stoichiometric mixed amounts of the cocrystal components in solid-state. In the initial research stages, the process can be even performed manually, by mortar and pestle. However, it may lead to reproducibility issues, so mechanical methods are preferable. Grinding methods by automatized equipment, like a ball or vibratory mill are suitable alternatives (DOUROUMIS; ROSS; NOKHODCHI, 2017). Grinding methods offer some operational advantages, such as less expensive and more environmentally friendly, compared to solution-based methods. Also, previous solvent solubilization of the cocrystal constituents is not required, which disregards issues relate to solubility differences between target-molecule and coformer, reducing possible harmful effects of the solvent on the solute-solute interactions. These grinding methods produce high purity and quality cocrystals, without or with negligible amounts of solvents. Sadly, grinding also presents drawbacks, and the main issue is the generation of amorphous materials, less stable than the crystalline form. Other issue concerns the risk of thermal degradation, due to mechanical stress, especially for heat-sensitive materials, such as polyphenols (FRISCIC; JONES, 2012; MALAMATARI *et al.*, 2017). Huang et al. (2014) studied the production of baicalein/nicotinamide cocrystals by slow evaporation (SE), rotary evaporation and neat grinding. Cocrystals prepared by three different methods showed similar PXRD patterns, indicating the same cocrystal. The authors claim that it indicates a clear advantage of the grinding method over SE and rotary evaporation because cocrystallization could be achieved even in the absence of organic solvent.

*Liquid assisted grinding* (LAG): also known as solvent-drop grinding is based on the addition of small quantities of solvent that act as catalyst, increasing the cocrystal formation kinetics. However, the solvent role is still not fully elucidated. For some systems , the liquid solvent changes the solid molecular orientation and conformation, increasing molecular collisions frequency. In other cases, the liquid phase performs as lubricant, wetting the solid surface and improving molecular diffusion. LAG carries the inherent issues of neat grinding,

besides additional problems as solvent disposal and environmental risks (RODRIGUES *et al.*, 2018). Sowa et al. (2014b) prepared new genistein/caffeine cocrystals by LAG method using eight different solvents separately (methanol, ethanol, isopropanol, acetone, ethyl acetate, acetonitrile, chloroform, and water). From the results, solvent type did not affect cocrystallization, i.e., similar cocrystals were obtained regardless the solvent used. The cocrystals by LAG were similar to those obtained by slow evaporation (section 2.3.2), suggesting a greener route to obtain genistein/caffeine cocrystals.

*Hot melt extrusion* **(HME):** a well-established method used in polymer and food industries. However, HME as cocrystallization technique is relatively recent, which combines simultaneous melting and mixing of target molecule and coformer by means of heated screw extruder (KARIMI-JAFARI *et al.*, 2018b). HME promotes intense mixing, shearing and plasticizing effects, improving surface contact of the components, enabling a solvent-free alternative for tailor cocrystals (GAJDA *et al.*, 2019a). The scale-up flexibility, continuous processing, and cost-effectiveness are promising features of HME, an alternative for cocrystal manufacture (CHAVAN *et al.*, 2018). Cocrystals production by HME is very recent, with no polyphenol applications detected in the literature. However, this is a promising method for manufacturing nutraceutical cocrystals. For example, Gajda et al. (2019b) investigated the addition of polymers and their crystallinity degree on HME cocrystallization of theophylline/nicotinamide (The/Nic) cocrystals. Comparing neat and polymer-assisted HME cocrystallizations, adding poloxamer (semicrystalline polymer) increased cocrystallization efficiency. Also, The/Nic cocrystals supplemented by poloxamer were stable after 12 months of storage at 25 °C/60 % RH conditions while The/Nic cocrystals supplemented by Soluplus® (amorphous polymer) showed significant structural modifications during storage. HME cocrystallization from polymeric matrix has unexplored potential. The extrusion may allow the production of polymeric materials embedded with cocrystals with varied forms (e.g. fibers, rods, pellets) and for different purposes (e.g. food-packages).

## 2.3.2 Solvent-based methods

A variety of solvent-based approaches have been used for synthesizing cocrystals. On these methods the solvent plays a central role, affecting cocrystal characteristics such as purity, shape, polymorphism and solvate tendency. The solvents are sellected based on parent components' solubility. In some cases, information about solid-liquid equilibrium is required for solvent selection. Mainly, if the solubilities of cocrystal components are too different, for

solvent-based methods, it affects the cocrystal purity and the success of the proposed route ( RODRIGUES et al., 2018; KARIMI-JAFARI et al., 2018).

*Slow evaporation* **(SE):** also called evaporative cocrystallization, is based on system supersaturation, caused by solvent evaporation, and is the crystallization driving force. SE is especially convenient to elucidate cocrystal structure. SE often allows growth of crystals suitable for single-crystal X-ray diffraction studies. Typically, hazardous solvent mixtures have been employed, disqualifying SE as a green method (KARIMI-JAFARI *et al.*, 2018b). In some SE cases, cocrystals are partially formed or even not formed, due to incongruent solubility of individual components in the solvent. When parent components present similar solubility in a solvent (congruent solubility), the phase diagram is symmetrical (**Figure 2.2a**), and pure cocrystal might be obtained in a wide range of compositions (region C). Otherwise, when two components show different solubilities (incongruent solubility), the phase diagram is less symmetrical (Figure 2 b), and pure cocrystal is obtained at narrow set of compositions (region C, **Figure 2.2b**) (STEED, 2013). Therefore, knowledge of phase diagram is usefull to determine SE experimental conditions. Hence, other methods are indicated to deal with incongruent systems (ALHALAWEH; VELAGA, 2010).
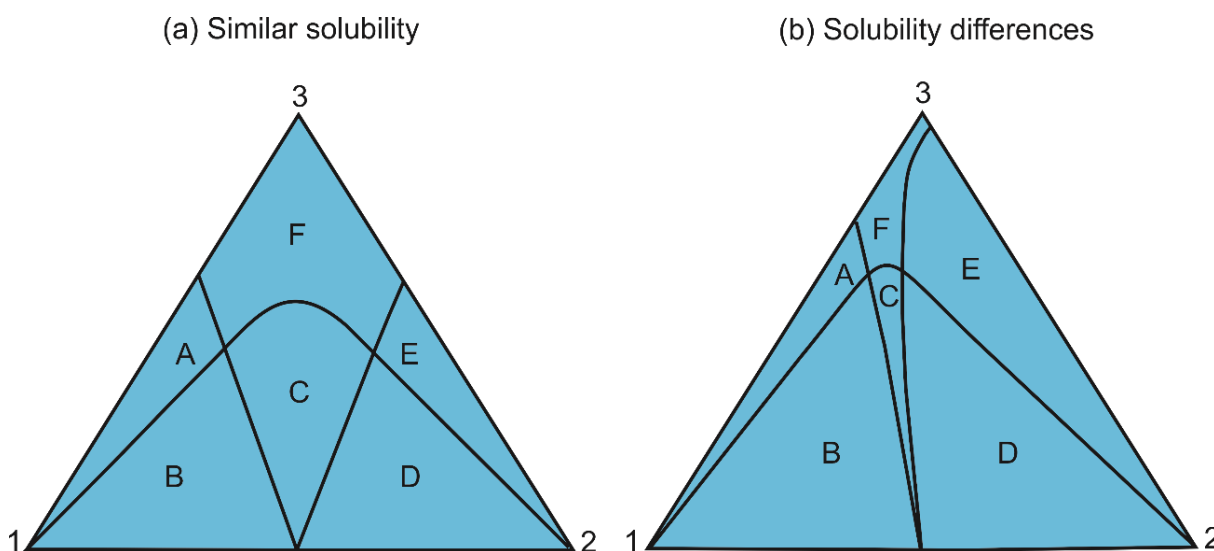


**Figure 2.2** - Phase diagram. (a) Similar solubilities between target-molecule and coformer (1 and 2) in solvent 3 and (b) different solubilities of 1 and 2 in 3. A: 1 + 3; B: 1 + cocrystal; C: cocrystal; D: 2 + cocrystal; E: 2 + 3; F: 1 + 2 in 3. From: Steed (2013)

The practical use of phase diagrams is limited once for its construction the solid phases (target-molecule, coformer and cocrystal) should be quantifiable by some method. In reality, the accurate measurement of cocrystalline phases is one of the biggest bottlenecks in cocrystal research, which turns these diagrams very rare in the literature. In the absence of phase

diagrams, and for practical purposes, the solubility of the individual polyphenols and coformers in a solvent may be useful to estimate the incongruent behavior. Therefore, in general, the cocrystal region becomes smaller as the solubility ratio between the cocrystal components increases (AHUJA *et al.*, 2020b).

   ***Isothermal Slurry Conversion* (ISC):** Unlike SE, which starts from clear solutions, the slurry method involves cocrystallization from a suspension of target-molecule and coformer. It takes place via solution-mediated phase transformation, where higher solute concentration favors nucleation and cocrystals growth (BUČAR et al., 2010; KARIMI-JAFARI et al., 2018). Cocrystals are naturally metastable in comparison with their parent components, and its formation is dependent on the component's thermodynamic behavior. A theoretical cocrystal slurry production, suggested by Zhang, Henry, Borchardt, & Lou (2007), stated that stable cocrystal is obtained from coformers at their critical chemical activity values. As a first approximation, a coformer chemical activity is the ratio of its solution concentration and its solubility on the solvent. Once overcoming the critical value, the cocrystal, with higher thermodynamic stability, spontaneously crystallizes, given sufficient time for nucleation and cocrystal growth. Then, for a successful cocrystal slurry route, the amount of coformer should be higher than its solubility in the solvent. Consequently, the process is often carried out with high solid content. Besides, auxiliary techniques such as ultrasound and microwave may improve the slurry cocrystal conversion. Ultrasound has a well-known positive effect on induction period, supersaturation conditions and metastable zone width, effects that favors pure cocrystals formation on unfavorable thermodynamic systems (incongruent solubility). It represents, on ternary phase diagrams, an expansion of pure cocrystal regions, compared to not ultrasonicated systems (APSHINGEKAR *et al.*, 2017). Microwaves provide much faster cocrystal production than conventionally heated slurry cocrystallization. The positive microwave effect goes beyond simple heating effect, also affecting the solution structure, and molecular movements, which enhance the opportunities for molecular collisions and interactions between solutes and solvent molecules (AHUJA *et al.*, 2020a). Caffeic acid phenethyl ester, a polyphenol commonly present in propolis, was successfully cocrystallized with coformers such as caffeine, isonicotinamide, and nicotinamide by microwave-assisted slurry. All cocrystals could be formed at mid-temperature (80 °C) and in a short time (1 min) compared to conventional heated slurry (KETKAR *et al.*, 2016).

## 2.3.2.1 Supercritical CO$_2$-Based Methods

   Supercritical carbon dioxide (SC-CO$_2$) has been successfully employed in cocrystal manufacturing, and the inspiring study showing its feasibility as cocrystals synthesis media was

published by Padrela et al. (2009). The authors used indomethacin–saccharin cocrystals as a model system and classified the cocrystallization according to the role of SC-$CO_2$ in the process, as solvent, antisolvent, or atomization enhancer.

*Cocrystallization with Supercritical solvent (CSS):* The cocrystallization by CSS uses SC-$CO_2$ as a solvent in a slurry/suspension composed by the parent components. SC-$CO_2$ may promote higher effective molecular interactions between reactants, facilitating the nucleation and cocrystals growth. By controlling SC-$CO_2$ conditions (temperature and pressure) it is possible to fine-tune its density and solvent power, which defines the cocrystal characteristics, such as purity and size distribution. CSS method is strongly dependent on pure components solubility on SC-$CO_2$, and the solubility of each solute in SC-$CO_2$ should be similar. Because cocrystal conversion rate is limited by convection, the process is generally carried out under stir. Finally, to increase cocrystallization versatility, small amounts of organic solvents may be added, acting as SC-$CO_2$ entrainer, which enables cocrystal formation, when pure SC-$CO_2$ does not produce the cocrystals (PADRELA *et al.*, 2009, 2015). In a recent study, Ribas et al. (2019) produced cocrystals of curcumin/nicotinamide, by CSS at fixed pressure and temperature conditions (9 MPa, 45 C) for 60 min and obtained cocrystals with particle size ranging from 25-35 μm. The results indicate CSS as more advantageous to prepare curcumin/nicotinamide cocrystals than the evaporative method because it does not demand organic solvent, and it is a fast process.

*Rapid expansion of supercritical solutions (RESS)*: RESS involves high pressure solubilization and saturation of SC-$CO_2$ with the starting materials. After this step, the mixture is depressurized through a nozzle into a drying chamber at atmospheric pressure. The depressurization is very fast (less than $10{-5}$ s), leading to solvent expansion, which reduces SC-$CO_2$ solvent power, providing cocrystal precipitation. This method has been underexplored, probably due to low solubility in SC-$CO_2$ of most studied molecules. Besides, large solubility differences between the target-molecule and coformer may lead to heterogeneous mixtures and then, non-stoichiometric supercritical solutions (MÜLLERS, PAISANA, & WAHL, 2015; PANDO; CABAÑAS; CUADRA, 2016a). Regarding polyphenols-based cocrystals, the most $CO_2$-soluble phenolics ($\sim 10^{-4}$ to $10^{-2}$ mole fraction), such as vanillin and cinnamic acid, have higher chances to produce RESS pure cocrystals, mostly using coformers at the same solubility range (e.g. caffeine and nicotinamide), while poorly $CO_2$-soluble phenolics, such as curcumin ($\sim 10$-8 to 10-6 mole fraction), have limited chance for RESS cocrystallization, where $CO_2$-antisolvent techniques should be preferred (CHEN; CHEN; TANG, 2009; JOHANNSEN;

BRUNNER, 1994; KOTNIK; ŠKERGET; KNEZ, 2011; ROJAS-ÁVILA *et al.*, 2016; ZHAN *et al.*, 2017).

***Gas antisolvent (GAS):*** In GAS technique, pressurized $CO_2$ is added to a high-pressure chamber containing the solute-solution, until desired pressure is obtained. While $CO_2$ is feeding, it dissolves into liquid solution, causing its expansion and decreasing its solvency ability, leading to solute crystallization (PANDO; CABAÑAS; CUADRA, 2016). GAS cocrystallization offers advantages over traditional methods. It allows a fast single-step process, provides a platform to control the particle size and morphology by fine-tuning the process pressure and temperature. Contrasting with mechanical methods, it reduces thermal and mechanical stress of the reactants. Also, GAS reduces organic solvent usage and reduces residual solvent in cocrystal powder when compared to traditional solvent-based methods (WICHIANPHONG; CHAROENCHAITRAKOOL, 2018b).

***Supercritical antisolvent (SAS):*** As in GAS method, SC-$CO_2$ is used as antisolvent to induce cocrystal precipitation from parent components solution. In SAS cocrystallization, SC-$CO_2$ and liquid solution are simultaneously sprayed into the high-pressure vessel through a nozzle. Then, the fluid dissolves into the solution droplets which become immediately supersaturated, leading to cocrystals nucleation and growth. After precipitation, the vessel is washed with pure SC-$CO_2$ to remove residual organic solvent from the final powder (PANDO; CABAÑAS; CUADRA, 2016). SAS and GAS methods share the same previously cited advantages over traditional methods. However, the SAS method, due to its continuous feeding, can promote new and unique molecular recognition events, which might result in new or polymorphic cocrystals, increasing the process versatility (PADRELA *et al.*, 2009).

## 2.4 BASIC COCRYSTAL CHARACTERIZATION TECHNIQUES

Experimentally, the cocrystallization of a specific polyphenol might lead to not cocrystallized undesirable solid forms, such as solvates, hydrates, polymorphs, salts, and co-amorphous solids. Therefore, based on this complex diversity of these possible solid products, the cocrystal characterization is a vital step in cocrystal development.

In principle, any analytical method able to distinguishing solid forms can be used to identify and characterize new cocrystals. In practice, the appropriate technique(s) selection depends on a series of factors, including equipment availability, necessary evidence, samples amount (available and required) and form (single crystal vs. powder). Generally, the characterization is performed by combining analytical methods, such as crystallography,

spectroscopy, microscopy, thermal analysis and others (REUTZEL-EDENS, 2012). These analytical procedures are briefly described as follows.

Single-crystal X-ray diffraction (SCXRD) probably is the characterization method that provides more structural information. In SCXRD, small crystals are exposed to an X-ray beam from all possible diffraction directions. The diffracted intensity and the correspondent diffraction angles are mathematically converted to a model that describes the electron density in the crystal. This model provides geometric information about the molecules, such as bond lengths and angles, torsion angles, and interplanar distances and geometries of the intermolecular interactions. However, this characterization method is strongly dependent on size and quality of single crystals produced. Once the production of single-crystals, convenient for SCXRD studies, cannot always be achieved, the Powder X-ray diffraction (PXRD) has been used as an alternative characterization method (PINDELSKA; SOKAL; KOLODZIEJSKI, 2017; REUTZEL-EDENS, 2012).

Because most cocrystals can only be prepared as microcrystalline powders, PXRD is a useful standard analysis. Although PXRD provides considerably less structural information than SCXRD, it differentiates the solid forms easily and inexpensively. Since distinct solid phases hold different set of diffraction peaks, the PXRD plot, with angles (°2θ) related to crystal lattice, can be used as a "fingerprint" that characterizes different crystal structures (PINDELSKA; SOKAL; KOLODZIEJSKI, 2017).

Thermal methods are also useful techniques for cocrystal characterization. These methods evaluate physical and/or chemical changes in testing materials with temperature variations (predefined heating or cooling). Differential Scanning Calorimetry (DSC) is the most widespread thermal method for cocrystals evaluation. It provides phase transitions that occur while the cocrystal sample is under heating (REUTZEL-EDENS, 2012).

The nature of the thermal events showed by DSC thermograms could indicates successful cocrystallization. The analysis generally compares the thermal events from the cocrystal, the individual components, and the physical mixture of the starting materials. If a trial cocrystal sample exhibits a DSC thermogram with single endothermic event, distinct from the melting points from individual components and from physical mixture, this is a high indication of cocrystal formation (SATHISARAN; DALVI, 2018). DSC analysis may be inconclusive if systems endothermic events are equal to the physical mixture, because it is not possible to associate the event with cocrystal formation, or eutectic mixture or in situ cocrystallization. Therefore, additional methods are necessary to confirm the cocrystal synthesis.

Vibrational spectroscopic techniques also provide useful complementary evidence of cocrystal formation. Mid-infrared spectroscopy (4000–400 cm$^{-1}$) has been more commonly used because of their availability, but other spectroscopic methods, as near-infrared (NIR) and Raman, have also been historically used to identify chemical structures (functional groups) based on characteristic fingerprints derived from vibrational modes. Spectroscopic analysis can identify hydrogen bonds in a cocrystal phase by comparing differences in vibrational modes exhibited by the pure components and the cocrystal (REUTZEL-EDENS, 2012).

Microscopic techniques have also been used to morphologically characterize cocrystals, specially Polarized Optical Microscopy (POM) (HE *et al.*, 2016), Fluorescence microscopy (FAN *et al.*, 2016), and Scanning Electron Microscopy (SEM) (PESSOA *et al.*, 2019).

In this section, the most commonly solid-state techniques used for cocrystal assessment have been briefly described. A detailed list of characterization methods, used to evaluate cocrystal properties, and covering traditional and advanced procedures, can be found elsewhere (PINDELSKA; SOKAL; KOLODZIEJSKI, 2017).

Because polyphenols can crystallize as hydrates, solvates, and different polymorphic forms, the cocrystallization can provides undesirable solid forms, which makes the cocrystal evaluation a huge challenge, particularly when DSC is inconclusive. Then, PXRD seems suitable to distinguish between cocrystal and pure component forms (polymorphs, hydrates, and solvates). For instance, quercetin has four structures deposited at CSD, quercetin anhydrous (CSD code: NAFZEC), quercetin monohydrate (CSD code: AKIJEK), quercetin dihydrate (CSD code: FEFBEX) and quercetin-DMSO solvate (CSD code: VUVHOM) (KLITOU et al., 2019; KLITOU et al., 2020). Typical polyphenol coformers, such as nicotinamide and caffeine, also present polymorphism. Therefore, a cautious analysis must consider possible polymorphic transformations of the pure component (like quercetin) and the coformers to avoid wrong conclusion of cocrystal formation. A recommended practice is to perform a control test for each cocrystal component, at the processing condition, to verify possible phase changes. Because the characterization methods might provide weak evidences or even be inconclusive about cocrystal formation, these techniques should be used in combination to provide sufficient evidences to support cocrystal formation.

## 2.5  AN OVERVIEW ONN POLYPHENOL-BASED COCRYSTALS

Phenolic compounds, such as polyphenols, are naturally present in fruits, vegetables, leaves, seeds and some foods and beverages, like tea, chocolate and wine, and its ingestion is highly indicated as a healthy habit. Nowadays, polyphenols are used as functional ingredient for food products and dietary supplements. Their beneficial effects depend on factors such as

intake, absorption, metabolism, and mainly bioavailability. Although polyphenols are abundant in food products, the *in vivo* effects are restricted because some of them are poorly absorbed due to low bioavailability(CHEN; CAO; XIAO, 2018). To overcome the low bioavailability, new polyphenol formulations have been proposed, including micro (CHEN *et al.*, 2019) and nanoencapsulation (MILINČIĆ *et al.*, 2019), emulsions and liposomes (PIMENTEL-MORAL *et al.*, 2018). Cocrystallization also emerges as alternative formulation to reduce the bioavailability drawbacks (HE *et al.*, 2017a; KETKAR *et al.*, 2016; LUO *et al.*, 2019b; ZHU *et al.*, 2017).

The main polyphenols that were successfully cocrystallized are summarized in this section. The SCOPUS database (www.scopus.com) was used to compile reseach papers and scientific trends. The survey, carried out on December, 2020, applied the following keywords/booleans: [("co-crystal") OR (cocrystal)] AND [(polyphenol*) OR (phenolic*)], with no constraint on publication year. In order to detect papers with polyphenols (e.g., flavonoids, phenolic acids, tannins), additional keyword/booleans were considered: OR (flav*) OR (phen* acid) OR (tannin*) OR (coumarin*). Besides, the polyphenol's common name and CAS numberes, from most abundant polyphenols, were used according to Phenol-Explorer database (http://phenol-explorer.eu/compounds).

Finally, special attention was given to polyphenol-based cocrystals which could be produced by safe coformers for food applications, and presented, at least, *in vitro* release studies, suggesting ability on dissolution modulation. **Table 2.2** shows a list of polyphenol-based cocrystals, summarizing relevant information such as conformers, stoichiometry, cocrystallization method, solvent used for cocrystal synthesis and its safety FDA classification, and n-parameter (ratio of solvent volume to sample weight). From Table 2.2, a significant number of reported polyphenol-based cocrystals are flavonoids, probably due to their low water solubility (log S) and bioavailability, compared to other polyphenols. The water solubility of several flavonoids such as quercetin, naringenin, and baicalein (values -3.06, -3.11, and -3.25, respectively) are lower than simple polyphenols like gallic acid (-1.54). Polyphenols predominantly belong to class II (low solubility and high permeability) or class IV (low solubility and low permeability) of the biopharmaceutics classification system (BCS), *i.e.*, their bioavailability is limited mainly due to their low water solubility (SUZUKI *et al.*, 2019). Since the main cocrystallization goal is to enhance the molecule bioavailability by tuning their solubility, researches focusing on water-solubility enhancement are frequent.

Different coformers combinations are also shown in **Table 2.2**. The main chemical classes of food-grade coformers, used for cocrystallization of food-related polyphenols, are

illustrated in **Figure 2.3** The components that form vitamin $B_3$ complex, such as nicotinamide, isonicotinamide, and picolinic acid are the most used coformers. These components, involved in important human biochemical reactions, are precursors of nucleotide coenzymes, which play an essential role in a wide variety of metabolic pathways, such as electron transport chain, among others (LITWACK, 2018).
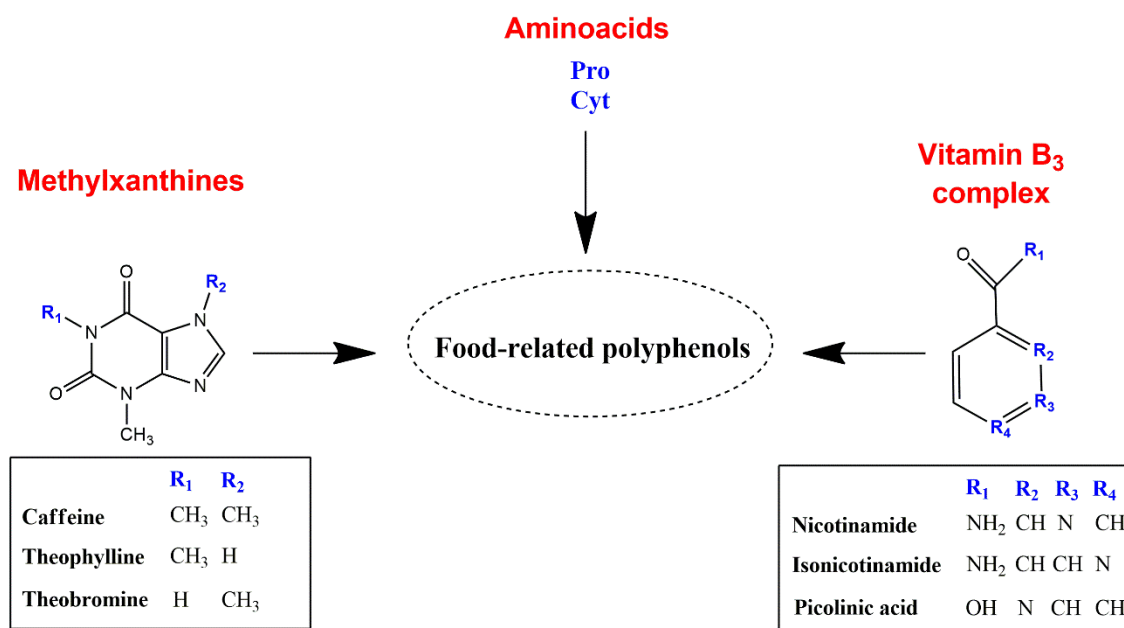


**Figure 2.3** -Major groups of food grade coformers used to produce polyphenol-based cocrystals.

Methylxanthines are also a meaningful group of molecules used as polyphenol coformers. They include caffeine, theophylline, and theobromine. The methylxanthines are alkaloids naturally occurring in high concentrations in various food products like tea, coffee, and chocolate, and present psychostimulant effects. They also have therapeutic potential against several neurodegenerative diseases such as Alzheimer's and Parkinson's (OÑATIBIA-ASTIBIA; FRANCO; MARTÍNEZ-PINILLA, 2017). They can also favor lipolysis, a key effect on fat depletion, weight loss, and obesity control (CARRAGETA *et al.*, 2018).

**Table 2.2**- Summary of polyphenol-based cocrystals available in the literature.

| Polyphenol/ Coformer[a] | Method[b] | Solvent | Solvent classification | η-parameter (μL/mg) | Reference |
|---|---|---|---|---|---|
| Cat/Asc (1:1) | Slurry | Ethanol | Class 3 | 62.31 | (SPIZZIRRI *et al.*, 2019) |
| Cat/Asc (1:1) | LAG | | | 0.24 | |
| Bai/Nic (1:3) | Slurry | Ethyl acetate | Class 3 | 706.88 | (PI *et al.*, 2019b) |
| Bai/Isonic (1:2) | LAS | THF/Hexane | Class 2/Class 2 | 116.73 | (ZHU *et al.*, 2017) |
| Bai/Caf (1:2) | Slurry | Methanol | Class 2 | 6.84 | |
| Bai/Bet (1:1) | SE | Methanol/Ethyl acetate (1:9, v/v) | Class 2/Class 3 | 198.41 | (ZHU *et al.*, 2017) |
| Bai/Bet (1:1) | LAG | Methanol | Class 2 | 0.30 | |
| Bai/The (1:1) | Slurry | Acetone | Class 3 | 88.89 | (LI *et al.*, 2018) |
| Bai/Nic (1:1) | SE | Ethyl acetate | Class 3 | 98.43 | (HUANG *et al.*, 2014) |
| Bai/Nic (1:1) | Rotary evaporation | | | 7.87 | |
| Dai/Isonic (1:1) | | | | 26.59 | (BHALLA *et al.*, 2019) |
| Dai/Tbr (1:1) | LAG | Ethanol | Class 3 | 23.03 | |
| Dai/Cyt (1:1) | | | | 27.39 | |
| Epi/Isonic (1:1)[c] | SE | Water/Methanol (1:1, v/v) | Class 3/Class 2 | 86.21 | (SMITH *et al.*, 2013) |
| Epi/Isonic (1:1)[c] | Slurry | | | 51.72 | |
| Epi/Nic (1:1)[d] | SE | | | 34.48 | |
| Epi/Nic (1:1)[d] | Slurry | | | 51.72 | |
| Epi/IsoAcid (1:1)[e] | SE | Water | Class 3 | 86.05 | |
| Epi/IsoAcid (1:1)[e] | Slurry | | | 51.63 | |
| Epi/IsoAcid (1:1) | SE | | | 86.05 | |
| Epi/IsoAcid (1:1) | Slurry | | | 51.63 | |
| Fis/Caf (1:1) | Cooling | Methanol | Methanol | 20.81 | (MOHITE *et al.*, 2019) |
| Fis/Nic (1:1) | | | | 24.49 | |
| Fis/Nic (1:1) | | Water | Class 3 | | (SOWA; ŚLEPOKURA; MATCZAK-JON, 2014a) |
| Fis/Nic (1:1) | | Methanol | Class 2 | | |
| Fis/Nic (1:1) | | Ethanol | Class 3 | | |
| Fis/Nic (1:1) | | 2-propanol | Class 3 | | |
| Fis/Nic (1:1) | | Acetone | Class 3 | | |
| Fis/Nic (1:1) | | Acetonitrile | Class 2 | | |
| Fis/Nic (1:1) | | Ethyl acetate | Class 3 | | |
| Fis/Nic (1:1) | | Chloroform | Class 2 | 0.35 | |
| Fis/Isonic (1:1) | LAG | Water | Class 3 | | |
| Fis/Isonic (1:1) | | Methanol | Class 2 | | |
| Fis/Isonic (1:1) | | Ethanol | Class 3 | | |
| Fis/Isonic (1:1) | | 2-propanol | Class 3 | | |
| Fis/Isonic (1:1) | | Acetone | Class 3 | | |
| Fis/Isonic (1:1) | | Acetonitrile | Class 2 | | |
| Fis/Isonic (1:1) | | Ethyl acetate | Class 3 | | |
| Fis/Isonic (1:1) | | Chloroform | Class 2 | | |
| Fis/Caf (1:1) | | Water | Class 3 | 0.30 | |

**Table 2.2** – (Continued)

| Polyphenol/ Coformer[a] | Method[b] | Solvent | Solvent classification | η-parameter (μL/mg) | Reference |
|---|---|---|---|---|---|
| **Fis/Caf (1:1)** | | Methanol | Class 2 | | |
| **Fis/Caf (1:1)** | | Ethanol | Class 3 | | |
| **Fis/Caf (1:1)** | | 2-propanol | Class 3 | | |
| **Fis/Caf (1:1)** | | Acetone | Class 3 | | |
| **Fis/Caf (1:1)** | | Acetonitrile | Class 2 | | |
| **Fis/Caf (1:1)** | | Ethyl acetate | Class 3 | | |
| **Fis/Caf (1:1)** | | Chloroform | Class 2 | | |
| **Fis/Nic (1:1)** | SE | Ethanol | Class 3 | 197.18 | |
| **Fis/Caf (1:2)** | SE | Ethanol | Class 3 | 119.86 | |
| **Fis/Isonic (1:1)** | Slurry | Methanol | Class 2 | 5.62 | |
| **Fis/Nic (1:2)** | Slurry | Ethanol | Class 3 | 4.35 | |
| **Fis/Nic (1:1)** | Slurry | Acetonitrile | Class 2 | 8.44 | |
| **Fis/Caf (1:1)** | Slurry | Ethyl acetate | Class 3 | 8.52 | |
| **Gen/Caf (1:1)** | LAG | Water | Class 3 | 0.29 | (SOWA; ŚLEPOKURA; MATCZAK-JON, 2014b) |
| **Gen/Caf (1:1)** | SE | Ethanol | Class 3 | 163.17 | |
| **Gen/Caf (1:1)** | Slurry | Methanol | Class 2 | 5.82 | |
| **Hes/PicAcid (1:1)** | | | Class 3 | 0.12 | (CHADHA *et al.*, 2017) |
| **Hes/Nic (1:1)** | LAG | Ethanol | Class 3 | 0.12 | |
| **Hes/Caf (1:1)** | | | Class 3 | 0.10 | |
| **Myr/Nic (1:2)** | Ultrasound-assisted Slurry | Methanol | Class 2 | 14.03 | (LIU *et al.*, 2016b) |
| **Myr/Pro (1:2)** | | Ethanol | Class 3 | 27.78 | (LIU *et al.*, 2016a) |
| **Nar/Isonic (1:2)** | SE | Acetonitrile | Class 2 | 116.28 | |
| **Nar/Isonic (1:2)** | Slurry | Ethyl acetate | Class 3 | 9.69 | |
| **Nar/PicAcid (1:1)** | Slurry | Ethyl acetate | Class 3 | 12.66 | |
| **Nar/Bet (1:1)** | Liquid diffusion | Dichloromethane/Ethanol/Hexane (1:2:12, v/v) | Class 2/Class 3/Class 2 | 385.60 | (LUO *et al.*, 2018) |
| **Nar/Bet (1:1)** | Slurry | Ethanol | Class 3 | 12.85 | |
| **Nar/Bet (1:1)** | | Acetonitrile | Class 2 | | |
| **Nar/Nic (1:1)** | | Ethanol | | 23.92 | |
| **Nar/Caf (3:2)** | Slurry | Acetone | Class 3 | 30.86 | (CUI *et al.*, 2019) |
| **Nar/Isonic (1:2)** | | Ethanol | | 23.92 | |

**Table 2.2** – (Continued)

| Polyphenol/ Coformer | Method[b] | Solvent | Solvent classification | η-parameter (µL/mg) | Reference |
|---|---|---|---|---|---|
| **Nar/Pro (1:1)** | | Ethanol | | 13.33 | (CUI *et al.*, 2019) |
| **Nar/Bet (1:2)** | | Ethanol | | 14.26 | |
| **Phl/Bet (1:1)** | LAS | Methanol/Dichloromethane | Class 2/Class 2 | 196.85 | (ZHANG *et al.*, 2019) |
| **Phl/Bet (1:1)** | LAG | Methanol | Class 2 | 0.39 | |
| **Que/Bet (1:2)** | SE | Ethanol/Ethyl acetate (1:4, v/v) | Class 3/Class 3 | 262.24 | |
| **Que/Bet (1:2)** | Slurry | Methanol/Ethyl acetate (v/v, 1:4) | Class 2/Class 3 | 17.48 | |
| **Que/Caf (1:1)** | SE | | Class 2 | 113.21 | (SMITH *et al.*, 2011) |
| **Que/Caf (1:1)** | Slurry | Methanol | Class 2 | 12.52 | |
| **Que/Isonic (1:1)** | SE | | Class 2 | 129.59 | |
| **Que/Tbr (1:1)** | SE | Water/Ethanol (1:2. v/v) | Class 3 | 96.53 | |
| **Pte/Caf (1:1)** | | Chloroform | Class 2 | | (SCHULTHEISS; BETHUNE; HENCK, 2010) |
| **Pte/Caf (1:1)** | LAG | Acetonitrile | Class 2 | 0.32 | |
| **Pte/Caf (1:1)** | | Ethanol | Class 3 | | |
| **Pte/Caf (1:1)** | | Nitromethane | Class 2 | | |
| **Pte/Caf (1:1)** | Vapor diffusion | Methanol/Water (1:10, v/v) | Class 2/Class 3 | 223.58 | |
| **Pte/Caf (1:1)** | Vapor diffusion | Ethanol/Water (1:10, v/v) | Class 3 | 223.58 | |
| **Res/Nic (1:1)** | | Acetone/Hexane/Toluene (1:1:1, v/v/v) | Class 3/Class 2/Class 2 | 85.63 | (HE *et al.*, 2017a) |
| **Res/Isonic (1:2)** | SE | Acetone/Hexane/Heptane (1:1:1, v/v/v) | Class 3/Class 2/Class 3 | 85.63 | |
| **Res/Pro (1:2)** | | Methanol/acetonitrile (1:1, v/v) | Class 2/Class 2 | 52.34 | |
| **Res/Pip (1:2)[e]** | Slurry | Isopropanol/Ethyl acetate/Water (2:4:1, v/v) | Class 3/Class 3/Class 3 | | (HE *et al.*, 2017b) |
| **Res/Pip (1:2)[e]** | | | | 50.08 | |
| **Res/Pip (1:2)[f]** | SE | Acetone/Acetonitrile (1:1, v/v) | Class 3/Class 2 | | |
| **Res/Pip (1:3)[f]** | | | | 36.89 | |
| **Res/Pip (1:2)[g]** | | Toluene/Ethyl acetate (1:1, v/v) | Calss 2/Class 3 | 50.08 | |
| **CAPhe/Caf (1:1)** **CAPhe/Nic (1:1)** **CAPhe/Isonic (1:1)** | Microwave-assisted slurry | Ethanol | Class 3 | 1.90 | (KETKAR *et al.*, 2016) |

[a]Cocrystals are represented as *Polyphenol/Coformer* abbreviations, numbers in parenthesis symbolize the cocrystals stoichiometry. *Polyphenols*: **Bai** – Baicalein; **Cat** – (+)-catechin; **Cur** – Curcumin; **Dai** – Daidzein; **Epi** – Epigallocatechin-3-gallate; **Fis** – Fisetin; **Gen** – Genistein; **Hes** – Hesperetin; **Myr** – Myricetin; **Nar** – Naringenin; **Phl** – Phloretin; **Pte** – Pterostilbene; **Que** – Quercetin; **Res** – Resveratrol; **CAPhe** – Caffeic Acid phenethyl ester. *Coformers:* **Asc** – L-(+)-ascorbic acid; **Bet** – Betaine; **Caf** – Caffeine; **Cyt** – Cytosine; **IsoAcid** – Isonicotinamide acid; **PicAcid** – Picolinic acid; **Isonic** – Isonicotinamide; **Nic** – Nicotinamide; **Pip** – Piperine; **Pro** – Proline; **Tbr** – Theobromine; **The** – Theophylline. [b] **LAG** – liquid-assisted grinding; **LAS** – Liquid antisolvent; **SE** – slow evaporation. c 5H2O cocrystal hydrate. [d] 9H2O cocrystal hydrate. [e] 3H2O cocrystal hydrate. [f] Acetonitrile/water solvate. [g] Toluene/water solvate.

Polyphenol interactions with other substances are advantageous in some cases, and, combined, can produce complementary, additive, or synergistic effect. For instance, studies have showed that the co-ingestion of maethylxantines like caffeine enhances the bioavailability of some flavonoids, such as flavan-3-ols, and epigallocatechin-3-gallate (Epi). The study by Fraga, Croft, Kennedy, & Tomás-Barberán (2019) suggests that the thermogenic effect of Epi from green tea extracts is partially due to flavanols and caffeine combination. These findings help to draw relevant cocrystal applications. A possible use for flavonoid/methylxanthine cocrystals could be fortification/supplementation of teas. These results illustrate that coformers used to synthetize polyphenol-based cocrystals may be explored beyond their effect as a lattice modifier; they might also be applied as a source of additional bioactive property to polyphenols.

In general, different polyphenol-based cocrystals are properly produced by conventional methods, especially slurry, grinding and slow evaporation methods (**Table 2.2**). Among these cocrystals, several are produced by Class 2 solvents from FDA residual solvents guide (**Table 2.2**). This guide divides common solvents into three levels according to their potential risk to human health: Class 1 are solvents to be avoided, due to known or suspected carcinogenesis; Class 2 are solvents with non-genotoxic animal carcinogens or causative agents of other irreversible toxicity such as neurotoxicity or teratogenicity; and Class 3 reunite solvents with low toxic potential to human being. Because of their inherent toxicity, Class 1 and Class 2 solvents should be minimal used or avoided, with their residual concentration limits respected (FDA, 1997, 2018). Class 1 and Class 2 solvents are particularly challenging due to the low limit of residual concentration in the final product. Cocrystals production using these solvents are a hard task, once the process might produce cocrystal solvates, which overtake the limits of residual solvent. This drawback was reported by He, Zhang, Wang, & Mei, (2017) which used solvent mixtures to produce cocrystals of resveratrol/piperine. Three out of five produced cocrystals were solvates with Class 2 solvents, acetonitrile and toluene. The chemical structures of these cocrystals, determined by single-crystal X-ray diffraction, revealed that all cocrystal solvates had the solvent-to-resveratrol molar ratio of 1:1, overcoming by far the residual limit.

The non-recommended solvents used for cocrystal production also result in environmental issues. Although useful, the FDA's classification is limited because it does not specify the environmental risks. Due to these limitations, other classifications have been developed (BYRNE *et al.*, 2016). One of the most complete solvent guides, including environment-related indicators, was developed by Prat et al. (2016). On this classification,

several Class 2-solvents as THF, methanol, and chloroform were labeled as 'problematic', whereas others like hexane and dichloromethane earned the 'hazardous' label. These solvents are linked with aquatic life toxicity, bioaccumulation, generation of harmful volatile organic compounds, and problems related to recycling and disposal. From the perspective of polyphenol-based cocrystal production, the solvents have an additional inconvenience because many cocrystals synthesized methods are solvent-consuming, as shown in Table 2.2 by $\eta$-parameter[1], the solvent: sample ratio (v/w). For instance, narigenin/betaine cocrystal (Nar/Bet (1:1)) was produced with high amount ($\eta$ = 385.60 $\mu$L/mg) of undesirable solvents such as dichloromethane and hexane.

New cocrystal synthesis for fine applications need to be aligned with the latest practices of cleaner development and production and should be as much 'green' as possible. For this purpose, the use of supercritical fluids is exceptionally high-powered. However, these protocols are still scarcely explored for polyphenol-based cocrystal synthesis. The first cocrystals for food applications provided by high pressure techniques were made by Pessoa *et al.* (2019). They produced resveratrol/nicotinamide (Res/Nic) cocrystal by GAS method, at 9 MPa and 45 °C. The PXRD pattern of Res/Nic revealed a not pure cocrystal, with the presence of non-cocrystallized pure components on the final material. A more systematic approach would identify the effect of process variables (pressure, temperature, and $CO_2$ flowrate) on cocrystal characteristics, such as purity and dissolution profile, to suggest possible applications. Despite the study limitations, the cocrystal showed higher dissolution rate than pure resveratrol in simulated physiological conditions at pH 6.8 and gastric environment (HCl 0.1 M), indicating that cocrystallized resveratrol could be more bioavailable.

Another drawback in polyphenol cocrystal formation is related to processing time. For instance, the slurry synthesis of (+)-catechin/L-(+)-ascorbic acid (Cat/Asc) cocrystals (SPIZZIRRI *et al.*, 2019) was achieve at 24h conversion, which limits the large scale process feasibility. Other cocrystals systems showed similar problem, like Bai/Nic cocrystal produced by slurry (PI *et al.*, 2019b), completed in 8h process.

Fast processes like Spray drying can overcome time limitation. This continuous single-step method transforms liquids (solutions, suspensions, slurries) into solid powders. It is a continuous, highly controllable, and fast process (ALHALAWEH; VELAGA, 2010). Although

---

[1] The $\eta$-parameter is the volume of solvent (in $\mu$L) divided by the sample weight (in mg).

no studies reported polyphenol cocrystallization by spray drying, some findings suggest it as a viable alternative. For instance, Alhalaweh et al. (2013) prepared theophylline cocrystals by spray drying, demonstrating favorable processing time and adequacy to manufacture pure cocrystals, even in incongruently systems, such as theophylline/nicotinamide. It gives flexibility in solvent selection, since the phase diagrams knowledge is less crucial if compared to slurry and evaporation methods.

Cocrystals have also been combined with other innovative techniques such as solid-lipid nanoparticles (SLNs), improving polyphenol application. Bazylińska et al. (2014) proposed to combine innovative methods to obtain unique materials composed by phosphatidylcholine-based solid-lipid nanocarriers loaded with polyphenol-based cocrystals. In this approach, cocrystals of baicalein/nicotinamide and myricetin/caffeine were synthetized by *Liquid assisted grinding* (LAG), and then embedded into SLNs by three different preparation techniques, i.e., solvent diffusion, hot homogenization-ultrasonification and microemulsification. Regardless the SLNs production method, the solubility modulation characteric of the cocrystals was preserved. Furthermore, SLNs were stable for nine months in colloidal and in freeze-dried forms. In our perspective, these are appealing results because they may expand food related applications of polyphenol-based cocrystals. Cocrystals loaded in lipid matrices can be better incorporated into oily foods compared to the free-form cocrystals.

## 2.5.1 Modulating the dissolution of food-relevant polyphenols

The health effect of polyphenols, a wide class of secondary metabolites, depends on their absorption, metabolism, and subsequent human bioavailability. Dietary polyphenols, often as esters, glycosides, or polymers, normally cannot be directly absorbed. Before absorption in human body, these compounds should suffer enzymatic reactions as methylation, glucuronidation, or sulfatation. Regardless specificities of each polyphenol, the general consensus is that polyphenol absorption may depend on its ability to be solubilized in gastrointestinal fluids (CHEN et al., 2018). In this context, polyphenol-based cocrystals have been dissoluted in several media, from pure water and aqueous buffers, to biorelevant gastrointestinal simulants, as Fasted State Simulated Gastric Fluid (FaSSGF) and Fasted State Simulated Intestinal Fluid Version 2 (FaSSIF-V2). Quantifying the polyphenol amount in each liquid sample over time provides the concentration-time curve, from which a dissolution profile can be extracted. Dissolution studies of polyphenol-based cocrystal have been performed at

various time and different media, as listed in Table 2.3. In this review the final polyphenol concentrations were used to evaluate the dissolution performance, calculated comparing the amount of polyphenol released by the cocrystal compared with the control (pure polyphenol powder), with the results expressed as fold change.

As can be seen from **Table 2.3,** cocrystallization has been suitable to modulate polyphenols dissolution performance. For instance, cocrystallization of caffeic acid phenethyl ester with nicotinamide (CAPhe/Nic (1:1)) provided high concentration of CAPhe in water for up to 24 hours, reaching CAPhe concentration in water 17.7-times higher than the control (KETKAR *et al.*, 2016). The dissolution modulation from cocrystallization proved to be effective not only in aqueous media, but also in different buffer systems and pH values. Cui et al. (2019) studied the dissolution of naringenin cocrystals in HCl (pH 1.2), acetate (pH 4.5), and phosphate buffer (pH 6.8). For all samples, a significant increment in dissolution performance was detected. For the narigenin/caffeine (Nar/Caf (3:2)) cocrystal, the gains in dissolution performance, related to control, were 2.14, 1.25, and 2.76-fold, at pH values of 1.2, 4.5, and 6.8, respectively.

The favorable effect of cocrystallization on increasing dissolution and apparent solubility of polyphenols has been associated with two critical steps: (i) generation of a metastable supersaturated state and (ii) preservation of this supersaturated state for a long period. This phenomenon has been reported as 'spring and parachute' effect (BAVISHI; BORKHATARIA, 2016a). During dissolution, cocrystal hydrogen bonds are dissociated, releasing coformer molecules (more water-soluble component) in the solution, forming metastable phases (amorphous and/or polymorphic) with polyphenol. Because of its favorable energy state, amorphous and/or polymorphic forms speed up the polyphenol dissolution, generating a temporary supersaturated state - the 'spring' effect. The maintenance of peak solubility, or 'parachute' effect, is dictated by the Ostwald's Law of Stages. The amorphous-like phase is converted to metastable polymorphs (still with high solubility), and then finally to the most thermodynamically stable polymorph (BABU; NANGIA, 2011; WEI *et al.*, 2018).

**Table 2.3** - In vitro dissolution performance of various polyphenol-based cocrystals.

| Polyphenol/Coformer | Dissolution media | Dissolution time | Dissolution performace | Reference |
|---|---|---|---|---|
| Bai/Nic (1:3) | FaSSIF-V2<br>FaSSGF | | ↑*1.74-fold*<br>↑*2.22-fold* | (PI *et al.*, 2019b) |
| Bai/Nic (1:3) | FaSSIF-V2<br>FaSSGF | 360 min | ↑*2.17-fold*<br>↑*2.54-fold* | |
| Bai/Caf (1:2) | HCl buffer (pH 2) [b]<br>Phosphate buffer (pH 4.5) [b] | | ↑*2.5-fold*<br>↑*1.5-fold* | (ZHU *et al.*, 2017) |
| Bai/Bet (1:1) | Phosphate buffer (pH 6.8) [b] | 250 min | ↑*1.73-fold* | (ZHANG *et al.*, 2019) |
| Bai/The (1:1) | HCl buffer (pH 1.2) [c]<br>Phosphate buffer (pH 6.8) [c] | 360 min | ↑*2.2-fold*<br>↑*7.1-fold* | (LI *et al.*, 2018) |
| Bai/Nic (1:1) | HCl buffer (pH 1.2)<br>Phosphate buffer (pH 6.8) | 60 min | ↑*1.50- fold*<br>↑*2.16-fold* | (HUANG *et al.*, 2014) |
| Epi/Isonic (1:1)<br>Epi/Nic (1:1) [#]<br>Epi/IsoAcid (1:1) [‖]<br>Epi/IsoAcid (1:1) | Water | | ↓*17.87-fold*<br>↓*8.13-fold*<br>↓*25.10-fold*<br>↓*19.18-fold* | (SMITH *et al.*, 2013) |
| Hes/PicAcid (1:1) | Phosphate buffer (pH 7.2) | 240 min | ↑*4-fold* | (CHADHA *et al.*, 2017) |
| Hes/Nic (1:1)<br>Hes/Caf (1:1) | | | ↑*4.5-fold*<br>↑*4-fold* | |
| Kae/Pro (1:2) | Water [b] | 360 min | ↑*1.8-fold* | (HE *et al.*, 2016) |
| Nar/Nic (1:1) | HCl buffer (pH 1.2)<br>Acetate buffer (pH 4.5)<br>Phosphate buffer (pH 6.8)<br>Water | | ↑*1.74-fold*<br>↑*1.88-fold*<br>↑*1.96-fold*<br>↑*3.15-fold* | (CUI *et al.*, 2019) |
| Nar/Caf (3:2) | HCl buffer (pH 1.2)<br>Acetate buffer (pH 4.5)<br>Phosphate buffer (pH 6.8)<br>Water | | ↑*2.17-fold*<br>↑*1.25-fold*<br>↑*2.76-fold*<br>↑*2.33-fold* | |
| Nar/Isonic (1:2) | HCl buffer (pH 1.2)<br>Acetate buffer (pH 4.5)<br>Phosphate buffer (pH 6.8)<br>Water | 90 min | ↑*2.34-fold*<br>↑*1.88-fold*<br>↑*2.90-fold*<br>↑*3.10-fold* | |
| Nar/Pro (1:1) | HCl buffer (pH 1.2)<br>Acetate buffer (pH 4.5)<br>Phosphate buffer (pH 6.8)<br>Water | | ↑*2.03-fold*<br>↑*1.67-fold*<br>↑*2.30-fold*<br>↑*2.38-fold* | |
| Nar/Bet (1:2) | HCl buffer (pH 1.2)<br>Acetate buffer (pH 4.5)<br>Phosphate buffer (pH 6.8)<br>Water | | ↑*2.17-fold*<br>↑*1.83-fold*<br>↑*1.15-fold*<br>↑*3.08-fold* | |
| Phl/Bet (1:1) | Phosphate buffer (pH 6.8) [b] | 250 min | ↑*1.58-fold* | (ZHANG *et al.*, 2019) |
| Phl/Nic1:1 | Phosphate buffer (pH 7.2) | 300 min | ↑*2.14-fold* | (HUANG, S. *et al.*, 2019a) |
| Phl/Isonic (1:1) | | | ↑*1.31-fold* | |
| Que/Bet (1:2) | Phosphate buffer (pH 6.8) [b] | 250 min | ↑*3.66-fold* | (ZHANG *et al.*, 2019) |
| Que/Nic (1:1) | Phosphate buffer (pH 7.4) | 360 min | ↑*2.71-fold* | (VASISHT *et al.*, 2016) |
| Que/PicAcid (1:1) | | | ↑*5.17-fold* | |

**Table 2.3** – (Continued)

| Polyphenol/Coformer | Dissolution media | Dissolution time | Dissolution performace | Reference |
|---|---|---|---|---|
| **Pte/Caf (1:1)** | Water | 300 min | ↑*23.66-fold* | (SCHULTHEISS; BETHUNE; HENCK, 2010) |
| **Res/Nic (1:1)** | Phosphate buffer (pH 2) [d] | | ↑*2.59-fold* | |
| | Phosphate buffer (pH4.6) [d] | | ↑*1.70-fold* | |
| | Phosphate buffer (pH 6.8) [d] | | ↑*1.72-fold* | |
| **Res/Isonic (1:2)** | Phosphate buffer (pH 2) [d] | 180 min | ↑*2.99-fold* | (HE *et al.*, 2017a) |
| | Phosphate buffer (pH4.6)[d] | | ↑*2.35-fold* | |
| | Phosphate buffer (pH 6.8) [d] | | ↑*2.48-fold* | |
| **Res/Pro (1:2)** | Phosphate buffer (pH 2) [d] | | Approximately one | |
| | Phosphate buffer (pH4.6) [d] | | ↑*1.30-fold* | |
| | Phosphate buffer (pH 6.8) [d] | | ↑*1.44-fold* | |
| **Res/Nic (1:1)** | HCl buffer (pH 1.2) | | ↑*1.10-fold* | (PESSOA *et al.*, 2019) |
| | Phosphate buffer (pH 6.8) | 90 min | ↑*1.10-fold* | |
| **Res/Nic (1:1)** | HCl buffer (pH 1.2) | | ↑*1.43-fold* | |
| | Phosphate buffer (pH 6.8) | | ↑*1.13-fold* | |
| **CAPhe/Caf (1:1)** | | | ↑*5.5-fold* | (KETKAR *et al.*, 2016) |
| **CAPhe/Nic (1:1)** | Water | 24 h | ↑*17.7-fold* | |
| **CAPhe/Isonic (1:1)** | | | ↑*7.5-fold* | |

[a]Cocrystals are represented as *Polyphenol/Coformer* abbreviations, numbers in parenthesis symbolize the cocrystals stoichiometry. **Polyphenols: Bai** – Baicalein; **Epi** – Epigallocatechin-3-gallate; **Hes** – Hesperetin; **Kae** – Kaempferol; **Nar** – Naringenin; **Phl** – Phloretin; **Que** – Quercetin; **Pte** – Pterostilbene; **Res** – Resveratrol; **CAphe** – Caffeic Acid phenethyl ester. **Coformers: Bet** – Betaine; **Caf** – Caffeine; **IsoAcid** – Isonicotinamide acid; **Isonic** – Isonicotinamide; **Nic** – Nicotinamide; **Pro** – Proline. [b] The dissolution media was supplemented with 0.5% Tween 80. [c] The dissolution media was supplemented with 0.2% SDS-Na. [d] The dissolution media was supplemented with 0.1% PVP K30. [e] 9$H_2O$ cocrystal hydrate. [f] $H_2O$ cocrystal hydrate.

HUANG et al. (2019b) compared the dissolution performance of phloretin/nicotinamide (Phl/Nic) and phloretin/isonicotinamide (Phl/Isonic) cocrystals. Despite the molecular similarity between nicotinamide and isonicotinamide, the authors produced cocrystals with distinct dissolution profiles. Phl/Nic cocrystal exhibited a clear and pronounced 'spring and parachute' effect, with maximum phloretin concentration, 6.6-times higher that the control (Phl), achieved at 15 min and maintained for 60 min. In contrast, Phl/Isonic cocrystal showed only 'spring' stage. The maximum Phl concentration was observed at 15 min, reaching 5.5-times higher than pure Phl solubility. However, just after 15 min, the Phl concentration decreased, and reduced continuously until PHL equilibrium solubility was reached. It has also

been reported that the hydrotropic property of some coformers, such as nicotinamide, can help maintain the supersaturation state (HUANG *et al.*, 2014).

Although less common, cocrystallization has also used to modulate the dissolution of polyphenols with the purpose of decrease its solubility. Smith et al. (2013) reported an example of this strategy. They used the cocrystallization to reduce the water solubility of epigallocatechin-3-gallate (Epi), which is the most abundant polyphenol in green tea and has been reported as high water-soluble but low permeable compound. Epigallocatechin-3-gallate cocrystals with isonicotinamide, nicotinamide, and isonicotinamide acid as coformers were successfully produced. All cocrystals were powerful in reducing the dissolution of Epi in water, with the best results for epigallocatechin-3-gallate/isonicotinamide acid (Epi/IsoAcid (1:1)‖) cocrystal hydrate, which showed a 25.10-fold reduction.

## 2.5.2 Modulating the bioavailability of food-relevant polyphenols

The results of *in vitro* dissolution trials are useful to initiate cocrystallization researches because it may indicate the most promising cocrystals (higher dissolution *in vitro* results) and their beneficial effect on enhancing the polyphenol bioavailability. However, because of the complexity of cocrystals absorption and metabolism, the *in vitro* results should be interpreted carefully, combined with complementary *in vivo* studies (BOLLA; NANGIA, 2016).

As far as we know, there are no *in vivo* studies regarding the bioavailability of polyphenol-based cocrystals in humans. The bioavailability studies have been performed using animal models, usually Wistar and Sprague–Dawley rats. Briefly, the tests are performed by supplying the animals with the cocrystal through some vehicle, such as granules, suspensed in water or dispersed in vegetable oil. At previously scheduled times, blood samples are collected and the polyphenols concentration in blood plasma is quantified. These data permit building plasma concentration-time curves, from which by fitting pharmacokinetic models, important parameters of bioavailability can be obtained.

**Table 2.4** summarizes the bioavailability parameters of various studies carried out on polyphenol-based cocrystals. The $t_{max}$ parameter represents the time to reach the maximum polyphenol concentration ($C_{max}$). The AUC symbolizes the area under the plasma concentration-time curve, $F_{rel}$ is the relative oral bioavailability, defined as the ratio between the AUC of cocrystal and the AUC of pure polyphenol. In general, cocrystallization has also been effective in bioavailability modulation, as observed in

**Table 2.4**.

Substantial increases in Frel were observed, especially for apigenin/theophylline (Api/The (1:2)) cocrystal, with approximately 6-fold enhancement in oral bioavailability compared with apigenin (Api).

**Table 2.4** - Oral bioavailability studies of polyphenol-based cocrystals.

| Polyphenol/ Coformer[a] | Pure Polyphenol | | | Cocrystal | | | | Reference |
|---|---|---|---|---|---|---|---|---|
| | $C_{max}$ (μg/mL) | $t_{max}$ (h) | AUC (μg.h/mL) | $C_{max}$ (μg/mL) | $t_{max}$ (h) | AUC (μg.h/mL) | $F_{rel}$ | |
| **Api/The (1:2)** | 0.67 | 2.22 | 5.22 | 6.80 | 0.27 | 31.70 | **6.07** | (HUANG, S. *et al.*, 2019b) |
| **Bai/Caf (1:2)** | 4.54 | 0.42 | 17.75 | 15.21 | 0.67 | 73.48 | **4.14** | (ZHU *et al.*, 2017) |
| **Bai/The (1:1)** | 2.50 | 5.40 | 23.94 | 6.06 | 10.00 | 147.59 | **6.16** | (LI *et al.*, 2018) |
| **Bai/Nic (1:1)** | 8.83 | 1.50 | 74.96 | 22.03 | 1.00 | 209.67 | **2.80** | (HUANG *et al.*, 2014) |
| **Dai/The (1:2)** | 0.93 | 1.16 | 8.56 | 2.76 | 0.26 | 12.80 | **1.49** | (HUANG, S. *et al.*, 2019b) |
| **Dai/Isonic (1:1)** | | | | 1.85 | 3.00 | 2.70 | **2.11** | (BHALLA *et al.*, 2019) |
| **Dai/Tbr (1:1)** | 0.87 | 4.00 | 1.28 | 1.33 | 3.00 | 2.21 | **1.72** | |
| **Dai/Cyt (1:1)** | | | | 1.61 | 3.00 | 2.45 | **1.91** | |
| **Epi/IsoNicAcid (1:1)** | | | | 0.35 | 0.5 | 0.91 | **1.37** | (SMITH *et al.*, 2013) |
| **Epi/Isonic (1:1)** | 0.34 | 0.13 | 0.66 | 0.13 | 0.50 | 0.38 | **0.57** | |
| **Epi/Nic (1:1)** | | | | 0.19 | 0.33 | 0.37 | **0.55** | |
| **Fis/Caf (1:1)** | 1.80 | 1.00 | 6.29 | 9.01 | 0.25 | 17.22 | **2.74** | (MOHITE *et al.*, 2019) |
| **Hes/PicoAcid (1:1)** | | | | 0.63 | 2.00 | 2.89 | **1.37** | (CHADHA *et al.*, 2017) |
| **Hes/Nic (1:1)** | 0.47 | 3.00 | 2.11 | 1.15 | 1.50 | 3.33 | **1.58** | |
| **Hes/Caf (1:1)** | | | | 1.27 | 1.50 | 3.39 | **1.60** | |
| **Isoqui/Nic (1:1)** | 0.45 | 0.25 | 1.25 | 0.53 | 0.38 | 1.49 | **1.19** | (XU *et al.*, 2016) |
| **Isoqui/Isonic (1:1)** | 0.45 | 0.25 | 1.25 | 0.90 | 0.16 | 2.38 | **1.90** | |
| **Kae/Pro (1:2)** | 7.83 | 6.00 | 39.55 | 36.79 | 4.66 | 178.68 | **4.52** | (HE *et al.*, 2016) |
| **Lut/Caf (1:1)** | 0.72 | 0.50 | 3.06 | 0.93 | 0.50 | 4.42 | **1.44** | (LUO *et al.*, 2019b) |
| **Myr/Pro (1:2)** | 0.43 | 4.00 | 3.88 | 1.49 | 2.60 | 11.51 | **2.97** | (LIU *et al.*, 2016a) |
| **Nar/Nic (1:1)** | | | | 2.91 | 0.08 | 2.37 | **0.81** | (CUI *et al.*, 2019) |
| **Nar/Caf (3:2)** | | | | 1.65 | 0.40 | 4.14 | **1.41** | |
| **Nar/Isonic (1:2)** | 0.51 | 2.20 | 2.93 | 3.39 | 0.08 | 4.26 | **1.45** | |
| **Nar/Pro (1:1)** | | | | 1.02 | 2.00 | 7.00 | **2.39** | |
| **Nar/Bet (1:2)** | | | | 1.71 | 3.60 | 14.38 | **4.91** | |
| **Que/Nic (1:1)** | 0.91 | 0.50 | 7.79 | 6.00 | 0.17 | 12.14 | **1.56** | (VASISHT *et al.*, 2016) |
| **Que/PicoAcid (1:1)** | | | | 7.83 | 0.08 | 13.63 | **1.75** | |

**Table 2.4** – Continued

| Polyphenol/ Coformer[a] | Pure Polyphenol | | | Cocrystal | | | | Reference |
|---|---|---|---|---|---|---|---|---|
| | $C_{max}$ (µg/mL) | $t_{max}$ (h) | AUC (µg.h/mL) | $C_{max}$ (µg/mL) | $t_{max}$ (h) | AUC (µg.h/mL) | $F_{rel}$ | |
| Que/Caf (1:1) | 0.29 | 0.50 | 0.12 | 2.61 | 0.08 | 0.50 | **4.01** | |
| Que/Caf (1:1) | 0.29 | 0.50 | 0.12 | 0.66 | 0.17 | 0.32 | **2.57** | (SMITH et al., 2011) |
| Que/Isonic (1:1) | | | | 1.40 | 0.17 | 0.68 | **5.46** | |
| Que/Tbr (1:1) | 0.29 | 0.50 | 0.12 | 0.84 | 0.08 | 1.24 | **9.93** | |
| Res/Nic (1:1) | | | | 0.48 | 0.37 | 2.09 | **1.17** | (HE et al., 2017a) |
| Res/Isonic (1:2) | 0.39 | 0.87 | 1.79 | 0.39 | 0.31 | 1.50 | **0.84** | |
| Res/Pro (1:2) | | | | 0.37 | 0.25 | 1.51 | **0.84** | |
| CAPhe/Nic (1:1) | 0.04 | 0.25 | 0.04 | 0.08 | 0.17 | 0.11 | **2.76** | (KETKAR et al., 2016) |

[a] Cocrystals are represented as *Polyphenol/Coformer* abbreviations, numbers in parenthesis symbolize the cocrystals stoichiometry. **Polyphenols**: **Api** – Apigenin; **Bai**– Baicalein; **Dai** – Daidzein; **Epi** – Epigallocatechin-3-gallate; **Fis** – Fisetin; **Hes** – Hesperetin; **Isoqui** – Isoliquiritigenin; **Kae**– Kaempferol; **Lut** – Luteolin; **Myr** –Myricetin; **Nar** – Naringenin **Que** – Quercetin; **Res** – Resveratrol; **CAPhe** – Caffeic Acid phenethyl ester. *Coformers*: **Caf** – Caffeine; **Cyt** – Cytosine; **Isonic** – Isonicotinamide; **IsoNicAcid** – Isonicotinaminic acid; **Nic** – Nicotinamide; **PicoAcid** – Picolinic acid; **Pro** – Proline; **Tbr** – Theobromine; **The** – Theophylline.

Most literature researches, summarized in the present review, deal with cocrystallization process to increase polyphenols solubility and, as a consequence, improve bioavailability. Cui *et al.* (2019) produced naringenin cocrystals with different cocrystal coformers, evaluated their solubility, dissolution rate, and the rats tissue distribution after oral administration, and the results shown relevant improvement of the cocrystal form, compared to pure naringenin. Notably, the naringenin/betaine cocrystal enabled the highest naringenin tissue distribution for all tested organs, unlike naringenin/betaine physical mixture and pure naringenin, indicating a positive correlation between the improvement on bioavailability, oral absorption and biodistribution of cocrystallized naringenin.

Cocrystallization have also been used to increase polyphenols bioavailability by deacreasing their aqueous solubility. Polyphenols such as epigallocatechin-3-gallate have received considerable attention due to numerous health-promoting bioactivities, been included in many dietary supplement formulations. However, reports have demonstrated their low bioavailability due to high-water solubility and low permeability. Then, Smith et al. (2013) produced different cocrystals with epigallocatechin-3-gallate (Epi), to increase its bioavailability by decreasing the water-solubility. All formed cocrystals successfully decreased

Epi water-solubility, particularly cocrystals formed with isonicotinic acid as coformer, which improved the Epi bioavailability.

In general, the increase in polyphenol bioavailability is related to dissolution enhancement and maintenance of high levels of polyphenol solution medium. However, the bioavailability of some biological molecules also depends on their permeability through cellular membranes. Cocrystallization enhanced in about 10-times (using Caco-2 model) the apparent pearmeability of oxyresveratrol through its cocrystallization with citric acid. The modulation of permeability seems to be a complex interrelation between the cocrystal structure, melting temperature, coformer solubility and permeability (SUZUKI *et al.*, 2019).

### 2.5.3 Modulating properties from cocrystals of food-relevant polyphenols

For the effective use of polyphenol-based cocrystals, as potential food ingredient or additive, it is necessary to evaluate their effect and stability in food-materials, to drive this emerging technology for the food area. In spite of the high potential, studies on this subject are extremely rare. One attempt to understand the cocrystal role in food media was proposed by Spizzirri et al. (2019), through cocrystals of catechin/ascorbic acid, applied in two commercial bottled tea beverages (peach and lemon) and black tea infusion. The cocrystals showed three-times higher solubility in the beverages than pure catechin, which improved the antioxidant attributes of the tea samples (bottled and infusion). Additionally, some studies showed that cocrystallization has been useful to improve in vitro antioxidant, antihemolytic, and anti-inflammatory activities of polyphenols (BHALLA *et al.*, 2019; CHADHA *et al.*, 2017; VASISHT *et al.*, 2016).

Besides, several naturally occurred polyphenols presented anticancer effects, and this subject has become very relevant (FRAGA *et al.*, 2019), with promising results showing higher anticancer effect achieved by cocrystallized polyphenols. Recently, myricetin (Myr) and dihydromyricetin (diMyr), both cocrystallized with berberine (Ber) chloride, demonstrated in vitro anticancer effect in HT-29 cancer cells (colorectal tumor model). Myr and diMyr cocrystals increased significantly the inhibitory rates compared with the control groups (pure Myr, diMyr, and Ber) (LI, P. *et al.*, 2020).

Cocrystallization can also modulate photoluminescence attributes. For instance, S. Huang et al. (2019) synthesized phloretin-nicotinamide (Phl/Nic) and phloretin-isonicotinamide (Phl/Isonic) cocrystals, with strong photoluminescence from Phl/Nic cocrystal,

although the Phl/Isonic cocrystal and pure Phl show no photoluminescence. This contrasting behavior in optical properties resulted from different intermolecular interactions and structural arrangements between the coformers and Phl. Luminescent properties of organic crystals have attracted significant interest due to their applications in optic devices, including biosensors for food applications. Cocrystals are often reported as unstable under controlled humidity, dissociating into pure constituents (THAKURIA *et al.*, 2019; ZHANG *et al.*, 2019). and changing their optic attributes (e.g., fluorescence emission wavelength). Therefore, a possible application of polyphenol-based cocrystals with optic features for food products would be as moisture sensor that changes its fluorescent color according to the moisture content.

Mechanical properties can also be modulated by cocrystallization. Resveratrol cocrystals produced by He et al. (2017b) showed superior tabletability (*i.e.* tablet-forming ability) compared to pure resveratrol. Similar findings were observed for other polyphenols-based cocrystals as curcumin (WONG *et al.*, 2018) and methyl gallate (SUN; HOU, 2008). Tabletability and plasticity are directly correlated, low plasticity materials have poor tabletability. Cocrystallization could improve plasticity of powders, leading to better tabletability (DAI; CHEN; LU, 2018).

Recently, relevant advances have been achieved on clarifying the cocrystallization effect on biological properties of polyphenols. Xue et al. (2020) showed the mechanism of in vitro inhibition of α-glucosidase by gallic acid/p-aminobenzoic acid (Ga/Paba) and gallic acid/glycine (Ga/Gly) cocrystals. Combining NMR analysis and molecular docking to understand the mechanism of possible enzyme inhibition, the authors found that hydrogen bond interactions between cocrystal components remain after cocrystals solubilization, and they are essential for the inhibitory activity. The results showed that α-glucosidase inhibition rate depends on the cocrystal coformer; while Ga/Paba increased α-glucosidase inhibition related to pure gallic acid, Ga/Gly decreased it, which, according to molecular docking results, is related to the affinity of the cocrystals with α-glucosidade. Ga/Paba maintained a more potent and stable binding with amino acid residues inside the enzyme cavity, while Ga/Gly forms weaker interactions just near the cavity mouth. Additional *in vitro* α-glucosidade inhibitory essays and *in vivo* of hypoglycemic activity essays corroborate with the molecular docking models, showing the feasibility of the mechanisms proposed.

The possibility of modulating the inhibition of α-glucosidase and hypoglycemic activity opens new opportunities for polyphenol reseach since several other polyphenols have been

reported to present important metabolic effects, such as α-glucosidase inhibitory, antidiabetic, and antiglycation activities, which can be explored by cocrystallization (SUN *et al.*, 2020).

## 2.6 CONCLUSIONS AND FUTURE OUTLOOK

The production of polyphenol-based cocrystals was summarized considering the use of food-grade coformers, and it has been showed that cocrystallization can modulate desirable polyphenol properties, widening their application for food related products. A broad and inovative overview of the cocrystallization methods was presented, reveling that conventional methods, remarkeably slurry, grinding and evaporation are the most used technologies to produce various cocrystals. It has been also noted that most researchers have focused on the pharmaceutical properties of polyphenols and/or their use as an active pharmaceutical ingredient. Then, considering the tunable aspects related to polyphenol cocrystallization, widening its application for food products, alternative methods for cocrystals production, such as supercritical fluids to provide "green" cocrystals, were also addressed. Finally, this review contributes to a new approach, evaluating the potential of cocrystallization as a way to modulate the properties of polyphenols, in the context of application in food area. Thereby, an increasing interest for cocrystal potentials may stimulate further investigation for food products development.

## CHAPTER 3 PRODUCTION OF QUERCETIN-NICOTINAMIDE COCRYSTALS BY GAS ANTISOLVENT (GAS) PROCESS

This work aimed to invetigate the role of process variables pressure, temperature, and quercetin-to-nicotinamide ratio on the characteristics of quercetin/nicotinamide cocrystals obtained by gaseous antisolvent (GAS) method.

This chapter was published as an article in the peer-reviewed journal *The Journal of Supercritical Fluids*. Impact factor (2022): 4.577. According to Elsevier subscription rules, the authors retain the right to include the article in a thesis.

**Graphical abstract**
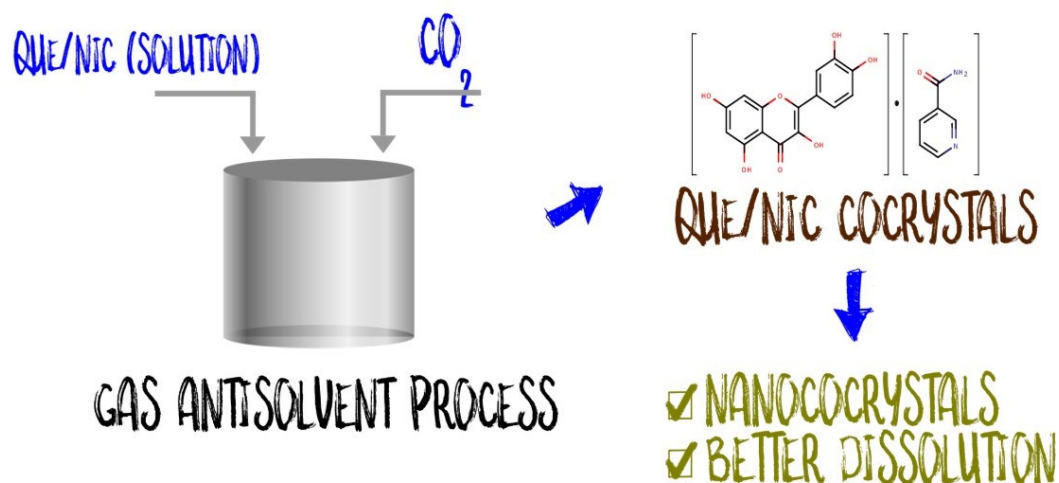
**Abstract**

Gas antisolvent (GAS), based on antisolvent feature of supercritical $CO_2$, was unlikely explored to obtain cocrystals of quercetin/nicotinamide (QUE/NIC). Cocrystallization is an emerging technique to improve physicochemical properties of active compounds such as quercetin. QUE/NIC cocrystals were prepared by GAS with acetone as solvent, and the resulting products were characterized by powder X-ray diffractometry (PXRD), differential scanning calorimetry (DSC), thermogravimetric analysis (TGA), Raman spectroscopy, scanning electron microscopy (SEM), high performance liquid chromatography (HPLC), and elemental analysis. GAS produced QUE/NIC cocrystals had higher dissolution performance, at pH of 1.2 and 6.8, compared to raw QUE, providing QUE release at least 2-times higher than raw QUE. These results indicate that GAS-processed QUE/NIC cocrystal is a promising solid formulation to improve quercetin's dissolution and bioavailability, with potential use in food and pharmaceutical applications.

## 3.1 INTRODUCTION

Quercetin (QUE) is a natural polyphenol synthesized by plants and an abundant micronutrient present in human diet. In nature, QUE is found as glycosides (conjugated to sugar moieties) or as aglycone. Quercetin aglycone is directly absorbed at the colon, while the glycoside form must be firstly deglycosylated by the colonic microbiota and then, absorbed as aglycone. Similar to other flavonoids, quercetin glycosides are generally more water-soluble than the aglycone form. However, the positive biological effects of quercetin on human health are predominantly attributed to the aglycone form (ALMEIDA *et al.*, 2018). Besides, studies have reported various biological activities associated to quercetin, such as antidiabetic (BULE *et al.*, 2019), anticancer (D'ANDREA, 2015), and anti-obesity effects (NABAVI *et al.*, 2015). However, quercetin has limited applications due to its low water solubility and subsequent poor bioavailability (MUKHOPADHYAY; PRAJAPATI, 2015). Therefore, much effort has been recently directed to overcome these issues. In general, studies have developed different release systems, including solid-lipid particles (ADITYA *et al.*, 2014), impregnated-polymer particles (GARCÍA-CASAS *et al.*, 2019), conjugated magnetic particles (RAJESH KUMAR *et al.*, 2014), among others. However, these systems also present several issues, including limited chemical and physical stability, low loading capability, residual organic solvent, toxicity, unknown safety, and/or constraints with regulatory aspects (WANG *et al.*, 2016).

Therefore, the cocrystallization rises as an emergent technique used to improve the solubility, dissolution rate, and bioavailability of different bioactive compounds. Cocrystals are crystalline solids formed by at least two types of molecules in the same lattice, the target-molecule and the coformer, in a stoichiometric ratio, and bonded by non-covalent intermolecular interactions, such as hydrogen bonds, halogen bonds, electrostatic interactions, π–π stacking, and van der Waals interactions. The modulated physicochemical properties strongly depend on the selected coformer, its physicochemical properties, and the crystalline lattice formed by the pair target-molecule/coformer. Usually, compounds most explored for use as cocrystal coformers are classified as GRAS (generally recognized as safe) because of their safety attributes to consumers (BERRY; STEED, 2017; DIAS; LANZA; FERREIRA, 2021).

Cocrystallization presents some advantages over formulation strategies usually applied to improve physicochemical properties of bioactive compounds, such as encapsulation and functionalization. The most remarkable advantages of cocrystallization, compared with traditional methods, are the improvement of active compound solubility/dissolution in biorelevant media; and the preservation of the molecular structure of chemical species. Once the cocrystallization does not involve structural modifications by chemical reaction, undesirable reactions that lead to inactive side products do not occur, i.e., cocrystallization preserves the biological activity of the components and, in some cases, improves their bioactivity (BOLLA; NANGIA, 2016) Besides, compared to the metastable free forms, such as amorphous phases, cocrystals are more stable due to their crystalline nature, with lower Gibbs free energy (BABU; NANGIA, 2011).

Despite the advantages reported, cocrystals are not a perfect approach for all materials and, depending on the system and cocrystallization method, they face diverse challenges such as physical instability, tendency to re-precipitation, residual organic solvent, and other drawbacks (KALE; ZODE; BANSAL, 2017). Thus, a bioactive formulation based on cocrystallization should be carefully studied to produce a final cocrystal which properly improves the physical properties of the original biocomponents.

There are numerous procedures used to prepare cocrystals, which can be mainly categorized as solvent-free or solution-based methods. The solvent-free methods involve the production of cocrystals by mechanical energy absorption, like dry grinding, liquid-assisted grinding, and hot-melt extrusion. Otherwise, the solution-based methods involve solution cocrystallization by supersaturation as the driving force; in this case, the solvent may affect the

cocrystal purity, polymorphic form, crystals size, and shape. This solution-based group comprises slow evaporation, antisolvent cocrystallization, slurry conversion, spray drying, among others (KARIMI-JAFARI *et al.*, 2018b; RODRIGUES *et al.*, 2018).

The above-mentioned methods often present drawbacks, such as low cocrystal conversion, scaling-up difficulties, thermal degradation, and excessive use of organic solvents. To overcome these limitations, processes based on supercritical $CO_2$ have been developed for cocrystals preparation due to the reduction in the organic solvent consumption, compared to classical methods. Besides, $CO_2$ is an eco-friendly solvent, innocuous, non-flammable, affordable, recyclable, and has accessible critical parameters (31.04 °C and 7.38 MPa) (CUADRA *et al.*, 2018).

Recently, researchers have shown an increasing interest in cocrystals obtained by gaseous antisolvent (GAS). This technique was initially developed as an alternative to micronize explosives (GALLAGHER *et al.*, 1989), and has shown a suitable alternative for formulating bioactive molecules (JAFARI *et al.*, 2015; KURNIAWANSYAH; MAMMUCARI; FOSTER, 2017; PHOTHIPANYAKUN; SUTTIKORNCHAI; CHAROENCHAITRAKOOL, 2013), and preparing cocrystals (KOTBANTAO; CHAROENCHAITRAKOOL, 2017; OBER; GUPTA, 2012; WICHIANPHONG; CHAROENCHAITRAKOOL, 2018a, 2018b), mostly due to the versatility in solvent selection, process similarities to conventional antisolvent, easy solid recovery, and ability to produce fine-tuned materials for particular applications (MACEACHERN; KERMANSHAHI-POUR; MIRMEHRABI, 2020). For GAS method, the compressed $CO_2$ is added to a solution containing the solutes (target molecule and coformer) until reaching the desired pressure. Then, $CO_2$ is incorporated into the liquid solvent, causing its expansion and decreasing the solvent power, which results in solute precipitation (PANDO; CABAÑAS; CUADRA, 2016).

GAS cocrystallization has some advantages compared to conventional methods. It is a rapid single-step process, and provides a tunable and versatile approach to produce cocrystals with different morphologies and particle sizes by adjusting operating parameters. Also, the thermal and mechanical stresses of the products are reduced, compared to mechanochemical processes. Furthermore, it reduced the use of organic solvent and minimizes the residual amount of solvent in the cocrystal when compared to some solution-based methods, such as liquid-antisolvent (OBER; MONTGOMERY; GUPTA, 2013)

Quercetin molecule **(Figure 3.1)** has five hydroxyl groups that can form intermolecular hydrogen bonds with various coformers. Particularly, quercetin presents a high tendency to form cocrystals with molecules with carbonyl and pyridyl groups, such as nicotinamide (NIC) **(Figure 3.1)** and its derivatives. Due to its high aqueous solubility and safety for humans, nicotinamide has been reported as a promising coformer (VASISHT *et al.*, 2016). Other therapeutic-relevant flavonoids, such as hesperetin (CHADHA *et al.*, 2017), fisetin, luteolin, genistein (SOWA; ŚLEPOKURA; MATCZAK-JON, 2013) were also cocrystallized with nicotinamide and its derivatives.

**Figure 3.1**-Chemical structures of quercetin and nicotinamide
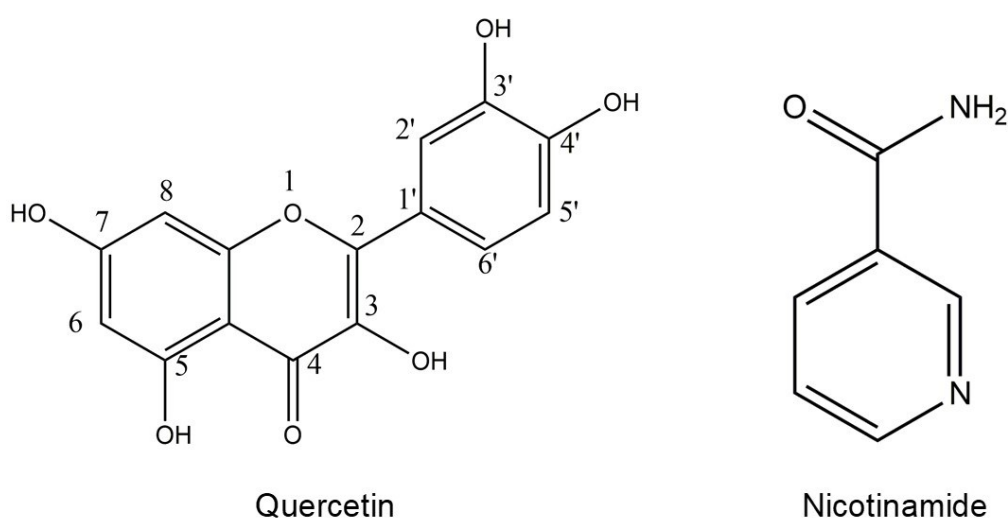


Quercetin cocrystals were successfully produced with some coformers, such as caffeine, theobromine, isonicotinamide (SMITH *et al.*, 2011), and isoniazid (LIU *et al.*, 2020). The first attempt to produced quercetin/nicotinamide (QUE/NIC) cocrystals was reported byVasisht et al. (2016) through liquid-assisted grinding, which improved the QUE dissolution profile, and also the antihaemolytic and antioxidant activities, compared to pure QUE. More recently, QUE/NIC cocrystals at 1:1 and 1:2 molar ratio were also prepared by Wu et al. (2020) using the slow evaporation method, and the produced cocrystals provided better dissolution and bioavailability performance compared to pure quercetin.

The above-mentioned studies support that improved quercetin dissolution and bioavailability could be achieved by cocrystallization, especially by means of supercritical processes. However, as far as we know, no previous study has investigated the use of GAS process for the production of quercetin/nicotinamide cocrystals. Therefore, the present research explores, for the first time, the effect of different processing parameters (temperature, pressure, and quercetin-to-nicotinamide molar ratio) on the production of quercetin/nicotinamide cocrystals by GAS, as a green alternative method to obtain bioactive/better-soluble cocrystals, with improved technological properties compared to traditionally produced cocrystal.

## 3.2 MATERIAL AND METHODS

### 3.2.1 Chemicals

All chemicals were purchased and used as received: quercetin (CAS No. 117-39-5, 98% m/m) from Chem-Impex International (Wood Dale, IL, USA); nicotinamide (CAS No. 98-92-0, 99% m/m) and dipotassium phosphate (CAS No. 7758-11-4, 98% m/m) from Vetec Sigma-Aldrich (Duque de Caxias, RJ, Brazil); monopotassium phosphate (CAS No. 7778-77-0, 98% m/m) and hydrochloric acid (CAS No. 7647-01-0, 37 % m/m) from Dinâmica (Indaiatuba, SP, Brazil); and acetone (CAS No. 67-64-1, 99.8% m/m) from Neon (Suzano, SP, Brazil); carbon dioxide (CAS No. 124-38-9, 99.9% m/m) from White Martins (São Paulo, SP, Brazil).

### 3.2.2 Cocrystallization by GAS process

The GAS assays were performed using a self-assembled high-pressure unit outlined and fully described by Pessoa et al. (2019). In short, this apparatus is composed by a 600 mL-volume stainless-steel vessel with two syringe pumps for $CO_2$ feeding, a set of ball valves, and two needle valves for flow rate control. Attached to the outlet valve, a PTFE-membrane filter (0.22 µm) linked to a polyethylene frit prevents material losses. Finally, a thermostatic bath maintains the $CO_2$ in the liquid phase while another one set the temperature in the high-pressure vessel.

Prior to processing (cocrystal formation by GAS method), solutions at various concentrations and molar ratios were ultrasonically prepared by dissolving QUE and NIC, simultaneously, in 35 mL of acetone (Ultronique Q3.0/37A, Ecosonics, Indaiatuba, SP, Brazil). For the 1:1 assays were used 302.23 mg of QUE and 122,2 mg of NIC, while for the 1:2 assays, 151,1 mg QUE and 122,2 mg of NIC were used. Then, each solution was filtered using a hydrophilic-PTFE syringe filter (0.45 µm). For each GAS assay, a different QUE/NIC solution was injected into the vessel, to evaluate the effect of different quercetin-to-nicotinamide molar

ratios. Cocrystallization was carried out by GAS method in four sequential steps: *(1) pressure equilibration*; *(2) system pressurization*; *(3) system stirring, and (4) product drying.*

   ***Pressure equilibration***: after the vessel assembly, to prevent pipe clogging due to the Joule-Thomson effect, $CO_2$ was slowly delivered into the vessel, with the outlet valve closed until the inside pressure equilibrates with $CO_2$ reservoir pressure (about 6 MPa). ***System pressurization***: compressed $CO_2$ (20 MPa) was continuously pumped into the vessel at a constant flow rate (10 mL·min$^{-1}$), under constant magnetic stirring, until reaching the processing pressure and temperature. ***System stirring***: as soon as the working pressure and temperature were reached, the $CO_2$ inlet valve was closed and the system was held stirring for 10 min, at constant working pressure and temperature, in order to better mix the phases, triggering the precipitation of cocrystals. ***Product drying***: Finally, with the outlet valve open, an additional amount of $CO_2$ (about 800 mL), at the same previous conditions of temperature and pressure, was continuously pumped into the vessel to remove the solvent possibly adsorbed in samples and present in the headspace above them. For reproducibility purposes, each cocrystallization procedure was performed in duplicate. The operational parameters evaluated for the cocrystallization were: temperature, of 35 and 45 °C; pressure of 8 and 10 MPa; and quercetin/nicotinamide ratio of 1:1 and 1:2 mol/mol. The level of the parameters was defined based on literature data (LONG *et al.*, 2021; NEUROHR *et al.*, 2013; PESSOA *et al.*, 2019; WICHIANPHONG; CHAROENCHAITRAKOOL, 2018b). Also, for all GAS assays, the solution volume and the $CO_2$ flow rate were kept constant.

### 3.2.3 Liquid antisolvent cocrystallization (LAS)

   The QUE/NIC solutions were prepared as reported at section 3.2.2, and added drop-wise in hexane (1:5 solution-to-hexane ratio), under stirring (500 rpm). Then, the suspensions (precipitates + mother liquor) were centrifugated at 3400 rpm for 10 minutes, and the supernatant was separated using a glass Pasteur's pipette. Wet precipitates were dried in dissector at room temperature. Finally, the produced samples were gently grounded using pestle and mortar, and sieved (200 mesh) to result a fine powder (KIM; YEO, 2015).

### 3.2.4 Cocrystal characterization

   The produced cocrystals were characterized and identified by the following techniques: powder X-ray diffractometry (PXRD), differential scanning calorimetry (DSC), thermogravimetric analysis (TGA), Raman spectroscopy, scanning electron microscopy (SEM), High performance liquid chromatography (HPLC), and elemental analysis.

The PXRD patterns were collected using a Rigaku MiniFlex600 powder diffractometer. Measurements were taken utilizing a copper X-ray source powered at 40 kV and 15 mA ($K_{\alpha1}$ 1.54059 Å), in θ-2θ scan mode. Scans were measured between 4°- 40° 2θ with a step size of 0.02° 2θ and with a scanning speed of 6°/min.

Differential scanning calorimetry (DSC) analyses were carried out on a differential scanning calorimeter (Jade DSC, Perkin Elmer, USA), outfitted with a 2P intracooler cooling system. Samples were placed in hermetic sealed aluminum pans, heated from 50 °C to 350 °C at a rate of 10 °C·$min^{-1}$, and under nitrogen flow (50 mL·$min^{-1}$). Thermogravimetric analysis (TGA) was performed on a TGA/DTG-60 equipment (Shimadzu, Japan), from 50 °C to 350 °C, at scan rate of 10 °C·$min^{-1}$, and under nitrogen flow of 100 mL·$min^{-1}$.

Raman spectral data were collected using a Raman spectrometer (Cora 5200, Anton Paar) with laser power at 450 mW and single wavelength at 785 nm. Powder samples were scanned from 100 to 2300 $cm^{-1}$ at spectral resolution of 2 $cm^{-1}$, and using an integration time of 5 s.

The morphology and the particle size distribution (PSD) of the produced cocrystals were analyzed by Scanning Electron Microscopy (SEM) using a JEOL JSM-6701 F microscope operating at 10 kV. Samples were mounted in stubs containing double-sided carbon tape and then gold-coated. For the construction of PSD, the length of particles (ca. >300) was measured from SEM images (x2500 magnification) using the ImageJ software (SCHNEIDER; RASBAND; ELICEIRI, 2012). The Rice estimator was used to calculate the number of bins on histogram charting (ALXNEIT, 2020). Number-based PSDs were constructed (**Figure A.10**), which enable the determination of the PSD parameters $d_{10}$, $d_{50}$, $d_{90}$, and span (HORIBA SCIENTIFIC, 2010; XU, 2014).

The QUE-to-NIC molar ratio in the processed powders was determined by HPLC, in a system coupled with photodiode array (PDA) detector (Shimadzu, Model Prominence LCMS-2020, Kyoto, Japan), providing an approximation for the cocrystal stoichiometry. Chromatography was performed on a Phenomenex Luna® C18(2) column (150 x 4.60 mm; 5,0 μm) using a mobile phase of aqueous phosphoric acid solution (0.1 %) and methanol, at 45:55 (v/v). A solid aliquot of each cocrystal sample (~15 mg) was dissolved in methanol (dilution factor: 10 times), filtered (0.22 μm), injected (10 μL) in the HPLC system at 30 °C, and eluted at 0.8 mL/min. QUE and NIC were detected at 254 nm, and the quantification was performed

using standard solutions prepared in methanol in suitable concentration range. For more details, please see supplementary data (**Figure A.2** and **Figure A.3**).

The QUE-to-NIC molar ratio from the processed powders was determined using CHN elemental analysis (PerkinElmer, model 2400 Series II) by calculating the relative percentage of carbon, hydrogen, and nitrogen in the materials.

### 3.2.5 Dissolution Studies

The dissolution profile of the cocrystal samples was evaluated based on the works by Zhu et al. (2017) and Pessoa et al. (2019), with minor modifications. The dissolution media used were potassium phosphate buffer (pH 6.8, 0.05 M) and 0.1 M HCl solution (pH 1.2). Samples (10 mg) were suspended in 100 mL of each simulating media at $37 \pm 0.5\ °C$, in 250-mL Erlenmeyer flasks incubated in a Dubnoff-type shaker (100 rpm). Liquid aliquots (2 mL) were withdrawn at scheduled time intervals (5, 10, 15, 20, 30, 40, 50, 60, 90, 120, 150, 180 min) and filtered through 0.45 μm hydrophilic-PTFE syringe filters. Immediately after each aliquoting, the same volume of fresh media (2 mL) was added to Erlenmeyer to keep constant volume of the dissolution system. The quercetin content from the collected samples was quantified spectrophotometrically at 366 nm using a microplate multi-reader (Tecan, Model Infinite M200). For quantification, a quercetin standard curve was prepared (**Figure A.1**). The dissolution profile of the cocrystals was performed in duplicate and the results expressed as concentration of quercetin released over time.

### 3.2.6 Statistical analysis

One-way analysis of variance (ANOVA) followed by Tukey's *post hoc* test was used to determine significant differences between yield means ($p < 0.05$). Besides, the Kruskal–Wallis test, followed by Dunn's test were also applied to evaluate statistical differences between the particle size ($d_{50}$) distributions obtained from different processing conditions ($p < 0.05$). Statistical analyses were performed with Minitab 17™ (Minitab Inc., State College, PA, USA).

## 3.3 RESULTS AND DISCUSSION
### 3.3.1 Cocrystallization by GAS process

Theoretically, for the feasibility of cocrystal production by GAS method, the target molecule and the coformer should be practically insoluble in the antisolvent ($CO_2$) and in the

mixture antisolvent/solvent, whilst soluble in the neat solvent. Comparing the parent components, while QUE is relatively less $CO_2$-soluble ($10^{-6}$ to $10^{-5}$ mole fraction) (FRANCO *et al.*, 2018), NIC is considerably more $CO_2$-soluble ($10^{-5}$ to $10^{-3}$ mole fraction) (KOTNIK; ŠKERGET; KNEZ, 2011).

Also, significant differences on the solubility of the components in a specific solvent could be deleterious to cocrystal formation by GAS method, once the less soluble reactant could precipitate first, impairing the cocrystallization process. Furthermore, the selected solvent should dissolve the materials (target component and coformer) in appropriate amount, ensuring good yield and productivity for the produced cocrystal. However, the higher is the solubility in a specific solvent at room pressure/temperature, higher is the chances for the components to be significantly soluble in the antisolvent/solvent mixture (i.e., $CO_2$ + an organic solvent), compromising the cocrystallization feasibility by GAS process. In this context, and based on solubility values reported at the literature for QUE and NIC in different organic solvents (ALESSI *et al.*, 2012; OUYANG *et al.*, 2018), we initially selected ethanol and acetone as solvent to perform the QUE/NIC cocrystallization by GAS method. The QUE solubility in ethanol and acetone is $3x10^{-4}$ and $5x10^{-5}$ molar fraction, respectively, while the NIC solubility in these solvents is $4.4x10^{-2}$ and $1.9x10^{-2}$ molar fraction, respectively (ALESSI *et al.*, 2012; OUYANG *et al.*, 2018).

For the GAS method, the use of acetone as solvent was more adequate than ethanol for processing of QUE/NIC cocrystals, once for ethanol, the PXRD analysis of the final product detected only pure QUE or QUE with few traces of NIC (~14.86 2θ) (**Figure A.4**). This may be explained by the GAS-ethanol behavior, which indicates a severe NIC loss during processing due to its considerable solubility in the supercritical mixture ($CO_2$ + ethanol). Also, according to our previous work by BALBINOT FILHO et al. (2021), it is demonstrated that the $CO_2$ triggered the precipitation of QUE and NIC from the ethanolic solutions, which occur at different $CO_2$ molar ratios, i.e., QUE precipitates at lower $CO_2$ concentrations compared to NIC. This means that during filling the vessel with $CO_2$ in GAS processing, QUE precipitates first, making it no longer available to bind with NIC, which could also explain the non-formation of cocrystals from ethanolic solution showed at **Figure A.4**. Besides, low precipitation yields are frequently reported in literature when using ethanol as the solvent (MUNTÓ *et al.*, 2008; SUBRA-PATERNAULT *et al.*, 2007). Therefore, acetone was the selected solvent for GAS method, because QUE and NIC would be probably less soluble at the

supercritical mixture ($CO_2$ + acetone), compared to ethanol. Besides, successful cocrystallizations employing acetone as solvent and NIC as coformer have already been reported (NEUROHR *et al.*, 2013; WICHIANPHONG; CHAROENCHAITRAKOOL, 2018b).

In principle, processing variables such as pressure, temperature, stirring rate, and type of solvent can affect the characteristics of the GAS precipitated materials. Pressure, temperature and the components ratio (target-to-coformer) have been reported as the most critical variables because of their ability to produce polymorphs and/or new cocrystals (CUADRA *et al.*, 2018; RODRIGUES *et al.*, 2016; SAMIPILLAI; ROHANI, 2019; TUMANOVA *et al.*, 2018), which could exhibit distinct physicochemical properties, affecting the product functionalities and applications. Considering this, the effects of pressure, temperature and QUE-to-NIC ratio on the GAS cocrystals characteristics were evaluated. The GAS assays were carried out at different conditions of pressure, temperature, and QUE-to-NIC ratio (section 3.2.2), defining the experiments conducted at near or above the binary system ($CO_2$ + acetone) critical point (CHANG *et al.*, 1997). These conditions can provide particles with different solid characteristics, such as morphology, size and size distribution, as result of differentiated mass transport, nucleation and crystal growth (LIU; LI; DENG, 2021). Besides, at these conditions, acetone presents abrupt reduction in solvation power due to the large liquid-phase volumetric expansion, inducing solid precipitation (SU, 2012).

The total yield values of processed cocrystals, particle sizes ($d_{10}$, $d_{50}$ and $d_{90}$), and span, according to the conditions of temperature, pressure and QUE-to-NIC ratio, are presented in **Table 3.1**. The assays conducted with 1:1 QUE-to-NIC ratio (runs #1- #4) show that pressure and temperature had almost no effect on yield, only assay #4 (10 MPa/45°C) showed a yield statistically significant different from other assays ($p<0.05$). The lower yield value from assay #4, compared to the other assays with 1:1 QUE-to-NIC ratio, may be probably due to: (1) higher solubilization of QUE and/or NIC in the supercritical mixture $CO_2$ + acetone at higher temperatures, which reduces the amount of precipitated material; (2) re-solubilization of the cocrystal in $CO_2$ + acetone and/or in pure $CO_2$ during the pressurization and/or drying step, respectively.

**Table 3.1** - Operational parameters (temperature, pressure, and QUE/NIC ratio) used at GAS assays for the productions of QUE/NIC cocrystals, and the yield, particle size and span results.

| Assay[1] | Pressure (MPa) | Temperature (°C) | QUE-to-NIC ratio (mol) | Yield (%)[2,4] | $d_{10}$ (nm) | $d_{50}$ (nm)[4] | $d_{90}$ (nm) | span |
|---|---|---|---|---|---|---|---|---|
| #1 | 8 | 35 | 1:1 | 68.9[a] ± 2 | 73.3 | 280.3[d] | 885.2 | 2.9 |
| #2 | 8 | 45 | 1:1 | 65.6[ab] ± 5 | 51.9 | 112.1[bc] | 385.4 | 3.0 |
| #3 | 10 | 35 | 1:1 | 69.1[a] ± 3 | 79.7 | 143.2[e] | 535.2 | 3.2 |
| #4 | 10 | 45 | 1:1 | 51.0[c] ± 3 | 54.4 | 121.1[b] | 402.8 | 2.9 |
| #5 | 8 | 35 | 1:2 | 55.5[abc] ± 1 | 42.5 | 96.3[ac] | 360.0 | 3.3 |
| #6 | 8 | 45 | 1:2 | 50.9[c] ± 4 | 52.0 | 114.1[bc] | 493.8 | 3.9 |
| #7 | 10 | 35 | 1:2 | 52.9[bc] ± 3 | 42.5 | 87.8[a] | 331.7 | 3.3 |
| #8 | 10 | 45 | 1:2 | 52.2[bc] ± 5 | 52.2 | 110.6[bc] | 343.9 | 2.6 |

[1] For all assays (runs) the solution volume and the $CO_2$ flow rate were kept constant. [2] Mean values (n=2) followed by the same superscripts do not differ from each other using Tukey´s test (p<0.05). [3] Yield = (collected amount/initial amount) x100. [4] Obtained from particle size distributions (Fig. S8, Supplementary data), median particle sizes ($d_{50}$) sharing the same letters does not differ statistically (p<0.05, Kruskal-Wallis test).

The effect of the process variables on yield is not easily defined because it depends on the solubilities of the pure components and the formed cocrystal. Probably, the relationship between the solubilities of the materials in the range of pressure and temperature studied works in "teeter-totter" fashion, i.e., the decreasing in solubility experienced by one of the components is followed by approximated equal increase in solubility, resulting in almost equal yield, however, this supposition should be validated with further work to determine the solubility of the components in $CO_2$+acetone. Also, the solubility of a target-molecule in presence of a coformer can be different than that of the pure target-molecule (REVELLI *et al.*, 2014), bringing complexity the thermodynamics behavior of the cocrystallization process, and should be further investigated. Similarly, to 1:1 assays, pressure and temperature had no effect on the yield for the assays carried out at 1:2 QUE-to-NIC ratio (runs #5- #8).

Considering the QUE-to-NIC ratio, the yield decreases by reducing the QUE amount, i.e., assays performed with 1:1 ratio (#1- #4) presented higher yield than using 1:2 ratio (runs #5- #8). Probably, because the feed solution is more diluted at 1:2 ratio (see section 2.2), compared to 1:1 ratio, which reduces the initial supersaturation, for the same $CO_2$ amount, therefore, less cocrystal precipitation is expected. Besides, the growth of smaller particles is favored, as can be seen at **Table 3.1**. Diluted solutions can also promote the growth of small particles, even lower than the cut-off size of the filter of the unit (220 nm), due to increase in nucleation instead of crystal growth, resulting in particle loss and consequently decreasing the yield (AMANI; SAADATI ARDESTANI; MAJD, 2021).

Pressure and temperature showed considerable effect on particle size mostly at 1:1 QUE:NIC ($d_{50}$, **Table 3.1**). At this ratio, the increment in temperature at constant pressure produced smaller particles, contrasting with some previous reports related to GAS-produced particles (AMANI; SAADATI ARDESTANI; MAJD, 2021; ESFANDIARI; GHOREISHI, 2015). According to Roy et al. (2011), temperature has a complex effect on particle size, acting in phase equilibrium behavior, solubility, supersaturation degree, and nucleation/growth rates, which may explain the diverse trends of temperature effect observed in literature. Some works have demonstrated that the increment in temperature can promote size reduction (PARK; YEO, 2008), size increment (YEO; LEE, 2004), or negligible effect given specific temperature range (CHANG; TANG; CHEN, 2008). The increase in pressure, at constant temperature, on the other hand, reduced the particle size ($d50$, **Table 3.1**). This result was similar to obtained by Esfandiari and Ghoreishi (2013), who studied the GAS precipitation of 5-Flourouracil with

$CO_2$. The pressure increases augment the $CO_2$ density, which enhances $CO_2$ solubility in organic solvents such as acetone (CHIU; LEE; LIN, 2008). Consequently, the liquid expansion is higher and the supersaturation state required to initiate particle precipitation occurs faster, favoring the nucleation mechanism and the growth of smaller particles (AMANI; SAADATI ARDESTANI; MAJD, 2021).

The QUE-to-NIC ratio affected more significantly the particle size of the produced cocrystals compared to the variation in pressure and temperature. Generally, at 1:1 ratio, the particles sizes and the variability between the samples were larger compared to 1:2 ratio. Using 1:1 ratio, the particle sizes ($d_{50}$) varied from 112.1 to 280.3 nm. Otherwise, for 1:2 ratio, smaller particles were produced (87.8-114.1 nm), and it can be related to the fact that the starting solution is more diluted, which increases nucleation instead of crystal growth. Besides, the span value, a measure of PSD homogeneity, was relatively high for all conditions studied (2.6 – 3.3). Smaller span values, typically lower than 1 indicate narrower particle size distributions (TRANG *et al.*, 2019).

As a drawback, the production of QUE/NIC cocrystals may also result in a wide variety of unwanted solid forms, not cocrystallized ones, such as QUE and NIC homocrystals, solvates, polymorphs, and their physical mixtures. Therefore, the analysis of the effect of processing parameters on the cocrystal yield must be associated with the identification and characterization of the produced cocrystal.

### 3.3.2 Characterizations of the produced cocrystals

*3.3.2.1 Powder X-ray diffractometry (PXRD)*

The PXRD analysis of the produced samples was carried out to evaluate the formation of the cocrystallized phases, due to the absence of single crystals. The resulting diffractograms were compared with those obtained for the pure components (QUE and NIC), where the presence of new diffraction peaks suggests cocrystallized phase. Then, the PXRD analysis for the commercial pure components and for the GAS-processed pure samples were evaluated to detect possible phase transitions to polymorphic and/or solvated forms induced by the GAS processing.

Wiscons and Matzger (2017) recommend tracking the possible phase transitions in the parent materials caused by the processing, to ensure that a significant number of differentiating peaks are present in the cocrystal sample, avoiding misinterpretation and misconclusions about

the cocrystal formation. In fact, QUE samples processed by GAS showed different diffractograms compared with the commercial sample (Fig. S3, Supplementary data), indicating that QUE suffer phase transition induced by the GAS processing. According to Borghetti et al. (2012), QUE presents different heat-interconvertible hydrated forms (pseudopolymorphs), and a comparison with the main diffraction peaks from the GAS-processed samples (4.66, 8.46, 14.2, and 26.8° $2\theta$), a clear phase transition is detected from dihydrated toward a mixed hydrated/anhydrous form, and can be attributed to the $CO_2$ drying effect. Despite that, GAS processing consistently produces the same solid QUE, for all conditions studied (**Figure A.5**), which were different than the commercial sample. Therefore, the cocrystal samples (QUE/NIC) were compared with QUE sample produced by GAS, rather than the commercial QUE. On the contrary, NIC samples show no phase transition attributed to GAS processing (**Figure A.6**), i.e., the commercial and the GAS-processed samples are essentially represented by polymorph I (the most stable NIC polymorph) (LI, X. *et al.*, 2020). This behavior has been previously reported for several $CO_2$-based processes at different conditions (CUADRA *et al.*, 2016; NEUROHR *et al.*, 2013; PESSOA *et al.*, 2019).

The PXRD patterns for the GAS processed QUE and NIC are compared with the samples of the produced cocrystal, at different GAS conditions, and shown at **Figure 3.2**. The cocrystals produced by GAS with acetone show diffraction peaks at 6.06, 7.14, 7.92,12.2,13.9, 15.92, 24.85, and 28.04° $2\theta,$ which cannot be attributed to the individual components. This behavior evidences the cocrystal formation because PXRD patterns are "fingerprints" of the crystal structures, representing the d-spacings between lattice planes formed by the molecules that form the cocrystal (PINDELSKA; SOKAL; KOLODZIEJSKI, 2017). The diffractograms from the different cocrystal processing runs are very similar, suggesting that, within the studied conditions, pressure, temperature and QUE-to-NIC ratio have no effect on the type of cocrystal produced.

Also, the PXRD patterns of the GAS-processed cocrystals are different from literature data for QUE/NIC cocrystals (PATIL; CHAUDHARI; KAMBLE, 2018; VASISHT *et al.*, 2016; WU *et al.*, 2020) obtained by liquid-assisted grinding, electrospraying, and slow evaporation, showing various peaks with diverse intensities at different diffraction angles. For instance, the pattern reported by Vasisht et al. (2016) for a 1:1 QUE/NIC cocrystal has characteristic diffraction peaks at 4.5, 8.8, 13.91, and 16.25°. While the pattern reported by Wu et al. (2020), also for a 1:1 cocrystal, exbibit characteristic diffraction peaks at 8.1, 8.9, 11, 14.1,

15.1, 17.7,18.8 and 19.8°. This behavior may indicate the processing influence on cocrystal characteristics because, also, the literature PXRD data for QUE/NIC cocrystals are different for each production methods used to provide the cocrystals. This suggest that the QUE/NIC cocrystal produced by GAS (the present work) may represent a new type of cocrystal, probably at 1:1 stoichiometry, as discussed at section 3.3.
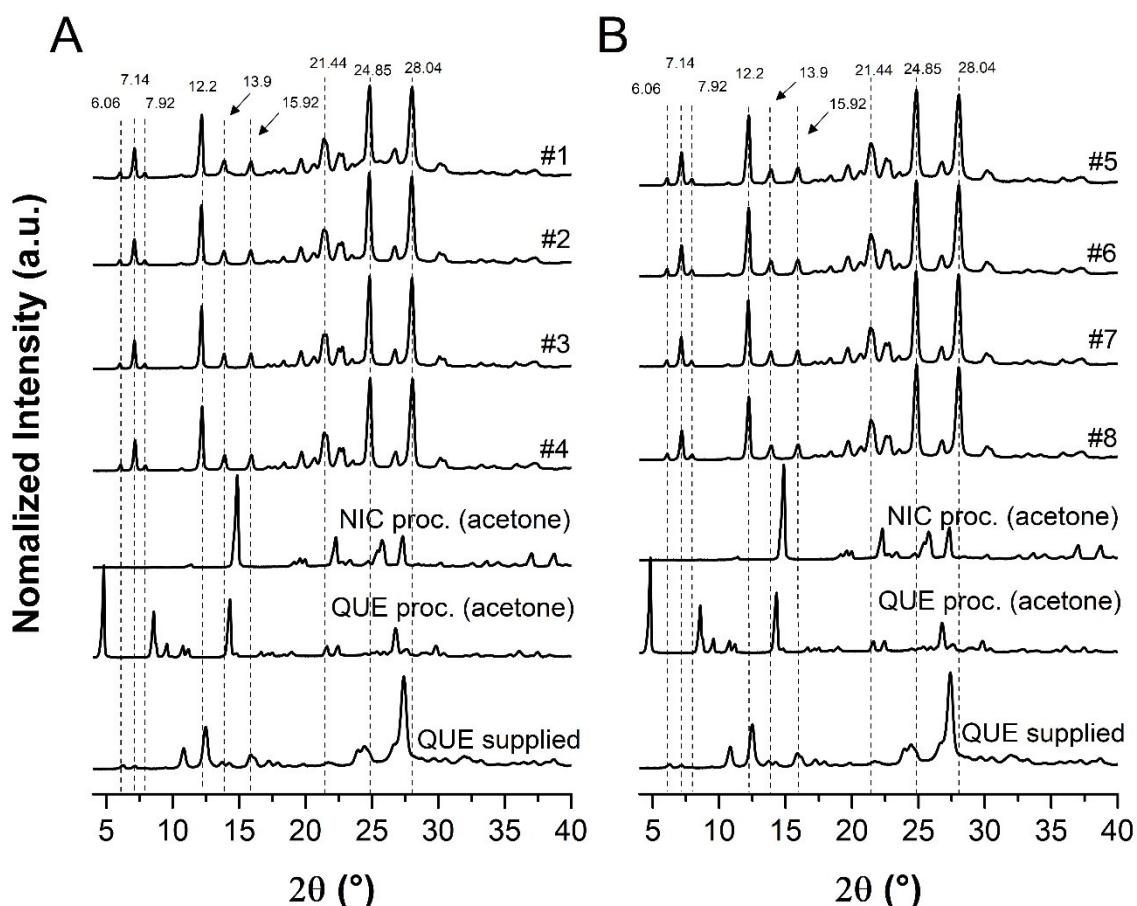


**Figure 3.2** - PXRD patterns of GAS-processed QUE and NIC samples and the formed cocrystals. (A) Samples processed with 1:1 QUE-to-NIC molar ratio (runs #1 - #4); (B) Samples processed with 1:2 QUE-to-NIC molar ratio (runs #5 - #8).

*3.3.2.2 Differential scanning calorimetry (DSC) and Thermogravimetric analysis (TGA)*

The samples were also thermally characterized by DSC. The melting points were determined by measuring the onset temperature of the peaks. The melting point of the pure components processed by GAS were compared with the produced cocrystals (**Figure 3.3A-B**). The pure components melting points match with literature data of 316 °C and 129°C for quercetin and nicotinamide (polymorph I), respectively (LI, X. *et al.*, 2020; WU *et al.*, 2020).
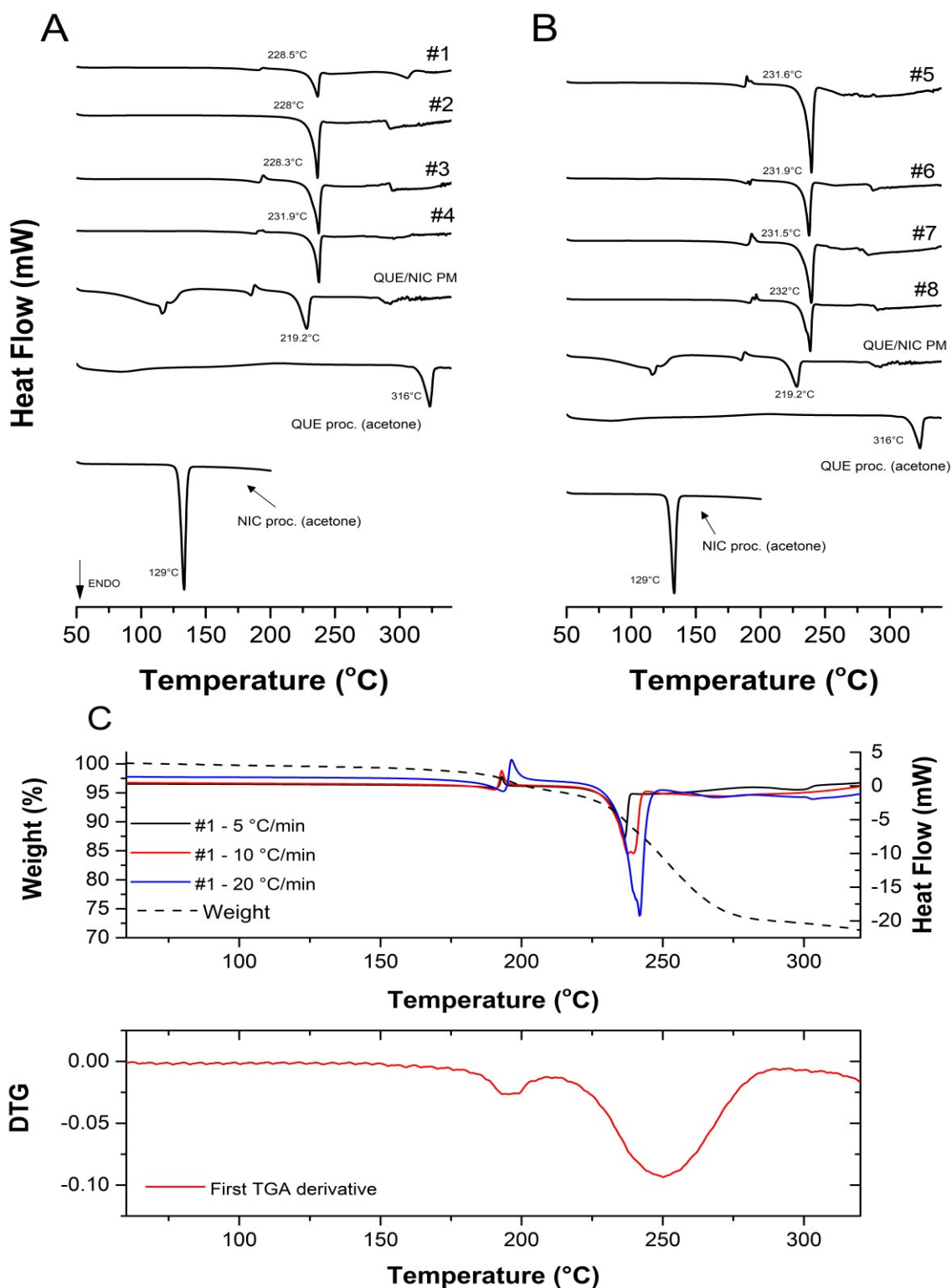
**Figure 3.3** - Thermal analysis of the GAS-processed QUE, and NIC; 1:1 physical mixture (QUE/NIC PM) and the formed cocrystals. (A) DSC runs of samples processed at 1:1 QUE-to-NIC molar ratio (runs #1 - #4); (B) DSC runs of samples processed at 1:2 QUE-to-NIC molar ratio (runs #5 - #8). (C) DSC runs of sample #1 at different heating rates and correspondent thermogravimetric analysis (TGA).

The distinct melting points of the cocrystal samples (~228-232°C), compared with the pure components, NIC (129°C) and QUE (316°C), suggest the formation of new crystalline phases, confirming a possible cocrystallization. The melting points of GAS-processed samples were very close to the published 1:1 cocrystals reported by Vasisht et al. (2016) (234.7) and Wu et al. (2020) (231.8 °C), which may indicate a possible polymorphic relationship between these phases, which should be investigated in future works.

Besides, DSC curves of the cocrystal samples did not present low- temperature thermal events indicating desolvation or dehydration, i.e., the samples are solvent-free particles. Additional DSC runs at different heating rates and using pin-holed pans, as well as thermogravimetric assay (**Figure 3.3C**), confirm the absence of hydrated phases (raw QUE) in the cocrystal powders. Besides, the physical mixture of QUE and NIC (1:1 molar ratio) was also evaluated by DSC, and the resulting curve (**Figure 3.3A**) showed an endothermic event at 219.2 °C, which is probably due to eutectic formation during DSC heating, as well documented in the literature (CHERUKUVADA; GURU ROW, 2014; RAJBONGSHI *et al.*, 2018). Finally, the thermic events related to the formation of cocrystals assessed by DSC (~228-232°C) corroborate well with PXRD data.

### 3.3.2.3 Raman spectroscopy

Raman spectroscopy is an important tool to investigate cocrystals formation because it is sensible to detect modifications in packing and intermolecular interactions at the solid structure. The recorded spectra detected possible intermolecular forces between QUE and NIC, which may be responsible for QUE/NIC cocrystal formation. As expected, all samples showed similar spectra (**Figure A.7**). For instance, the spectra for run #1, compared to GAS-processed QUE and NIC, are shown at **Figure 3.4**, where the QUE main bands are related to (C4=O) stretching (1660 cm$^{-1}$), (C2=C3) stretching (1616 cm$^{-1}$), and phenyl and benzo rings (C=C) stretching (1595 and 1561 cm$^{-1}$). The bands at 1500 and 1300 cm$^{-1}$ describe a set of coupled vibrational modes of (C=C) stretching and in-plane (C-H) and (C-OH) bending (BORGHETTI *et al.*, 2012; CORNARD; MERLIN, 2002). The NIC spectrum showed a very strong band at 1043 cm$^{-1}$ assigned to the pyridine ring in-plane bending. Also, medium intensity bands are present at 1392, 1597, 1616, and 1677 cm$^{-1}$, corresponding to Amide III, pyridine ring stretching, Amide II, and Amide I vibrations, respectively (CASTRO *et al.*, 2013).
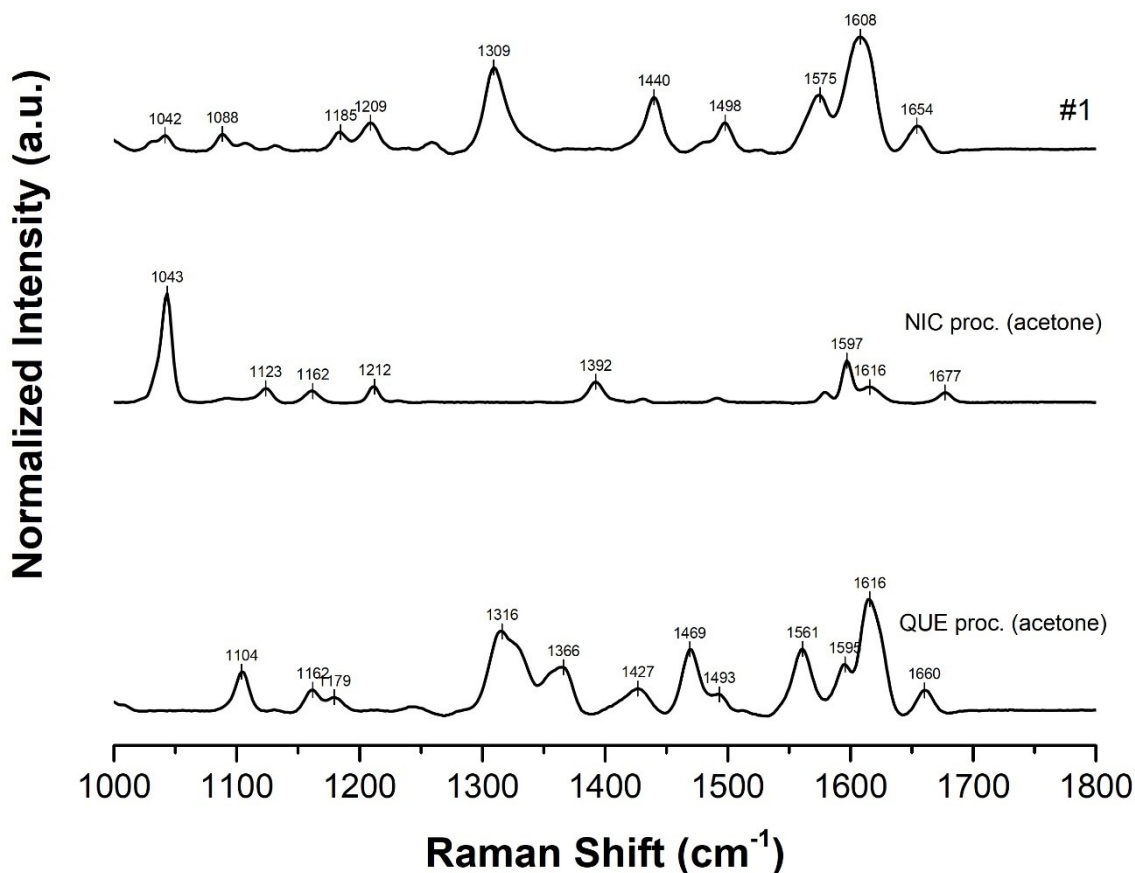
**Figure 3.4** - Raman spectra of run #1 and GAS-processed QUE and NIC samples.

As expected, some peaks from run #1 showed slight differences in positions, intensities and peak shapes compared to the starting materials. The most significant changes were observed at stretch vibration of C=O group of QUE (red-shifted from 1660 to 1654 cm$^{-1}$) and of amide, from NIC spectrum (1677 cm$^{-1}$), which was extinguished at run #1. These phenomena may occur due to the intermolecular carbonyl-amide interactions between QUE and NIC. Also, comparing NIC and run #1 spectrum, a remarkable decrease in peak intensity at 1043 cm$^{-1}$ (pyridine ring in-plane bending) was noted, suggesting that the NIC pyridine ring would be involved in molecular interactions at the cocrystallized product. In fact, structural studies by single-crystal XRD have reported similar interactions between flavonoids cocrystallized with pyridinecarboxamides as nicotinamide and isonicotinamide (SMITH *et al.*, 2011; SOWA; ŚLEPOKURA; MATCZAK-JON, 2013).

*3.3.2.4 Product morphology*

SEM images of the commercial QUE and NIC, the physical mixture, and the cocrystal samples produced by GAS by three different assays (run #1, #4 and #5) are given at **Figure 3.5.**

The SEM analysis showed that the morphology of the GAS cocrystals **(Figure 3.5d-f)** differs from those of the parent components **(Figure 3.5a-b)**, suggesting a different solid material, much probably a cocrystal. Although straight conclusions about cocrystal formation cannot be given by analyzing solely the SEM morphology, these results, alongside with PXRD, DSC and Raman analysis (sections 3.2.1-3.2.3), aid to a better characterization of the product (cocrystals formed by GAS method). The cocrystal samples **(Figure 3.5d-f)** had a needle-shaped morphology with noticeable particle agglomeration. The agglomerated cocrystal particles showed sizes ranging from 10 μm to several hundred of micrometers, as supported at the Supplementary material (**Figure A.8a-c**). In contrast, QUE (**Figure 3.5a**) had irregular flake-like structures, NIC (**Figure 3.5b**) featured block-shaped particles, and the particles on physical mixture (**Figure 3.5c**) were consistent with the simple mixture of pure components.
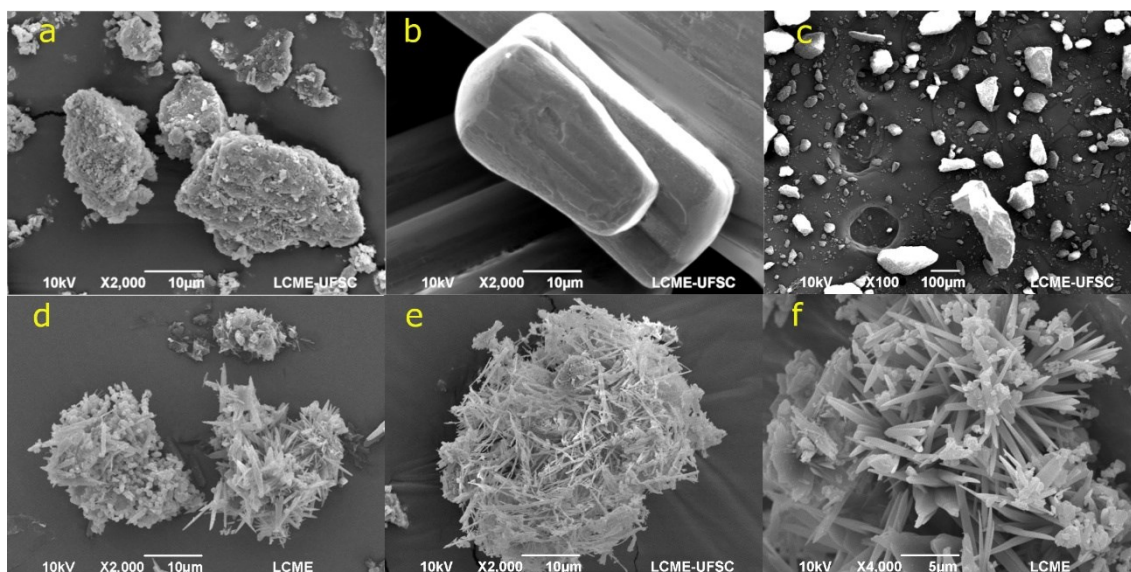


**Figure 3.5** - SEM images of (a) commercial QUE, (b) commercial NIC, (c) (1:1) physical mixture of QUE and NIC, (d) run #1, (e) run #4, (f) run #5.

*3.3.2.5 The effect of processing parameters on the cocrystallization outcome*

Collectively, X-ray diffraction, calorimetric and spectroscopic data indicate that the processing parameters, within the range evaluated, does not play a significant role in the cocrystal characteristics, i.e., the same crystalline product is produced regardless the pressure or temperature used for its production. Comparing the fed QUE-to-NIC ratio with that from the processed samples, after GAS processing (**Table 3.2**), the HPLC data suggest that all samples changed their ratio to 1:1 QUE-to-NIC. Also, the values of percentage of carbon, hydrogen, and nitrogen determined for all samples (**Table 3.2**), are consistent with the calculated values for 1:1 QUE:NIC (considering $C_{21}H_{16}N_2O_8$: C: 59.43%; H: 3.80%; N: 6.60%). These results suggest that the cocrystal formed has a 1:1 stoichiometry.

The fundamental challenges in determining the stoichiometry of GAS-processed samples are related to the changes in the final powder composition due to material loss and to precipitation of non-cocrystallized precursors, which may result in excess of starting materials at the final powder, complicating the stoichiometry determination. To circumvent this issue, an assay using liquid antisolvent (LAS) (section 3.1.1.3.) was performed to reproduce the QUE/NIC cocrystal obtained by GAS. LAS process may enable centrifuge separation of cocrystallized product from the solubilized precursors, increasing the sample purity and contributing to stoichiometry determination. However, comparing PXRD results from LAS samples (**Figure A.9**, **Table A.2**) with GAS samples (**Figure 3.2**), no similarity was detected, indicating that GAS method may have produced a cocrystal different from LAS.

The results of X-ray diffraction, calorimetric, spectroscopic, and powder composition were well reproducible within the GAS samples. Also, the absence of pure cocrystal formers on the GAS samples were confirmed by PXRD, DSC, and TGA. Therefore, it seems plausible that the QUE-to-NIC ratio from the final powder is in proximity to the stoichiometry suggested for the cocrystal (1:1). Still, for unequivocal determination of the cocrystal stoichiometry, allied with complete structural evaluation, advanced crystallographic analysis, such as single-crystal diffraction, PXRD along with NMR-crystallography, or synchrotron X-ray powder diffraction (synchrotron-PXRD) must be further used.

**Table 3.2** - Operational parameters evaluated in the GAS experiments and the summary of the results for quercetin content in the samples.

| Assay[1] | Pressure (MPa) | Temperature (°C) | Fed QUE:NIC ratio (mol:mol) | QUE:NIC ratio on powders (mol:mol)[2] | Elemental analysis[3] |
|---|---|---|---|---|---|
| #1 | 8 | 35 | | 1:1.06 | C: 58.78%; H: 3.66%; N: 5.79% |
| #2 | 8 | 45 | | 1:0.90 | C: 58.90%; H: 3.74%; N: 6.36% |
| #3 | 10 | 35 | 1:1 | 1:0.95 | C: 58.98%; H: 3.72%; N: 6.23% |
| #4 | 10 | 45 | | 1:0.94 | C: 58.89%; H: 3.69%; N: 6.33% |
| #5 | 8 | 35 | | 1:1.01 | C: 58.77%; H: 3.62%; N: 6.75% |
| #6 | 8 | 45 | | 1:1.05 | C: 58.96%; H: 3.69%; N: 6.66% |
| #7 | 10 | 35 | 1:2 | 1:1 | C: 58.65%; H: 3.55%; N: 6.78% |
| #8 | 10 | 45 | | 1:0.96 | C: 59.12%; H: 3.70%; N: 6.63% |

[1] For all runs the solution volume and the $CO_2$ flow rate were kept constant. [2] Quantified by HPLC-PDA. [3] Calculated for 1:1 QUE:NIC ratio ($C_{21}H_{16}N_2O_8$): C: 59.43%; H: 3.80%; N: 6.60%.

Complete structural evaluation of cocrystals produced by supercritical methods is challenging. According to Pando, Cabañas, and Cuadra (2016), new cocrystals should firstly be prepared by conventional methods, for then be reproduced by supercritical methods, then, the production of GAS samples, without previous conventional data, is a challenge. Because the chemical environment in supercritical state may modify the crystal lattice (ROY *et al.*, 2011), the synthesis of supercritical-based single-crystals from the cocrystals is arduous, even using supercritical-produced powders as seeds. Only very recently a single-crystal from a cocrystal was produced at supercritical conditions (VAKSLER *et al.*, 2021), where high quality mefenamic acid/nicotinamide single-crystal was successfully produced, enabling the cocrystal structure determination by single-crystal diffraction, avoiding the use of synchrotron-PXRD.

Besides, once supercritical methods produce powdered micronized materials, powder-based crystallographic methods as synchrotron-PXRD can be an alternative to structure elucidation, despite the limited access to synchrotron facilities (only about 70 synchrotron facilities around world) (LIGHTSOURCES.ORG, 2022). Finally, PXRD associated with NMR-crystallography seems be the best alternative, since these analyses are more common and feasible. Therefore, PXRD associated with NMR-crystallography analysis should be recommended for validation studies.

### 3.3.3 Dissolution studies

The quercetin stability in cocrystal form, and the ability of the cocrystal to maintain high concentration of quercetin at gastrointestinal environment were evaluated through dissolution assays conducted at different pH values (section 3.2.5). Dissolution profiles obtained at pH 1.2 and 6.8 are shown at **Figure 3.6.** The cocrystal samples showed higher dissolution rates, for both pH values, compared to pure QUE. For instance, in acid medium (pH 1.2), samples #1 and #5 released about 2-times higher amount of QUE than raw QUE powder at 180 min. At pH 6.8, a similar release profile was also observed for sample #1, which promoted an increment of 2.3-fold in QUE content compared to pure QUE at 180 min, while sample #5 showed a relative high increment in the first 20 min (1.7 times), but followed by successive slight concentration decreases until reaching a concentration correspondent to an increment of about 1.3-fold (180 min).

Slight differences in the dissolution rate and the amount of released QUE by samples #1 and #5 can be attributed to differences between the particle size distributions. In general, smaller particles promote higher amount of dissolved solute. On the contrary, sample #5 had lower dissolution performance compared to sample #1, even with smaller particles ($d_{50}$ 96.3 vs 280.3 nm). Unfortunately, excessive size reduction does not only increase the amount of dissolved solute, but also increase the supersaturation degree, the driving-force for solute precipitation, reducing the dissolution. This behavior has been frequently reported, where the proposed methods to overcome this drawback may include the addition of polymers and surfactants into cocrystals powders, to inhibit solute precipitation by reducing nucleation from bulk solution (HUANG, Y. *et al.*, 2019; RODRÍGUEZ-RUIZ *et al.*, 2022; SALAS-ZÚÑIGA *et al.*, 2019; ZHENG *et al.*, 2019). In the same vein, highly soluble cocrystals, such as formed by very small particles, can catalyze solute precipitation by powder surface nucleation, which shortens the

onset crystallization time for cocrystal to pure solute conversion, depleting the solute concentration in bulk solution (MACHADO *et al.*, 2020).
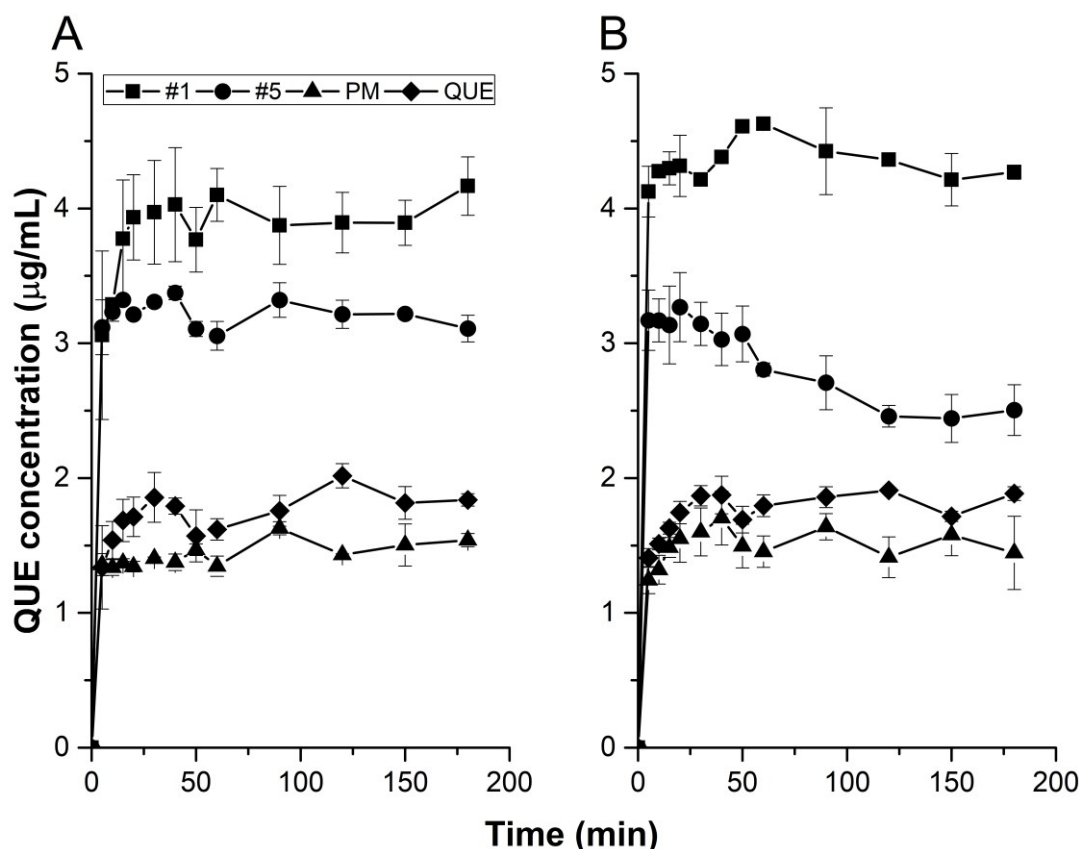


Figure 3.6 - Dissolution profiles of (■) sample #1, (●) sample #5, (♦) commercially supplied QUE, and (▲) physical mixture in (A) HCl solution (0.1 M, pH 1.2) and (B) phosphate buffer (pH 6.8) at 37 °C.

Dissolution results clearly show an expressive improvement in the apparent solubility and dissolution profile of QUE when cocrystallized with NIC. As QUE drawbacks are mostly related to its low solubility in aqueous medium, these enhancements promoted by cocrystallization widen the range of applications of this molecule on food and pharmaceutical applications.

## 3.4 CONCLUSIONS

The production of QUE/NIC cocrystals by the GAS method at different process conditions was explored. Cocrystals of QUE/NIC were successfully synthesized and characterized. The influence of temperature, pressure, and quercetin-to-nicotinamide ratio of

the GAS method was not relevant to modify the type and/or polymorphism of the cocrystal produced, although they mainly affect the yield of the produced powder. The use of GAS with $CO_2$ and acetone was effective to produce quercetin cocrystals with a stoichiometry of 1:1, different from those obtained by conventional cocrystallizations. Also, the QUE/NIC cocrystal produced by GAS, widens the use $CO_2$-based methods for cocrystallization, contributing to new QUE formulation strategies by cocrystallization. Dissolution behavior at different pH values showed better performance of GAS produced cocrystals (higher QUE dissolution) compared with pure quercetin. Also, GAS is an eco-friendly process since it is conducted at moderate temperature, and about 90% of the solvent used is supercritical $CO_2$, which is a renewable green solvent. Besides, the mostly higher initial investment costs of the high-pressure methods, compared to low-pressure methods, can be compensated by reduction of operational energy costs and also the reuse of the main solvent ($CO_2$). The economic aspects and life cycle need to be also studied for better application of this method. The increased in vitro dissolution performance suggests that the GAS-produced cocrystal may be used for enhancing bioavailability of quercetin, which is a natural product with wide range of applications.

# CHAPTER 4 PRODUCTION OF QUERCETIN-PROLINE COCRYSTALS BY MEANS OF GAS ANTISOLVENT (GAS)

This work aimed to invetigate the role of process variables pressure, temperature, and quercetin-to-proline ratio on the characteristics of quercetin/proline cocrystals obtained by gas antisolvent (GAS) method.

This chapter was submitted as an article in the peer-reviewed journal *Crystal Growth & Design*. Impact factor (2022): 4.076.

**Graphical abstract**
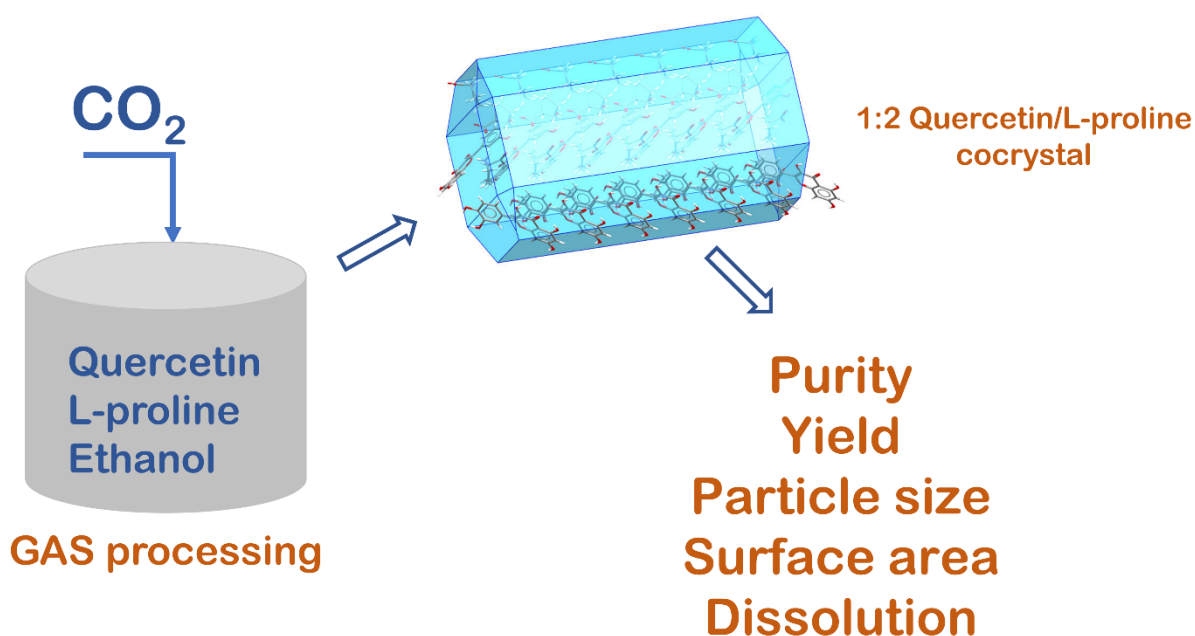
**Abstract**

Gas antisolvent (GAS) processing, based on supercritical $CO_2$, was firstly explored to obtain quercetin/L-proline (QUE/PRO). Cocrystallization is a novel mode to enhance physicochemical properties of poorly bioavailable molecules such as quercetin. QUE/PRO cocrystals were prepared by GAS with acetone as solvent, and the resulting powders were characterized by powder X-ray diffractometry (PXRD), differential scanning calorimetry (DSC), Raman spectroscopy, scanning electron microscopy (SEM), and Surface area determination (BET method). GAS process promoted higher yield compared to liquid antisolvent (LAS) processing. The ratio between QUE and PRO was the most relevant processing parameter, affecting the cocrystal yield, purity, particle size, and surface area. The QUE/PRO cocrystals produced by GAS presented better dissolution performance compared to LAS produced cocrystals, providing QUE release at least 1.3-times higher at pH 1.2, and 1.5-times higher at pH 6.8. These results indicate that GAS-processing is a promising approach to produce QUE/PRO cocrystals with improved quercetin's dissolution and bioavailability properties, with potential use in diverse applications.

4.1 INTRODUCTION

Quercetin (QUE) is a flavonoid with important biological properties (e.g., antioxidant, anti-cancer, anti-inflammatory, and anti-obesity), and because of its low water-solubility, presents poor bioavailability (CHEN; ZHOU; JI, 2010; D'ANDREA, 2015). To overcome this issue, several formulation approaches have been design, such as solid-lipid nanoparticles, nanoemulsions, biopolymer-particles, and others. Although, these formulation strategies present disadvantages such as low encapsulation loading, fast release, low stability, undesirable taste (KARIMI-JAFARI *et al.*, 2018b). Then, cocrystallization has emerged as an alternative methodology to increase the apparent water-solubility and dissolution of molecules with poor bioavailability like QUE, besides, this method generally rides out the problems faced by the typical formulations, providing also beneficial effect on bioavailability (DIAS; LANZA; FERREIRA, 2021; KARIMI-JAFARI *et al.*, 2018b). Diverse methods have been employed for cocrystal production, which can be classified as: (i) solution-based methods, where the cocrystal formation is achieved by supersaturating a solution of parent components; and (ii) solid-state methods, where the cocrystallization is induced by thermal and frictional energy (KARIMI-JAFARI *et al.*, 2018b). These methods have several issues, such as incomplete conversion,

undesirable amorphization, and thermal degradation (solid-state methods). In the case of solution-based methods, the main problems are related to the formation of single component crystals, solvate formation, and low yield. In this context, supercritical-based methods have been proposed as an alternative for cocrystal production, mainly in replacement of solution-based methods such as slow evaporation, cooling and slurry crystallization methods (DIAS; LANZA; FERREIRA, 2021). The supercritical-based methods like GAS, Supercritical antisolvent (SAS), Rapid Expansion of Supercritical Solutions (RESS), Cocrystallization with supercritical solvent (CSS) present environmental appealing, due to the use of green solvents, solvents recycling, and low solvent and energy consume (MACEACHERN; KERMANSHAHI-POUR; MIRMEHRABI, 2020). Gaseous antisolvent (GAS) technique is a supercritical-based cocrystallization method that uses the capacity of supercritical fluids in causing liquid expansion, decreasing the solvency ability of organic solvents, and leading to solute crystallization. This approach affords a fast single-step process, and improves the control of the cocrystal morphology and particle size by means of the processing parameters (e.g., pressure, temperature, flow-rate) adjustment (LONG *et al.*, 2021; WICHIANPHONG; CHAROENCHAITRAKOOL, 2018b).

GAS method has been successfully employed for the micronization of drugs, pigments, coprecipitation of bioactive-polymeric materials among other applications (PANDO; CABAÑAS; CUADRA, 2016; ZIELINSKI *et al.*, 2021), however the use of GAS method for cocrystallization is quite recent. Studies comprising the role of the process variables on the outcome of GAS-cocrystallizations are rare (MACEACHERN; KERMANSHAHI-POUR; MIRMEHRABI, 2020), hence generalizations about effect of process parameters are not straightforward. Nevertheless, and considering the scarce literature available, it seems that the effect of process parameters strongly depends on the chemical and physicochemical properties of the parent molecules. For instance, for the system composed by posaconazole/4-aminobenzoic acid, pressure and temperature had significant effect on cocrystal purity, although they have almost no effect on size and crystal habit (LONG *et al.*, 2021). On the contrary, for the system carbamazepine/saccharin, which cocrystals were prepared by SAS technique (continuous version of GAS processing), pressure and temperature played an important role on cocrystallization outcome (inducing polymorphism), and affecting in the product morphology, producing particles from plate-like to needle-like agglomerates (CUADRA *et al.*, 2018). The ratio between the parent components is another parameter hardly

studied. The rare literature available shows that the fine-tuning of the parent components ratio may improve the purity of the produced cocrystal (NEUROHR *et al.*, 2013), nevertheless, there are no information of its effect on the product polymorphism for $CO_2$-based methods. Even though, some studies using conventional methods, such as liquid-assisted grinding and slow evaporation have shown that variations in the parent components ratio provide cocrystals with different polymorphic forms and with improved properties (e.g., physical stability, dissolution) (SAIKIA; PATHAK; SARMA, 2021; TUMANOVA *et al.*, 2018).
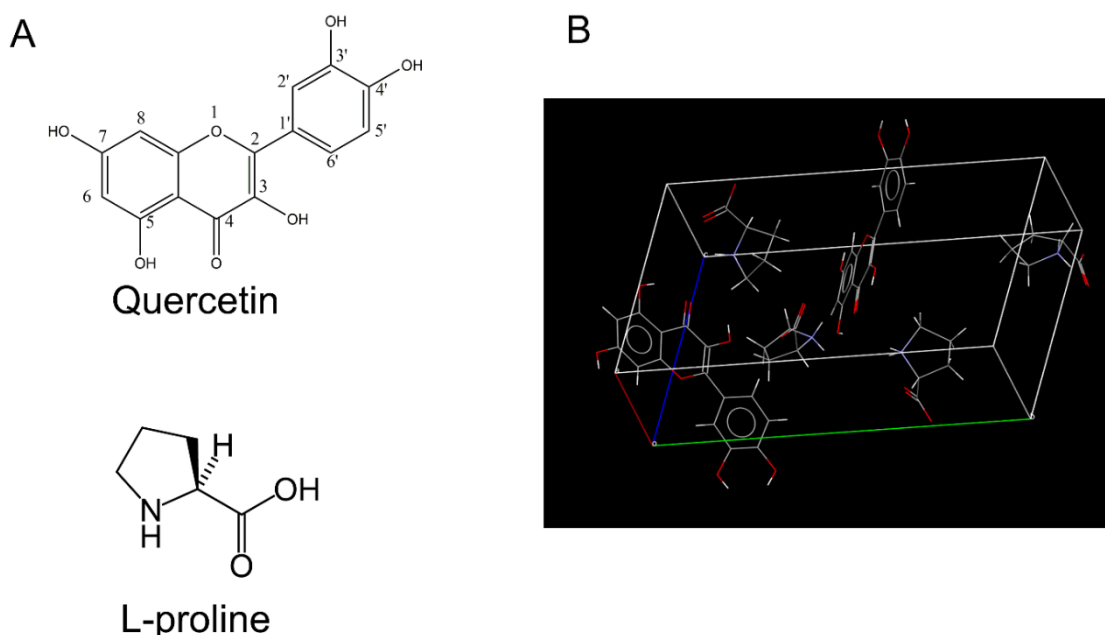


Figure 4.1- (A) Chemical structures of quercetin and L-proline. (B) Unit cell of 1:2 quercetin/L-proline cocrystal (CSD code: EJERES)(HE *et al.*, 2016) .

QUE cocrystals with dissolution improvement have been produced by conventional methods and using GRAS coformers (*Generally Recognized as Safe* by the US-FDA), such as nicotinamide (VASISHT *et al.*, 2016; WU *et al.*, 2020), caffeine (SMITH *et al.*, 2011), and L-proline (PRO) (HE *et al.*, 2016). Among the QUE cocrystals produced using GRAS coformers, quercetin/L-proline (QUE/PRO) (**Figure 4.1**) is the most promising solid form because of its superior ability in modulating the QUE dissolution.

To the best of our knowledge, cocrystals with QUE have not yet been produced by GAS method. Therefore, our objective is to study the QUE/PRO cocrystallization, as a model system, by GAS method, and also evaluate the effect of process parameters (pressure, temperature, and

quercetin-to-proline molar ratio) on the cocrystal characteristics, and examine the differences of the cocrystals produced by GAS method and by conventional method (slurry).

## 4.2 MATERIAL AND METHODS

### 4.2.1 Chemicals

Quercetin dihydrate (CAS No. 117-39-5, 98% m/m) was purchased from Chem-Impex International (Wood Dale, IL, USA); L-proline (CAS No. 174-85-3, 98,5% m/m), monopotassium phosphate (CAS No. 7778-77-0, 98% m/m) and hydrochloric acid (CAS No. 7647-01-0, 37 % m/m) were purchased from Dinâmica (Indaiatuba, SP, Brazil); dipotassium phosphate (CAS No. 7758-11-4, 98% m/m) was purchased from Vetec Sigma-Aldrich (Duque de Caxias, RJ, Brazil); ethanol (CAS No. 64-17-5, 99.5% m/m) and ethyl acetate (CAS No. 141-78-6, 99.5% m/m) were purchased from Neon (Suzano, SP, Brazil); carbon dioxide (CAS No. 124-38-9, 99.9% m/m) from White Martins (São Paulo, SP, Brazil).

### 4.2.2 Solution Preparation

QUE/PRO solutions were prepared by dissolving simultaneously, appropriate amounts of QUE and PRO in 30 mL of ethanol, in order to produce solutions of 1:1 and 1:2 QUE-to-PRO molar ratios, and with the help of an ultrasound bath. The solutions were filtered using a hydrophilic-PTFE syringe filter (0.45 µm) to remove any undissolved material. The amount of parent components used to form the solutions were: 302.2 mg and 115.1 mg of QUE and PRO, respectively, to obtain a solution of 1:1 QUE-to-PRO mol ratio, while 151.1 mg and 115.1 mg of QUE and PRO were used, respectively, to obtain a solution of 1:2 QUE-to-PRO mol ratio.

### 4.2.3 Cocrystallization by GAS process

The GAS unit used for the cocrystallizations assays was schematically described elsewhere (PESSOA *et al.*, 2019). In brief, it consists of a precipitation chamber comprising a 600 mL-volume stainless-steel jacked autoclave, linked to a thermostatic bath for temperature control; two syringe pumps (ISCO 500D) for $CO_2$ feeding; a set of ball valves, and two needle valves for flow rate control. Coupled to the outlet, a PTFE-membrane (0.22 µm) mounted in a polyethylene frit prevents material losses. Also, a digital pressure transmitter (Smar, LD301) and a K-type thermocouple ($\pm$ 2 °C) were used to monitor the processing pressure and temperature.

Following, each QUE/PRO solution was inserted into the vessel to evaluate the effect of variation in pressure, temperature, and QUE-to-PRO mol ratios. The GAS cocrystallization

assays were carried out in four sequential steps, *(1) pressure equilibration; (2) system pressurization; (3) system stirring, and (4) product drying*, described as follows.

**Pressure equilibration**: to prevent tube clogging due to abrupt $CO_2$ expansion (Joule-Thomson effect), the system pressure was equilibrated with slow filling the vessel with $CO_2$, while maintaining the outlet valve closed, and by means of a $CO_2$ reservoir at 6 MPa. System pressurization: compressed $CO_2$ (20 MPa) was continuously fed into the vessel at a constant flow rate (10 mL·min-1), under magnetic stirring, until reaching the processing pressure and temperature. **System stirring**: immediately after the working pressure and temperature were reached, the $CO_2$ inlet valve was closed and the system was held under stirring for 10 min, at constant pressure and temperature, inducing the precipitation of cocrystals. **Product drying**: Finally, with the outlet valve open, an additional amount of $CO_2$ (about 800 mL), at the same previous conditions of temperature and pressure, was continuously pumped into the vessel, removing the headspace solvent and the solvent amount adsorbed at the particle surfaces. For reproducibility purposes, each cocrystallization procedure was performed in duplicate. The operational parameters evaluated for the cocrystallization were: temperature, of 35 and 45 °C; pressure of 8 and 10 MPa; and quercetin/proline ratio of 1:1 and 1:2 mol/mol. The level of the parameters was defined based on literature data (LONG *et al.*, 2021; NEUROHR *et al.*, 2013; PESSOA *et al.*, 2019; WICHIANPHONG; CHAROENCHAITRAKOOL, 2018b). Also, for all GAS assays, the solution volume and the $CO_2$ flow rate were kept constant.

### 4.2.4 Slurry cocrystallization

For comparison with the GAS-produced cocrystals, QUE/PRO cocrystals were synthesized by slurrying method (HE *et al.*, 2016; LUO *et al.*, 2018). Briefly, 302.2 mg of QUE and 230.2 mg of PRO were stirred in 5 mL of ethyl acetate/ethanol mixture (1:1, v/v) for 24h at room temperature. The resulting material was then isolated by centrifugation, oven-dried at 50 °C overnight, and gently crushed using a pestle and mortar. Phase confirmation was addressed by PXRD (**Figure B.1**).

### 4.2.5 Powder X-ray diffraction (PXRD)

PXRD patterns were obtained using a Rigaku MiniFlex600 diffractometer (Rigaku, Japan) equipped with a copper X-ray tube (Kα = 1.54059 Å) and a detector D/teX. Data were recorded in θ-2θ scan mode, at a tube voltage of 40 kV, tube current of 15 mA, with a step size of 0.02°, and scanning speed of 6°/min.

### 4.2.6 Thermal analysis

Differential scanning calorimetry (DSC) of the samples was performed using a Jade DSC (Perkin Elmer, USA). During the DSC experiments the samples were weighed directly in hermetic sealed aluminum pans, heated from 50 °C to 350 °C at a rate of 10 °C·$min^{-1}$, under nitrogen flow (50 mL·$min^{-1}$).

### 4.2.7 Raman spectroscopy

The Raman spectroscopy was carried out in a Cora 5200 Raman instrument (Anton Paar, Austria), equipped with a 785 nm laser as excitation source (power 450 mW). The samples were analyzed as powder and their Raman spectra were acquired from 100 to 2300 $cm^{-1}$ at spectral resolution of 2 $cm^{-1}$, and using an integration time of 5 s.

### 4.2.8 Morphology and the particle size distribution (PSD).

The morphology and the particle size distribution (PSD) of the produced cocrystals were evaluated by Scanning Electron Microscopy (SEM) using a JEOL JSM-6701 F microscope operating at 10 kV. Samples were mounted in stubs containing double-sided carbon tape and then gold-coated. For PSD evaluation, the length of particles (ca. >200) was measured from SEM images (x2500 magnification) using the *ImageJ* software (SCHNEIDER; RASBAND; ELICEIRI, 2012). Number-based PSDs diagrams were created (**Figure B.2**), allowing the determination of the PSD parameters $d_{10}$, $d_{50}$, $d_{90}$ (representing the length of 10, 50 and 90% of the particles, respectively) and span, which represents ($d_{90}$-$d_{10}$/$d_{50}$) (HORIBA SCIENTIFIC, 2010; XU, 2014).

### 4.2.9 Specific surface area determination (BET method).

Samples were accurately weighed and subjected to nitrogen adsorption at Autosorb-1 equipment (Quantachrome Instruments, USA). Then, the Brunauer, Emmett and Teller (BET) model was fitted to sample isotherms for specific surface area determination (multi point BET method) (INTERNATIONAL ORGANIZATION FOR STANDARDIZATION, 2010).

### 4.2.10 Dissolution Studies

For each run, accurately weighed powder samples of approximately 10 mg were suspended in 250-mL Erlenmeyer flasks containing 100 mL of each dissolution media. Potassium phosphate buffer (pH 6.8, 0.05 M) and 0.1 M HCl solution (pH 1.2) were selected as dissolution media to mimic the gastrointestinal environment. The dissolution studies were conducted in a Dubnoff-type shaker at a rotation speed of 100 rpm at 37 °C. Liquid samples were collected at scheduled time intervals (5, 10, 15, 20, 30, 40, 50, 60, 90, 120, 150, 180 min)

and the withdrawn suspensions were filtered through 0.45 μm hydrophilic-PTFE syringe filters prior to spectrophotometric analysis. The quercetin content from the collected samples was quantified spectrophotometrically at 366 nm using a microplate multi-reader (Tecan, Model Infinite M200). For determination of QUE amount, a standard curve was prepared (1-10 μg.mL$^{-1}$, y=0.055x-0.030, R$^2$=0.997). The dissolution profile of the cocrystals was performed in duplicate and the results expressed as concentration of quercetin released over time.

## 4.3 RESULTS AND DISCUSSION

### 4.3.1 Cocrystallization by GAS process

To investigate the effect of pressure, temperature, and QUE-to-PRO mol ratio on the formation of QUE/PRO cocrystals, a study using a design of 3-factors and 2-levels was performed (**Table 4.1**). At 1:1 QUE-to-PRO mol ratio (assays #1-#4) the parameters pressure and temperature present no significant effect on the precipitation yields of the cocrystals. Otherwise, using the 1:2 QUE-to-PRO mol ratio (assays #5-#8), the significant effect of pressure and temperature on the cocrystal yield may related to the $CO_2$ density, i.e., the lowest yield was provided at the higher $CO_2$ density (0.7128 g·mL$^{-1}$), assay #7, with yield of 51.7%. Also, the $CO_2$-densities at runs #5, #6, and #8, are probably not so different from each other to cause significant difference on yield. A similar outcome was observed by Cuadra et al. (2018), who studied the effect of pressure and temperature on the precipitation yield of carbamazepine/saccharin cocrystals obtained by SAS method. They reported that a pressure increases of 5 MPa (0.15 g·mL$^{-1}$ in density) caused a reduction of 15% on yield.

The yield of the precipitated material depends on the complex relationship between the solubilities of the pure components and the cocrystal in the supercritical mixture ($CO_2$ + ethanol), which data are still a gap on the literature. Although straightforward conclusions cannot be drawn without experimental solubility data of all components, a general trend can be established. Since amino acids as PRO are practically insoluble in supercritical $CO_2$ (STAHL *et al.*, 1978), the decreasing in yield may be mostly attributed to higher QUE solubilization at high $CO_2$ densities (FRANCO *et al.*, 2018). This might lead to higher amount QUE in the supercritical phase, which is no longer available to be cocrystallized with PRO and then it is lost during the drying step ($CO_2$ flushing).

**Table 4.1**- Operational parameters (temperature, pressure, $CO_2$ density, and QUE/PRO ratio) used at GAS assays for the productions of QUE/PRO cocrystals, and the yield results.

| Assay[1] | Pressure (MPa) | Temperature(°C) | $CO_2$ density[2] ($g \cdot mL^{-1}$) | QUE-to-PRO ratio (mol) | Yield (%)[3,4] | Solid form obtained[5] |
|---|---|---|---|---|---|---|
| #1 | 8 | 35 | 0.4191 | | 78.8[ab] ± 0.6 | |
| #2 | 8 | 45 | 0.2411 | | 75.4[abc] ± 2.6 | Cocrystal + QUE (anhydrous) |
| #3 | 10 | 35 | 0.7128 | 1:1 | 80.8[a] ± 0.6 | |
| #4 | 10 | 45 | 0.4983 | | 76.6[ab] ± 4.3 | |
| #5 | 8 | 35 | 0.4191 | | 68.7[bc] ± 1.4 | |
| #6 | 8 | 45 | 0.2411 | | 64.7[c] ± 1.1 | Cocrystal |
| #7 | 10 | 35 | 0.7128 | 1:2 | 51.7[d] ± 6.1 | |
| #8 | 10 | 45 | 0.4983 | | 69.4[abc] ± 1 | |

[1] For all assays (runs) the solution volume and the $CO_2$ flow rate were kept constant. [2] $CO_2$ density data from. Anwar and Carroll, (2015). [3] Mean values (n=2) followed by the same superscripts do not differ from each other using Tukey´s test ($p < 0.05$). [4] Yield = (collected amount/initial amount) x100. [5] Determined by PXRD (see section *4.3.2.1.*).

The yields of the GAS-processed samples (**Table 4.1**) were typically superior to that obtained by slurry cocrystallization (51.7 – 80.8 vs 58.4%, respectively). The yield of samples produced by slurry method can vary widely, based on the operating conditions. Although, the slurry cocrystallization typically operates with higher initial mass of starting materials compared to GAS processing, significant material loss due to residual solubility in the solvent can occur, reducing the yield (KARIMI-JAFARI *et al.*, 2018b). Nevertheless, a decrease in yield due to material loss and residual solubility can occur in GAS process as well, but in less extent compared to slurry, because the solubility of the precursors is generally lower in the supercritical phase ($CO_2$+ethanol) than in the solvent at low pressure (ethanol). For example, QUE solubility is roughly 10-times lower in $CO_2$+ethanol than in pure ethanol at room conditions (CHAFER *et al.*, 2004; RAZMARA; DANESHFAR; SAHRAEI, 2010).

The QUE-to-PRO mol ratio parameter play a significant role in the cocrystallization outcome by GAS. The use of a 1:2 ratio of parent components provided samples composed by 1:2 QUE/PRO cocrystal with high purity (**Table 4.1**). Otherwise, using a 1:1 ratio, i.e., increasing the amount of QUE in relation to PRO, no new cocrystal polymorph could be obtained, but powders composed by a mixture of 1:2 QUE/PRO cocrystal and non-cocrystallized QUE (anhydrous form).

Cocrystals may be stoichiometrically distinct from the initial ratio between the precursors. This phenomenon is known as stoichiomorphism, as described by Salzillo et al.

(2016) while explaining different stoichiometric cocrystals from the same parent components. For instance, Tumanova et al. (2018)evaluated the formation of proline/naproxen cocrystals by liquid-assisted grinding method and show that cocrystallization from 1:2 and 2:3 proline/naproxen mixtures form proline/naproxen cocrystal with stoichiometry of 2:3, whereas the use of 2:1 proline/naproxen mixtures provided cocrystals with stoichiometry 1:1. Likewise, Neurohr et al. (2013) processed naproxen/nicotinamide cocrystal by GAS with initial ratios of 1:1, 1:2 and 2:1, and found that regardless the initial ratio, naproxen and nicotinamide self-organize to form a cocrystal with a 2:1 stoichiometry. The stoichiometry variation of cocrystals is not fully understood. Nevertheless, according Tumanova et al. (2018), the stoichiometry is related to solid-state transitions of the former components, leading to a most kinetically favored cocrystal phase. Saikia et al. (2021) suggest that the formation of different stoichiometric cocrystals is mainly affected by the type of precursors involved, the solvent selected, and the cocrystallization method used.

A general stoichiometric relation was proposed by Tothadi and Phadkule (2019), theorizing that if each entity of the active-molecule/coformer pair has two different functional groups, with ability to form complementary hydrogen bonds, there always be a probability of obtaining cocrystals with variable stoichiometries. Then, considering the present study, each parental component exhibit only one type of functional group able to form complementary hydrogen bonding, i.e., QUE with a weakly acidic O−H moieties, generally acting as hydrogen bond donors, and PRO with a carboxylate zwitterion ($COO^-$), capable to form persistent charge-assisted $COO^- \cdots O-H$ hydrogen bonding with QUE (HE *et al.*, 2016). These characteristics could explain the stoichiometry ratio of (1:2), obtained for the QUE/PRO cocrystals, regardless variations at GAS conditions of pressure, temperature, and the initial ratio of the parent components.

Our findings related to the effect of parent QUE-to-PRO ratio are also in accordance with Neurohr et al. (2013), which showed that one of the cocrystal components, obtained by GAS process is in excess compared to the cocrystal stoichiometry, and this excess amount may precipitate as homocrystals due to its higher concentration above the compound solubility in the solvent used. According to the results presented at **Table 4.1**, the excess of QUE from the 1:1 QUE-to-PRO assays was probably large enough to allow the precipitation of QUE as homocrystals, whereas in the assays using the 1:2 ratio, the QUE amount was not sufficient to surpass the QUE solubility limit.

The thermodynamic aspects behind the formation of pure cocrystals or mixtures of cocrystals and homocrystals depend on the ternary phase diagrams (TPD), delimiting the zones of coexistence of all components (cocrystal, active molecule, coformer, solvent, and antisolvent). Determination of TPDs is tedious, time consuming, expensive, generally incomplete, and very rare, even for simpler ternary systems, often related to conventional cocrystallizations. Moreover, TPDs concerning supercritical mixtures, focused on designing supercritical-aided cocrystallizations, are still a challenge and, to the best of our knowledge, none of these studies have been published to date.

## 4.3.2 Characterizations of the produced cocrystals

### 4.3.2.1 Powder X-ray diffractometry (PXRD).

The solid phase obtained in the GAS samples was determined by Powder X-Ray Diffraction (PXRD), and the patterns from each produced samples were compared to those patterns of pure QUE, PRO, and the QUE/PRO cocrystal simulated from the single crystal X-ray data (HE *et al.*, 2016). For the GAS samples processed at 1:1 QUE-to-PRO ratio (assays #1– #4), all studied conditions resulted in the formation of a mixture of the 1:2 QUE/PRO cocrystal and pure QUE (**Figure 4.2**). Discounting the small displacements of characteristic peaks at sample patterns with respect to reference pattern (CSD: EJERES) (HE *et al.*, 2016), which may be caused by sample thermal expansion or displacement. Most of the characteristic peaks from the samples from **Figure 4.2** (9.36, 11.98, 14.74, and 15.48° $2\theta$) matched with the cocrystal reference (CSD: EJERES) (HE *et al.*, 2016). Besides, peaks around 4.46 and 12.82° $2\theta$ can be attributed to the formation of anhydrous QUE during GAS processing (**Figure B.3**) (BORGHETTI *et al.*, 2012; FILIP *et al.*, 2013), indicating a remaining amount of unreacted QUE, while the absence of the PRO main peaks, at 8.84 and 19.36° $2\theta$, indicates that it was consumed during cocrystallization. On the contrary, the GAS processing using a 1:2 QUE-to-PRO ratio (assays #5 - #8) produced high-purity 1:2 QUE/PRO cocrystal, without unprocessed parent components, as can be concluded by comparing the PXRD patterns of the cocrystal reference major peaks from **Figure 4.3**, with those of assays #5 - #8.
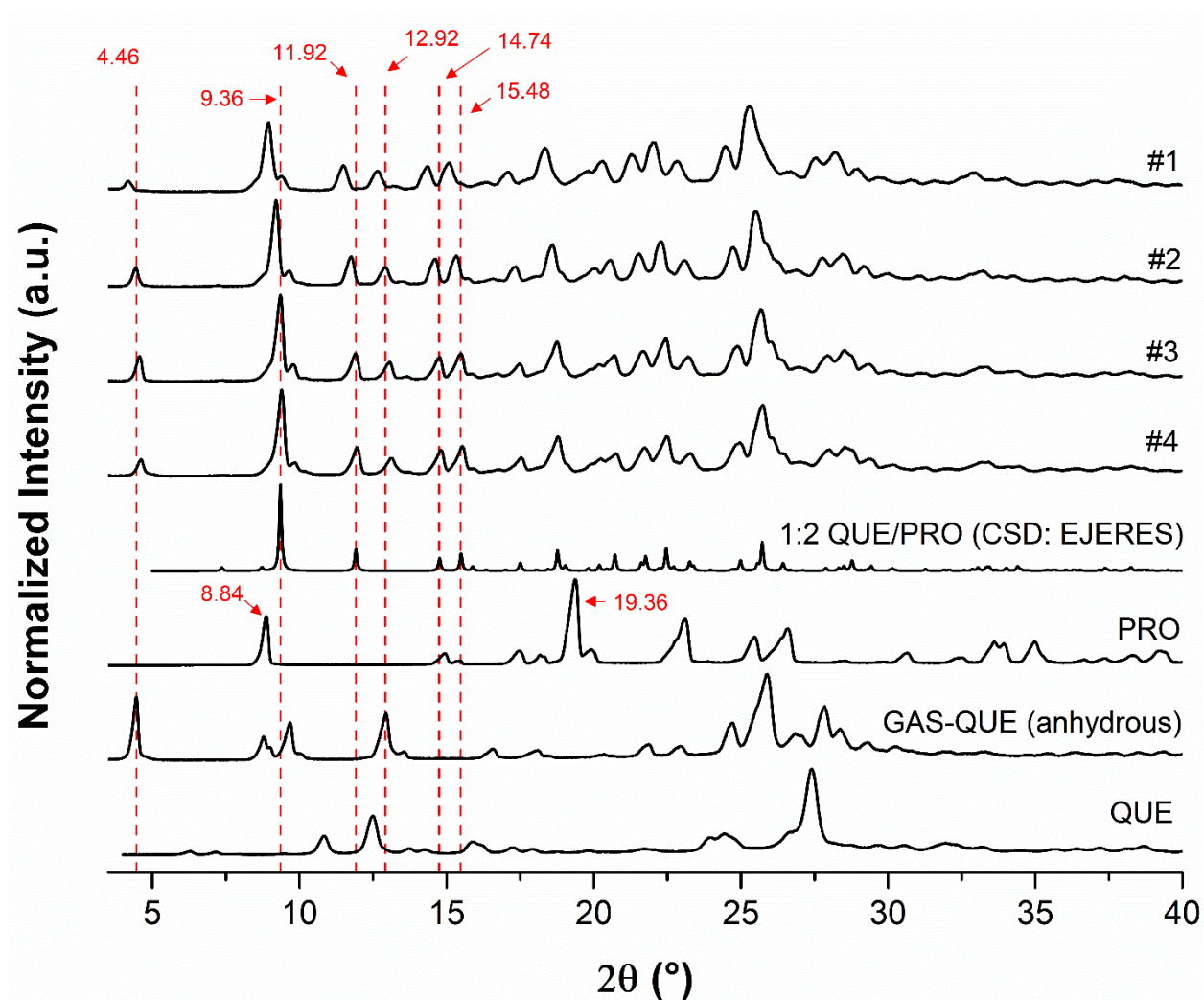
**Figure 4.2** - Powder X-ray diffraction patterns of samples processed by the GAS method at 1:1 QUE-to-PRO mol ratio (assays #1-#4), QUE/PRO cocrystal reference from the Cambridge Structural Database (CSD code: EJERES) (HE *et al.*, 2016), raw PRO, raw QUE, anhydrous QUE obtained by GAS processing (GAS-QUE).
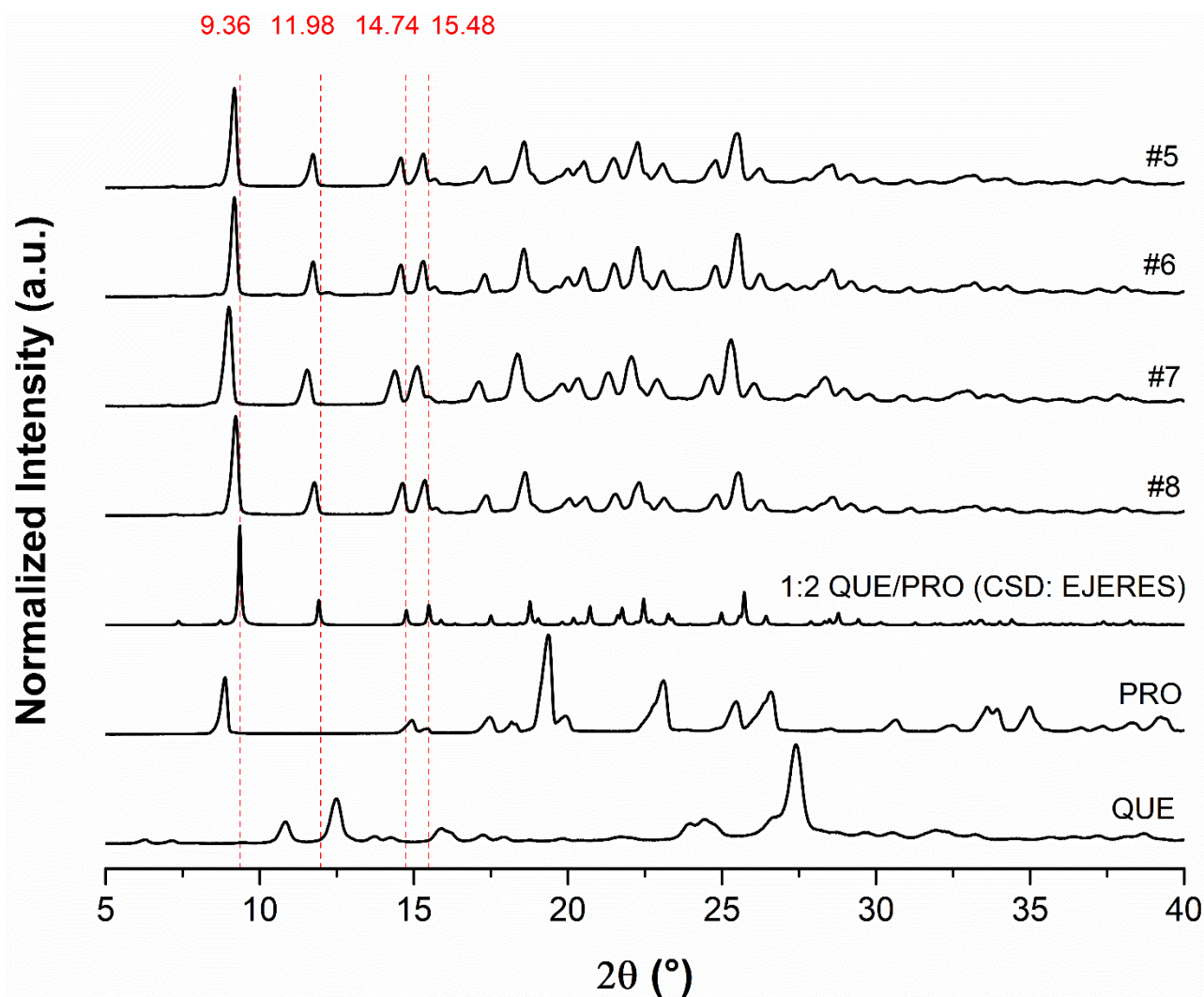
**Figure 4.3** - Powder X-ray diffraction patterns of samples processed by the GAS method at 1:2 QUE-to-PRO mol ratio (assays #5-#8), QUE/PRO cocrystal reference from the Cambridge Structural Database (CSD code: EJERES) (HE *et al.*, 2016), raw PRO, raw QUE.

*4.3.2.2 Differential scanning calorimetry (DSC).*

The thermal behavior of the starting components and QUE/PRO cocrystal was conducted by differential scanning calorimetry (DSC) to assess the cocrystal formation. The DSC graphs of the starting components (**Figure 4.4**) showed well agreement with literature, QUE showed well defined melting point at 311 °C (BORGHETTI *et al.*, 2012), while PRO melts at 232.9 °C, then it decomposes by increasing temperature (POKORNÝ *et al.*, 2021). All samples processed by GAS (**Figure 4.4**) presented an endothermic event around 225 - 227 °C (onset temperature), which is consistent with the results previously reported by He (HE *et al.*, 2016) for 1:2 QUE/PRO cocrystal (~227°C).
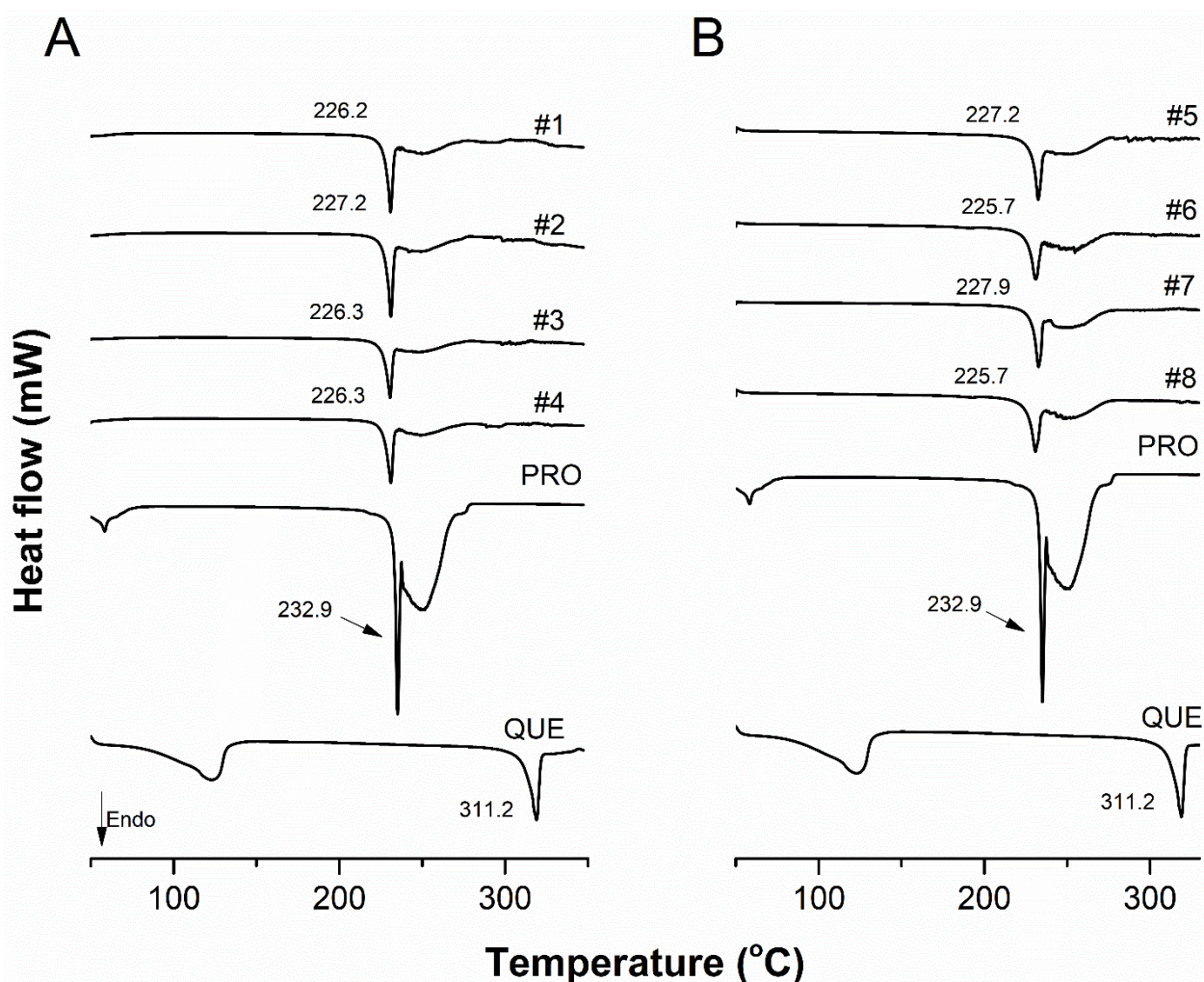
**Figure 4.4** - Differential scanning calorimetry (DSC) heating curves of the GAS-processed QUE/PRO cocrystals and raw QUE and PRO. (A) Samples processed at 1:1 QUE-to-PRO mol ratio (runs #1 - #4); (B) Samples processed at 1:2 QUE-to-PRO mol ratio (runs #5 - #8).

Although the unreacted amount of QUE is present at samples from assays #1-#4 (as confirmed by PXRD, **Figure 4.2**), the effect of this amount of unreacted QUE in the DSC curves was not perceptible, probably because the cocrystal decomposes just after its melting, as can be confirmed by the baseline shift following the thermic event (**Figure 4.4**).

### 4.3.2.3 *Raman spectroscopy*

Generally, homocrystals and cocrystals show distinct Raman spectra due to different intermolecular interactions at the solid structure, which can be used to assess cocrystal

formation. Changes in peak shape, intensity, and the displacement of functional group bands from the cocrystal spectrum (**Figure 4.5**), compared with that from the parent components spectra, can indicate intermolecular hydrogen bonding due to cocrystal formation. As expected, the spectrum of the pure components (**Figure 4.5**) was consistent with literature. The QUE most significant bands are assigned to (C4=O) stretching (1660 cm$^{-1}$), (C2=C3) stretching (1616 cm$^{-1}$), and phenyl and benzo rings (C=C) stretching (1595 and 1561 cm$^{-1}$), while the bands at 1497 and 1307 cm$^{-1}$ are related to a series of coupled vibrational modes of (C=C) stretching and in-plane (C-H) and (C-OH) bending (BORGHETTI *et al.*, 2012; CORNARD; MERLIN, 2002). The principal bands in PRO spectrum are ascribed to (NH$_2^+$) bending (1620 cm$^{-1}$); aliphatic (CH$_2$) groups (about 1470 and 1450 cm$^{-1}$); (COO$^-$) asymmetric and symmetric stretching (1550 and 1377 cm$^{-1}$, respectively); ring stretching and variation of COO$^-$ group (900 and 919 cm$^{-1}$, respectively) (CÁRCAMO *et al.*, 2012; SHIMPI *et al.*, 2014). The Raman spectra of QUE, PRO, and GAS-produced cocrystals are shown at **Figure 4.5** and the most significant changes in the cocrystal spectra in relation with the former components are listed at **Table 4.2**.

The spectra from the cocrystal shows significant changes at ring stretching vibration and variation of COO$^-$ group of PRO (900 and 919 cm$^{-1}$, respectively), which appeared as sharp peaks in PRO spectrum, whereas practically disappeared at the cocrystal spectra. Similarly, the band related to pyrrolidine ring deformations of PRO (451 cm$^{-1}$) is absent in the cocrystal spectra. In addition, subtle sifts were observed in cocrystal spectra at the region of symmetric stretching of COO$^-$ (from 1377 to 1362 cm$^{-1}$) and at hydroxyl-related regions, from 1307 to 1316 cm$^{-1}$; and from 1497 to 1494 cm$^{-1}$. Taken together, these findings indicate that the produced QUE/PRO cocrystals are mainly driven by N–H···O and O–H···O hydrogen bonding interactions, which is in accordance with the crystal structure previously reported by He [5].
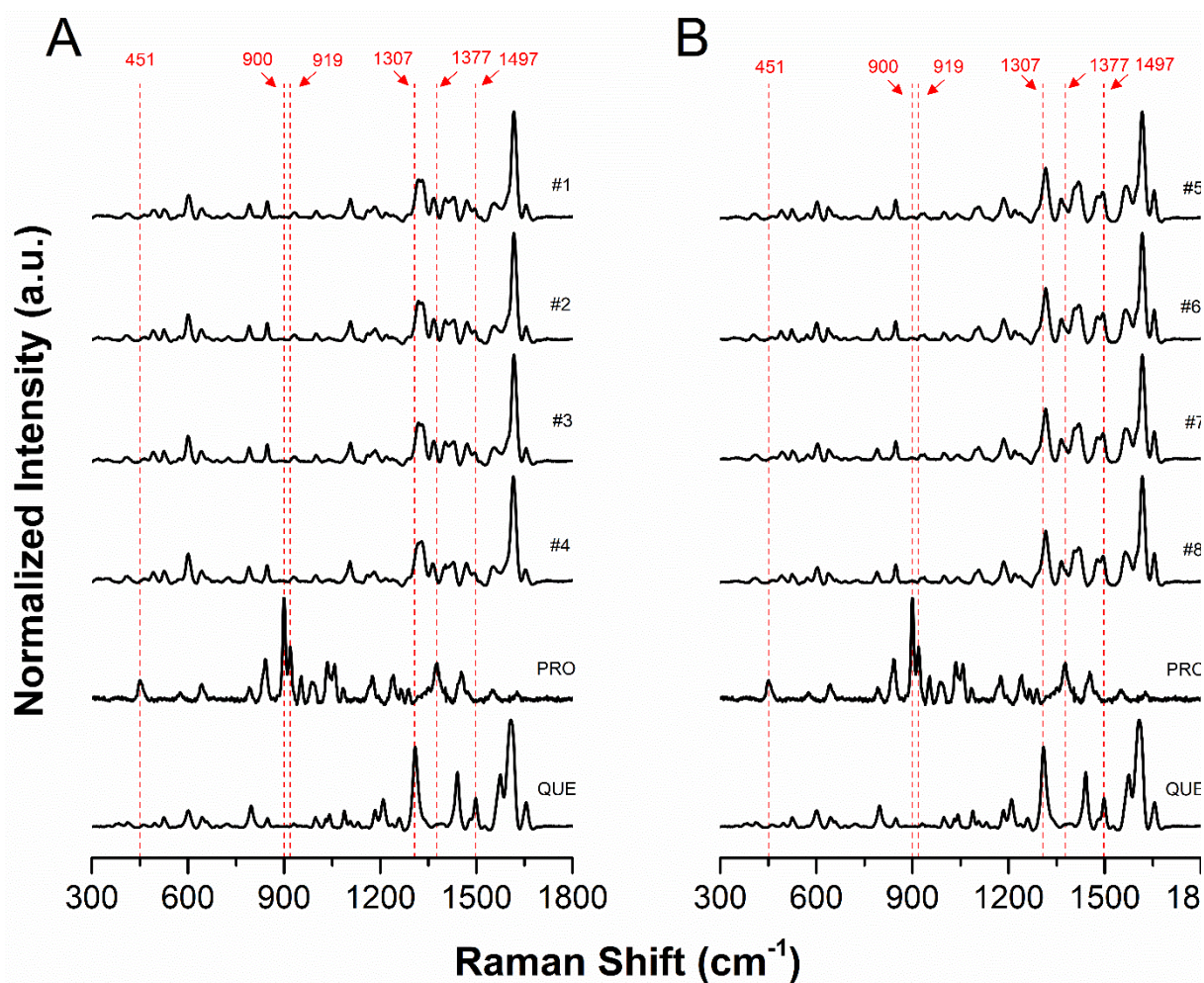
**Figure 4.5** - Raman spectra of the GAS-processed QUE/PRO cocrystals and raw QUE and PRO. (A) Samples processed at 1:1 QUE-to-PRO mol ratio (runs #1 - #4); (B) Samples processed at 1:2 QUE-to-PRO mol ratio (runs #5 - #8).

**Table 4.2** - Raman spectra of QUE, PRO and QUE/PRO cocrystals produced by GAS processing.

| Vibrational modes | Raman shift (cm-1) | | |
|---|---|---|---|
| | QUE | PRO | QUE/PRO |
| νPyrro. ring | - | 900 | absent |

**Table 4.2** – (Continued)

| | | | |
|---|---|---|---|
| νC-COO- | - | 919 | practically absent; large reduction on intensity |
| Pyrro. ring deformation | - | 451 | practically absent; large reduction on intensity |
| νsCOO- | - | 1377 | 1362 |
| Coupled νbenz. ring and δOH. | 1307 | - | 1316 |
| Coupled νbenz. ring; δC-H; and δOH. | 1497 | - | 1494 |

*ν:* stretching; $\nu_s$: symmetric stretching; *δ*: bending; Pyrro: Pyrrolidine; Benz: Benzene.

### *4.3.2.4 Morphology, particle size distribution (PSD), and specific surface area*

SEM images of 1:2 QUE/PRO cocrystals obtained by assays #1–#7 are shown at **Figure 4.6**. Pressure, temperature, and QUE-to-PRO ratio had a very weak effect on the morphology of the precipitated cocrystals, and the samples from all processing conditions showed similar needle-like morphologies. Otherwise, the GAS and LAS samples had different morphologies (needle-like vs flocculated particles, respectively). This disparity can be attributed to cocrystallization process, solvent used, and to the additional milling procedure required after LAS processing, which can alter the cocrystal morphology, affecting the dissolution performance of the of particles formed (CHIKHALIA *et al.*, 2006; LI *et al.*, 2019; WANG; LIANG, 2017).

Regarding PSDs, QUE-to-PRO ratio had a significant effect on particle size (**Table 4.3**). In overall, at 1:2 ratio, the particles sizes of the formed cocrystals were smaller compared to samples processed at using the 1:1 ratio (0.171-0.265 µm vs 0.264-2.593 µm, respectively). At 1:2 ratio, the starting solution is more diluted compared to the starting solution at 1:1 ratio, therefore initial supersaturation ratio is lower, which favors nucleation instead of crystal growth, resulting in smaller particles. On the other hand, pressure and temperature variations did not show a clear effect on particle size of the produced cocrystals. In fact, the effect of these variables could be hard to evaluate, due to their influence in different aspects of the crystallization, often antagonistically. For instance, an increase temperature augments the supersaturation because of its positive effect on mass transfer due to better dissolution of $CO_2$ in solution caused by improvement of diffusion and reduction of liquid interfacial tension.

Oppositely, an increase in temperature reduces the solute solubility in the solution, decreasing the supersaturation degree (GALLAGHER *et al.*, 1992; JESSOP; SUBRAMANIAM, 2007).
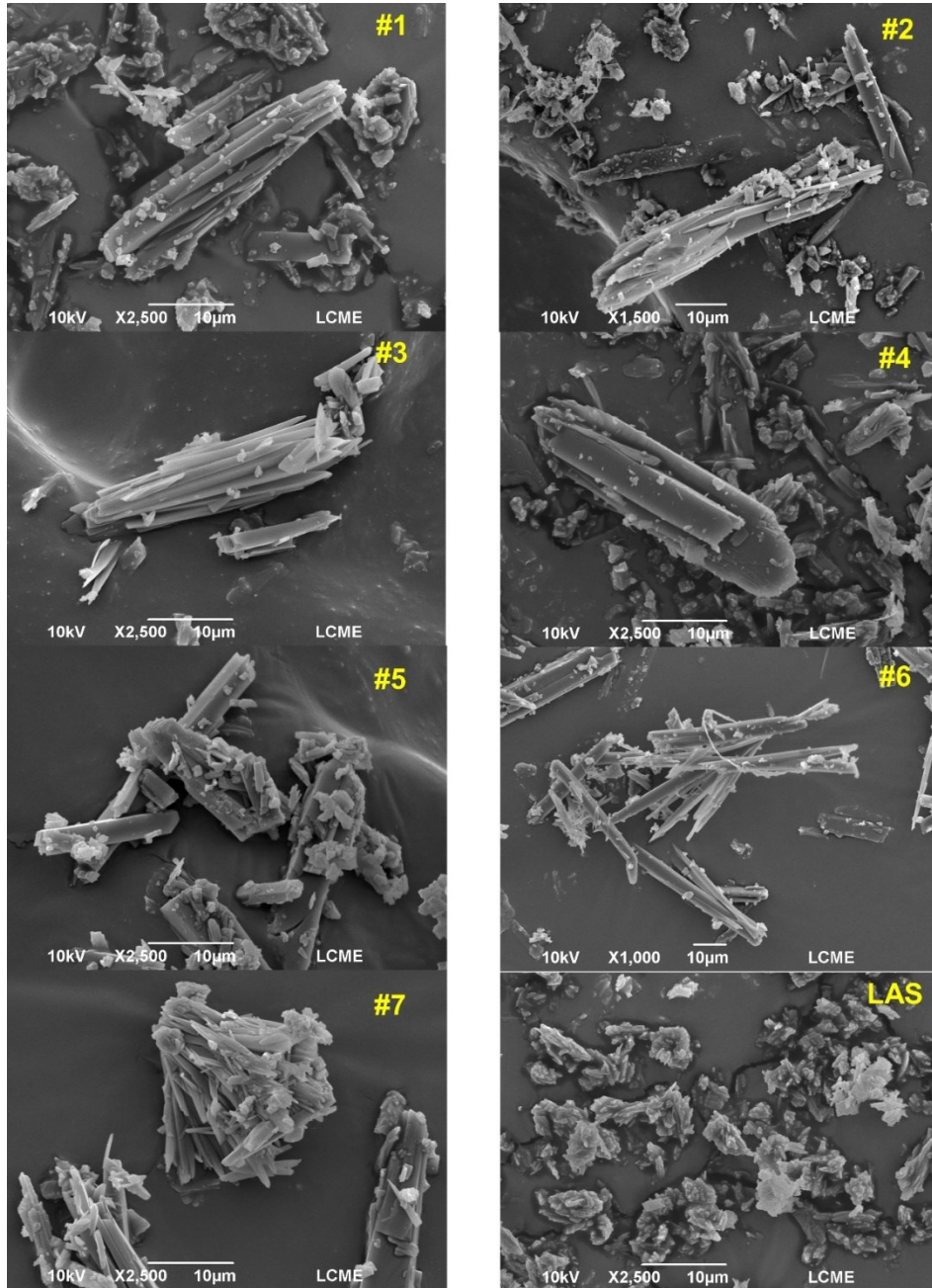


**Figure 4.6** - SEM images of the GAS (#1-#7) and LAS processed cocrystals.

As the supersaturation degree is the driven-force behind crystallization, affecting nucleation/growth rates and finally the particle sizes, this may explain because the effect temperature depends mostly of the range of temperature (ROY *et al.*, 2011).

Table 4.3 - Particle size distributions of QUE/PRO cocrystals produced by GAS.

| Assay[1] | P (MPa) | T (°C) | $CO_2$ density[2] (g·mL$^{-1}$) | QUE-to-PRO ratio (mol) | $d_{10}$ (μm) | $d_{50}$ (μm)[3] | $d_{90}$ (μm) | span |
|---|---|---|---|---|---|---|---|---|
| #1 | 8 | 35 | 0.4191 | | 0.876 | 1.776[a] | 5.458 | 2.6 |
| #2 | 8 | 45 | 0.2411 | | 1.054 | 2.497[a] | 8.704 | 3.1 |
| #3 | 10 | 35 | 0.7128 | 1:1 | 0.083 | 0.264[bc] | 1.375 | 4.9 |
| #4 | 10 | 45 | 0.4983 | | 1.028 | 2.593[a] | 9.778 | 3.4 |
| #5 | 8 | 35 | 0.4191 | | 0.071 | 0.171[b] | 0.813 | 4.3 |
| #6 | 8 | 45 | 0.2411 | | 0.062 | 0.193[bc] | 1.751 | 8.8 |
| #7 | 10 | 35 | 0.7128 | 1:2 | 0.076 | 0.265[bc] | 2.640 | 9.7 |
| #8 | 10 | 45 | 0.4983 | | 0.065 | 0.228[bc] | 2.827 | 12.1 |

[1] For all assays (runs) the solution volume and the $CO_2$ flow rate were kept constant. [2] $CO_2$ density data from Anwar and Carrol (2015). [3] Median particle sizes ($d_{50}$) values followed by the same superscripts do not differ from each other using Kruskal-Wallis test, followed by Dunn's test ($p < 0.05$).

In relation to cocrystal surface area, the BET analysis results for GAS processed samples, from assays #5-#8 (purest cocrystal samples), and the LAS sample are shown at **Figure 4.7A**. Within GAS processed cocrystals, sample #5 showed the highest surface area (8.881 m$^2$·g$^{-1}$), which may be related to its lower median particle size compared to other GAS-samples (**Figure 4.7B**)(SERRANO *et al.*, 2016).

However, comparing samples #5 with the LAS sample, the inverse relationship between surface area and particle size it is not clear, i.e., LAS sample has higher surface area related to sample #5 (10.370 vs 8.881 m$^2$·g$^{-1}$, respectively), even having higher median particle size (1.18 vs 0.171 μm, respectively). This behavior is possibly related to differences in the morphology of GAS and LAS samples (needle-like vs flocculated, respectively). Similar trend was also

observed by Serrano et al. (2016), studying surface area and particle size of sulfadimidine/4-aminosalicylic acid cocrystal with different crystal habits (morphologies).
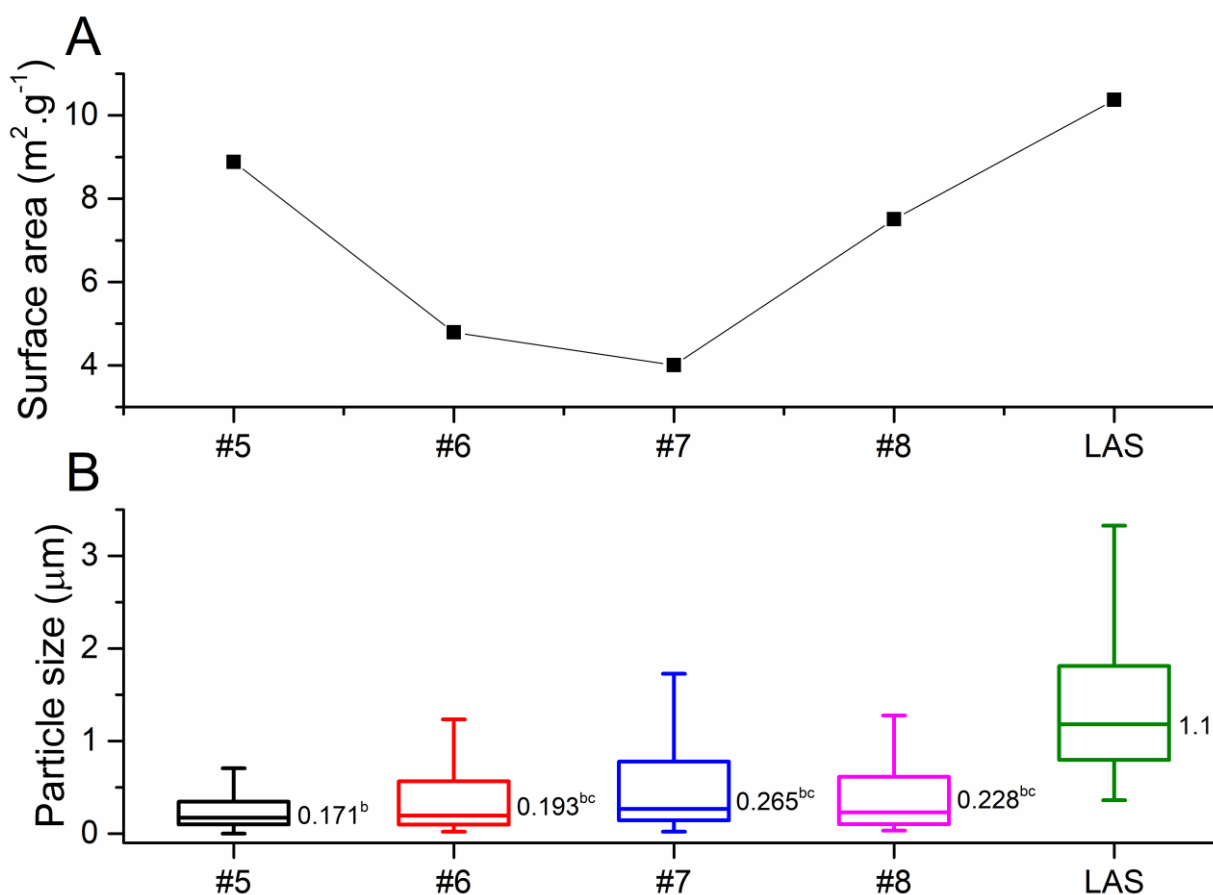


**Figure 4.7** - (A) Surface area and (B) box-plot particle size distributions of QUE/PRO cocrystals produced by GAS and LAS processing.

*4.3.2.5 Dissolution studies*

Dissolution test was performed to evaluate the potential impact of GAS cocrystallization on improving QUE dissolution compared to LAS cocrystallization. As shown at Figure 4.8, the cocrystal produced by GAS (sample #5) was superior in dissolution performance than LAS sample, in both dissolution media used (pH 1.2 and 6.8). It means that, higher supersaturated level of QUE was achieved if compared to pure QUE powder. At pH 1.2 (**Figure 4.8A**), the GAS-produced cocrystal reaches the maximum concentration (~8.5 µg·mL$^{-1}$) at about 20 min and could sustain supersaturated values (from 8.5 to 4 µg·mL$^{-1}$) for 180 min, whereas the LAS produced cocrystal attains a significant lower maximum value (~3.6 µg·mL$^{-1}$) at same time

period, maintaining an inferior level of supersaturation compared to GAS sample. In other words, the cocrystal produced by GAS had better dissolution performance and it was more stable than the cocrystal obtained by LAS.

Similarly, at pH 6.8 (**Figure 4.8B**) the cocrystal obtained by GAS was able to generate and sustain for a significant period (180 min), supersaturation levels of QUE higher than those achieved by the LAS cocrystal. For instance, the GAS produced cocrystal achieved the maximum concentration ($\sim$9.7 $\mu g \cdot mL^{-1}$) at about 60 min, maintaining at least a 1.5-fold higher concentration concerning LAS cocrystal sample.

Analyzing the shape of dissolution curves of the GAS produced cocrystal, it can be noted an initial fast release at pH1.2 (**Figure 4.8A**), with rapid decrease in concentration. This phenomenon is called "spring effect" and can be attributed to the quick conversion of cocrystallized QUE to more soluble metastable solid phases, which tends to solubilize and recrystallize rapidly in a short period of time, producing a concentration peak in dissolution curve. On the other hand, at quasi-neutral pH (**Figure 4.8B**), the GAS produced cocrystal showed a controlled QUE delivery due to the "spring and parachute" mechanism, which is characterized by the gradual transformation of cocrystallized QUE to metastable solid forms, following the Ostwald's Law of Stages ("parachute")(BAVISHI; BORKHATARIA, 2016).

The better cocrystal characteristics provided by GAS method, such as purity, yield surface area, particle size, and dissolution performance, suggests this high-pressure procedure and an alternative to produce QUE/PRO cocrystals, with useful various applications in pharmaceutical and food industries. The present results enlighten the role of the process variables (pressure, temperature, and ratio between the parent components) on the cocrystal characteristics, and can be useful for the cocrystallization of similar molecules such as flavonoids and amino acids, by using GAS or SAS methods.
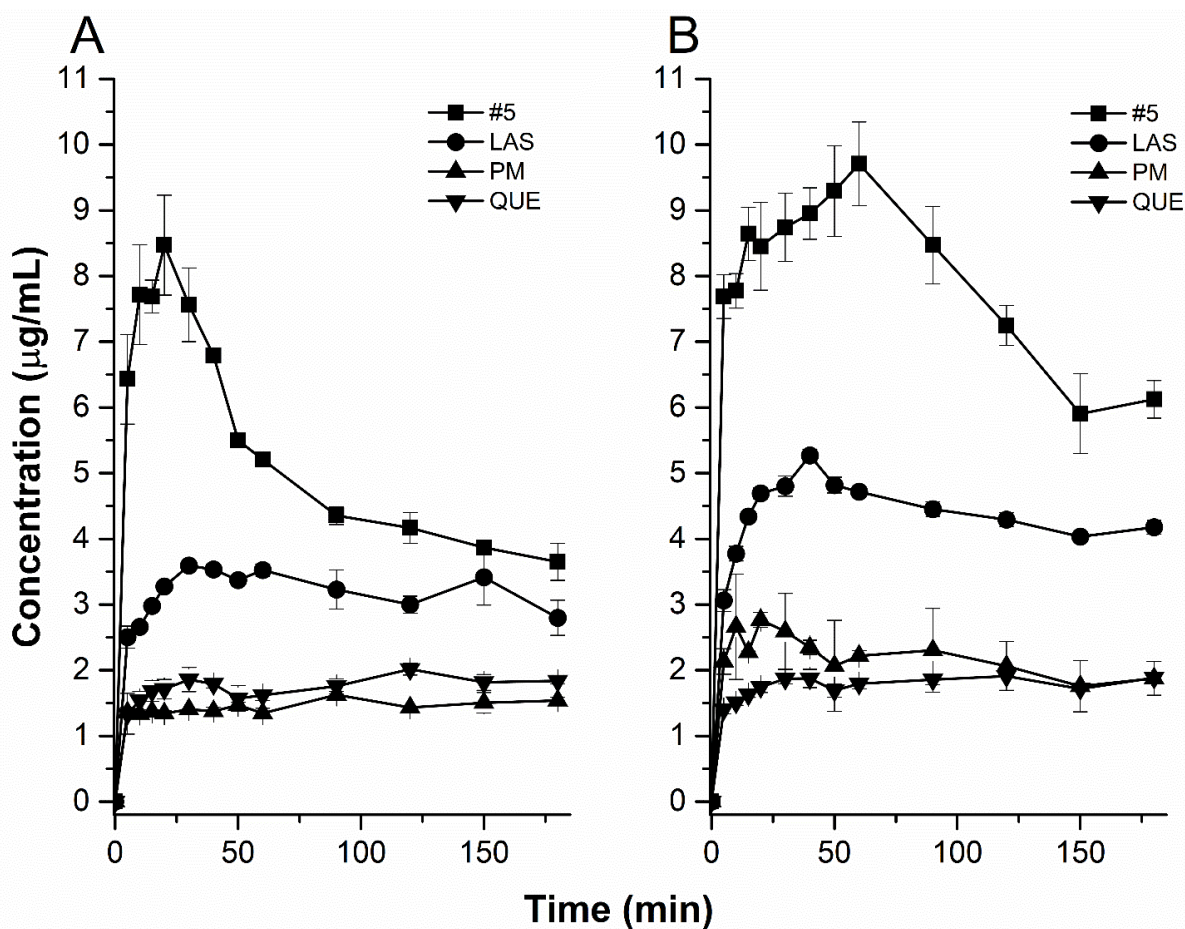
**Figure 4.8** - Dissolution profiles of (■) sample #5, (●) LAS sample, (▲) physical mixture, and (▼) commercially supplied QUE in (A) HCl solution (0.1 M, pH 1.2) and (B) phosphate buffer (pH 6.8) at 37 °C.

## 4.4 CONCLUSIONS

The production of QUE/PRO cocrystals by the GAS method at different process conditions was explored for first time. The 1:2 QUE/PRO cocrystals were successfully produced and characterized. The influence of temperature, pressure, and quercetin-to-nicotinamide ratio of the GAS method was not relevant to modify the type and/or polymorphism of the cocrystal produced, within the processing conditions studied. The ratio between QUE and PRO was the variable that most influenced the cocrystal characteristics, increasing yield and purity, reducing the particle size and providing powders with appropriated surface area. The use of GAS method with $CO_2$ and ethanol (solvent) was effective to produce 1:2 QUE/PRO cocrystals with higher yield compared to that obtained by conventional cocrystallization (LAS).

Dissolution behavior at different pH values showed better performance of GAS produced cocrystals (higher QUE dissolution) compared with LAS produced cocrystal and pure quercetin. Also, GAS process proved to be a viable alternative to LAS process, because it provided powders with better characteristics, as improved yield, and suitable particle size and surface area. GAS showed also be a better solution to process QUE/PRO cocrystals due to its advantage from the unit operation viewpoint, because GAS processing allows produce powders with adequate properties in a single step, while for LAS processing, additional unit operations, such as centrifugation, drying, and milling, are necessary to obtain the final product. Besides, at moderate temperatures, GAS is an eco-friendly process (about 90% of the solvent used is a renewable green solvent, the $CO_2$). Finally, the study expands the use $CO_2$-based methods for cocrystallization, contributing for the knowledge of factors that affect cocrystallization outcome and promoting the development of new QUE formulation strategies by cocrystallization.

**CHAPTER 5 COMPARISON BETWEEN QUERCETIN COCRYSTALS AND THEIR OBTAINING ROUTES**

One of the most important goals on the study of new routes for cocrystallization is to drawn general conclusions based on a few experiments performed with some key molecules (model compounds). The coformers used in this study (NIC and PRO) were selected because of their distinct chemical groups and per consequence, different type of association with QUE. NIC is a pyridinecarboxamide, which is capable to form hydrogen bonding with QUE using the nitrogen in pyridine ring and the amide group. While PRO forms charge-assisted hydrogen bonding with QUE by carboxylate group. Also, these chemical differences result in distinct solubility behaviors, which are essential to understand the role of solubility relationships between former components at cocrystallization by SC-$CO_2$ antisolvent methods. Although our study does not encompass a deep investigation about the role of the parent components solubilities on the success of cocrystallizations by SC-$CO_2$ antisolvent methods, our findings can be considered as a starting point to explore coformers with different solubilities on SC-$CO_2$ + organic solvent, providing qualitative insights about their possible relationships to form cocrystals.

As mentioned at Chapter 2, the success of cocrystallization routes based on solution methods is strongly influenced by the difference between the cocrystal formers (parent components) in a determined solvent or solvent/antisolvent mixture. If the solubility difference between the precursors is too large, the cocrystal formation is unlikely, because one of them will precipitate first, being no longer available to form cocrystal from the bulk solution. This limitation is the main disadvantage of conventional solution methods such as evaporation and liquid antisolvent. In literature, SC-$CO_2$ antisolvent methods, such as supercritical fluid enhanced atomization (SEA), have been claimed as an alternative to overcome this issue kinetically, surpassing the barrier of solubility difference by fast precipitation (PADRELA *et al.*, 2014). However, SC-$CO_2$ antisolvent methods, such as SEA and GAS, are also solution-based methods, i.e., the cocrystal is formed by saturating a parental solution with $CO_2$. Therefore, the issues originated from solubility difference can also be present. In our perspective, SC-$CO_2$ antisolvent methods probably do not work for any barrier of solubility (difference of solubility), and there must be some solubility difference that is unlikely to be kinetically overcome.

In fact, for the mixture of QUE/NIC processed with ethanol as solvent, no cocrystal was formed (**Figure A.4**), but rather a mixture of the parent components (rich in QUE) was obtained. While, for QUE/NIC mixture processed using acetone, cocrystals were obtained by all experimental conditions (**Figure 3.2**). These two mixtures are useful examples of systems with different degree of incongruency (solubility difference). The QUE/NIC mixture in ethanol is very incongruent (large solubility difference), at room conditions, NIC is about 29-times more soluble than QUE. Whereas, the acetonic mixture of QUE/NIC is less incongruent, the NIC solubility is 2.3-times higher than QUE solubility (CHEBIL *et al.*, 2007; OUYANG *et al.*, 2018; RAZMARA; DANESHFAR; SAHRAEI, 2010).

Comparing our results from GAS route with SEA procedure proposed by Padrela et al. (2014), the GAS processing (the present work) had inferior capacity in overcoming high incongruency. The solubility difference around 30 (QUE/NIC in ethanol) was probably too much to be surpassed by GAS, while for SEA, solubility differences with a factor of 38 could be overcome, resulting in pure cocrystals. In our study, the supersaturating condition provided by fixed $CO_2$ flow rate at 10 mL.min$^{-1}$ was probably fast enough to surpass kinetically just the low solubility difference of the QUE/NIC mixture in acetone. Therefore, for positive effect in the high incongruent system such as QUE/NIC mixture in ethanol, probably faster saturation conditions need to be achieved. By increasing the $CO_2$ flow rate, or in essence, the supersaturation rate, faster saturating conditions can be obtained, which may result in positive impact on processing of high incongruent systems. However, further investigation should be performed to determine the role of flow rate increments on the rate of supersaturation, and its capacity to surpass solubility barriers of systems with high incongruent behavior.

It is important bear in mind that the current methods capable to handle with systems with high solubility differences, such as SEA and spray-dry, work by instantaneous atomization of solution droplets, thus the mass transfer at these methods is very fast and it is improbable to achieve the rate of supersaturation obtained by GAS method. However, significant increase in supersaturation may be achieved by using mass transfer enhancers, such as impellers with different geometries, or applying different methods of $CO_2$ feeding, or even by associating GAS method with ultrasound treatment.

Another interesting outcome is related to the way the GAS processing deals with excess amounts of parent components in relation to the stoichiometry of the formed cocrystal. Processing QUE/PRO cocrystal with an excess amount of QUE (1:1 mol ratio) in relation to

the cocrystal stoichiometry (1:2 mol ratio) leads to impure powders (cocrystal + QUE). Once QUE has low solubility in $CO_2$ and $CO_2$+ethanol, it remains in the powders after processing. Otherwise, the processing of QUE/NIC cocrystal with NIC in excess leads to pure cocrystal samples, i.e., the system discards any excess amount of NIC (1:2 molar ratio) in relation to the cocrystal stoichiometry that the system is prone to form (1:1 molar ratio), because of the moderate solubility of NIC in $CO_2$ and $CO_2$+acetone.

This latter finding is especially useful for the discovery of new cocrystal forms produced by GAS method. At screening steps, the use of different molar ratios of coformers with moderate solubility in $CO_2$ and $CO_2$ + organic solvent can be advantageous because the excess amount of coformer in relation to cocrystal stoichiometry can be removed from samples if it is not cocrystallized. This may provide purer samples, facilitating the characterization steps, once less analytic signals will be present in the samples, which can expand the possibilities to discover new forms.

**CHAPTER 6 FINAL CONSIDERATIONS**

6.1 CONCLUDING REMARKS

In this work, a new $CO_2$-based preparation route for quercetin cocrystals was explored for the first time. This contribution comprises the development of new procedures for two different quercetin (QUE) cocrystals: (i) quercetin/nicotinamide (QUE/NIC) and (ii) quercetin/L-proline (QUE/PRO), as well as the study of effect of processing parameters pressure, temperature, and QUE-to-coformer molar ratio on the characteristics of the QUE cocrystals.

Both formed QUE cocrystals could be prepared by using supercritical antisolvent technology (the GAS method). However, the role of process parameters on some cocrystal characteristics was quite distinct depending of the quercetin cocrystal. For the QUE/NIC cocrystal, regardless of the level of process parameters, high purity QUE/NIC cocrystals were produced. While for the QUE/PRO cocrystal, samples with high cocrystal purity were obtained only using a QUE-to-PRO ratio equal to 1:2.

The production routes proposed here provided high yields for both cocrystal systems. For both, the QUE-to-coformer ratio was the parameter that most influenced the yield, providing higher yields increasing the ratio, or in essence, reducing the overall concentration. As yield, particle size was also strongly affected by the ratio between the parent components. For both cocrystals systems, the increase in the QUE-to-coformer ratio (i.e., decrease in overall concentration) provided cocrystals with smallest particle size.

Regarding the QUE/NIC cocrystal, its confirmation and characterization was challenging because of the absence of determined crystal structure. Despite that, by combining PXRD, DSC, TGA, Raman spectroscopy, SEM, HPLC, and elemental analysis, it was possible to assure the cocrystal formation and its stoichiometry.

Also, both GAS-produced QUE cocrystals showed suitable dissolution performance in simulated gastrointestinal environment (pH 1.2 and pH 6.8), being capable to achieve and maintain high supersaturated QUE levels for significant time interval.

This study consisted of an unprecedent investigation, focused on the development of an alternative platform for the production of quercetin cocrystals using environmental-friendly technologies involving $CO_2$. It was possible to look into role the process variables related to GAS cocrystallization and comprehend their effect in the final properties of the QUE cocrystals.

The pioneerism of this work can be used to expand the possibility of obtaining other QUE cocrystals with other coformers having moderated to negligible solubility in supercritical phase. Besides, our findings can be helpful for the development of new procedures for cocrystallization of other polyphenols by GAS processing, providing fundamental knowledge for the success of these further procedures. Finally, our findings can help drive the $CO_2$-usage and supercritical fluid technology towards nobler applications, expanding the spectrum of applications for quercetin as well.

## 6.2 FUTURE WORKS

Considering the outcomes presented in the present work, some general ideas are presented for complementary investigation:

- To produce single crystals of QUE/NIC cocrystal and to solve its crystal structure.
- To investigate the role of other process parameters, such as $CO_2$ flow, stirring, and pressurization rate on the characteristics of QUE cocrystals.
- To develop a multivariate calibration model based on PXRD and Raman data for precise quantification of QUE cocrystal in mixtures of the parent materials.
- To study the kinetics of cocrystallization for QUE cocrystals processed by GAS.
- To investigate the *in vivo* bioavailability of GAS-processed QUE cocrystals.
- To evaluate the stability of QUE cocrystal on food simulants (lipophilic and hydrophilic).

# REFERENCES

ABRAMOV, Yuriy A.; LOSCHEN, Christoph; KLAMT, Andreas. Rational Coformer or Solvent Selection for Pharmaceutical Cocrystallization or Desolvation. **Journal of Pharmaceutical Sciences**, [*s. l.*], v. 101, n. 10, p. 3687–3697, 2012.

ADITYA, N.P. *et al.* Development and evaluation of lipid nanocarriers for quercetin delivery: A comparative study of solid lipid nanoparticles (SLN), nanostructured lipid carriers (NLC), and lipid nanoemulsions (LNE). **LWT - Food Science and Technology**, [*s. l.*], v. 59, n. 1, p. 115–121, 2014.

AGUILAR-VELOZ, Laura Maryoris *et al.* Application of essential oils and polyphenols as natural antimicrobial agents in postharvest treatments: Advances and challenges. **Food Science & Nutrition**, [*s. l.*], v. 8, n. 6, p. 2555–2568, 2020.

AHUJA, Dipali *et al.* Microwave assisted slurry conversion crystallization for manufacturing of new co-crystals of sulfamethazine and sulfamerazine. **CrystEngComm**, [*s. l.*], v. 22, n. 8, p. 1381–1394, 2020a.

AHUJA, Dipali *et al.* Solution and calorimetric thermodynamic study of a new 1 : 1 sulfamethazine–3-methylsalicylic acid co-crystal. **CrystEngComm**, [*s. l.*], v. 22, n. 20, p. 3463–3473, 2020b.

ALESSI, P. *et al.* Supercritical antisolvent precipitation of quercetin systems: Preliminary experiments. **Chemical and Biochemical Engineering Quarterly**, [*s. l.*], v. 26, n. 4, p. 391–398, 2012.

ALHALAWEH, Amjad *et al.* Theophylline Cocrystals Prepared by Spray Drying: Physicochemical Properties and Aerosolization Performance. **AAPS PharmSciTech**, [*s. l.*], v. 14, n. 1, p. 265–276, 2013.

ALHALAWEH, Amjad; VELAGA, Sitaram P. Formation of Cocrystals from Stoichiometric Solutions of Incongruently Saturating Systems by Spray Drying. **Crystal Growth & Design**, [*s. l.*], v. 10, n. 8, p. 3302–3305, 2010.

ALMEIDA, A. Filipa *et al.* Bioavailability of Quercetin in Humans with a Focus on Interindividual Variation. **Comprehensive Reviews in Food Science and Food Safety**, [*s. l.*], v. 17, n. 3, p. 714–731, 2018.

ALXNEIT, Ivo. Particle Size Distributions from Electron Microscopy Images: Avoiding Pitfalls. **The Journal of Physical Chemistry A**, [*s. l.*], v. 124, n. 48, p. 10075–10081, 2020.

AMANI, Mitra; SAADATI ARDESTANI, Nedasadat; MAJD, Navid Yeganeh. Utilization of supercritical CO2 gas antisolvent (GAS) for production of Capecitabine nanoparticles as anti-cancer drug: Analysis and optimization of the process conditions. **Journal of CO2 Utilization**, [*s. l.*], v. 46, p. 101465, 2021.

ANWAR, S; CARROLL, J J. **Carbon Dioxide Thermodynamic Properties Handbook**. Beverly, MA: Scrivener Publishing, 2015-. ISSN 1098-6596.v. 1

APSHINGEKAR, Prafulla P. *et al.* Synthesis of Caffeine/Maleic Acid Co-crystal by Ultrasound-assisted Slurry Co-crystallization. **Journal of Pharmaceutical Sciences**, [*s. l.*], v. 106, n. 1, p. 66–70, 2017.

BABU, N. Jagadeesh; NANGIA, Ashwini. Solubility Advantage of Amorphous Drugs and Pharmaceutical Cocrystals. **Crystal Growth & Design**, [*s. l.*], v. 11, n. 7, p. 2662–2679, 2011. Disponível em: https://pubs.acs.org/doi/10.1021/cg200492w.

BALBINOT FILHO, C.A. *et al.* Precipitation of quercetin and nicotinamide in carbon dioxide + ethanol systems at high pressures: Phase equilibrium data for antisolvent processes. **Fluid Phase Equilibria**, [*s. l.*], v. 533, 2021.

BAVISHI, Dhara D.; BORKHATARIA, Chetan H. Spring and parachute: How cocrystals enhance solubility. **Progress in Crystal Growth and Characterization of Materials**, [*s. l.*], v. 62, n. 3, p. 1–8, 2016. Disponível em: https://linkinghub.elsevier.com/retrieve/pii/S0960897416300584.

BAZYLIŃSKA, Urszula *et al.* Engineering of phosphatidylcholine-based solid lipid nanocarriers for flavonoids delivery. **Colloids and Surfaces A: Physicochemical and Engineering Aspects**, [*s. l.*], v. 460, p. 483–493, 2014.

BERRY, David J.; STEED, Jonathan W. Pharmaceutical cocrystals, salts and multicomponent systems; intermolecular interactions and property based design. **Advanced Drug Delivery Reviews**, [*s. l.*], v. 117, p. 3–24, 2017.

BHALLA, Yashika *et al.* Daidzein cocrystals: An opportunity to improve its biopharmaceutical parameters. **Heliyon**, [*s. l.*], v. 5, n. 11, p. e02669, 2019.

BOLLA, Geetha; NANGIA, Ashwini. Pharmaceutical cocrystals: walking the talk. **Chemical Communications**, [*s. l.*], v. 52, n. 54, p. 8342–8360, 2016. Disponível em: http://xlink.rsc.org/?DOI=C6CC02943D.

BOND, Andrew D. Fundamental Aspects of Salts and Co-crystals. *Em*: WOUTERS, Johan; QUÉRÉ, Luc (org.). **Pharmaceutical Salts and Co-crystals**. Cambridge, UK: RSC Publishing, 2012. p. 9–28.

BORGHETTI, G.S. *et al.* Physicochemical properties and thermal stability of quercetin hydrates in the solid state. **Thermochimica Acta**, [*s. l.*], v. 539, 2012.

BRUNNER, Gerd. Applications of Supercritical Fluids. **Annual Review of Chemical and Biomolecular Engineering**, [*s. l.*], v. 1, n. 1, p. 321–342, 2010.

BUČAR, Dejan-Krešimir *et al.* A 1:1 Cocrystal of Caffeine and 2-Hydroxy-1-Naphthoic Acid Obtained via a Slurry Screening Method. **Journal of Chemical Crystallography**, [*s. l.*], v. 40, n. 11, p. 933–939, 2010.

BULE, Mohammed *et al.* Antidiabetic effect of quercetin: A systematic review and meta-analysis of animal studies. **Food and Chemical Toxicology**, [*s. l.*], v. 125, n. November 2018, p. 494–502, 2019.

BYRNE, Fergal P. *et al.* Tools and techniques for solvent selection: green solvent selection guides. **Sustainable Chemical Processes**, [*s. l.*], v. 4, n. 1, p. 7, 2016.

CÁRCAMO, J. J. *et al.* Proline and hydroxyproline deposited on silver nanoparticles. A Raman, SERS and theoretical study. **Journal of Raman Spectroscopy**, [*s. l.*], v. 43, n. 6, p. 750–755, 2012.

CARRAGETA, David F. *et al.* Anti-obesity potential of natural methylxanthines. **Journal of Functional Foods**, [*s. l.*], v. 43, p. 84–94, 2018.

CASTRO, Jose L. *et al.* Surface-enhanced Raman scattering of picolinamide, nicotinamide, and isonicotinamide: Unusual carboxamide deprotonation under adsorption on silver nanoparticles. **Journal of Colloid and Interface Science**, [*s. l.*], v. 396, p. 95–100, 2013.

CHADHA, Kunal *et al.* Cocrystals of Hesperetin: Structural, Pharmacokinetic, and Pharmacodynamic Evaluation. **Crystal Growth & Design**, [*s. l.*], v. 17, n. 5, p. 2386–2405, 2017. Disponível em: http://pubs.acs.org/doi/10.1021/acs.cgd.6b01769.

CHAFER, Amparo *et al.* Solubility of quercetin in supercritical $CO_2$ + ethanol as a modifier: Measurements and thermodynamic modelling. **Journal of Supercritical Fluids**, [*s. l.*], v. 32, n. 1–3, p. 89–96, 2004.

CHANG, Chiehming J. *et al.* Densities and P-x-y diagrams for carbon dioxide dissolution in methanol, ethanol, and acetone mixtures. **Fluid Phase Equilibria**, [*s. l.*], v. 131, n. 1–2, 1997.

CHANG, Yun-Ping; TANG, Muoi; CHEN, Yan-Ping. Micronization of sulfamethoxazole using the supercritical anti-solvent process. **Journal of Materials Science**, [*s. l.*], v. 43, n. 7, p. 2328–2335, 2008.

CHAVAN, Rahul B. *et al.* Continuous manufacturing of co-crystals: challenges and prospects. **Drug Delivery and Translational Research**, [*s. l.*], v. 8, n. 6, p. 1726–1739, 2018.

CHEBIL, Latifa *et al.* Solubility of Flavonoids in Organic Solvents. **Journal of Chemical & Engineering Data**, [*s. l.*], v. 52, n. 5, p. 1552–1556, 2007. Disponível em: https://pubs.acs.org/doi/10.1021/je7001094.

CHEN, Lei *et al.* A review on advanced microencapsulation technology to enhance bioavailability of phenolic compounds: Based on its activity in the treatment of Type 2 Diabetes. **Trends in Food Science and Technology**, [*s. l.*], v. 85, n. November 2018, p. 149–162, 2019.

CHEN, Lei; CAO, Hui; XIAO, Jianbo. Polyphenols: absorption, bioavailability, and metabolomics. *Em*: GALANAKIS, Charis M. (org.). **Polyphenols: Properties, Recovery, and Applications**. Duxford, UK: Woodhead Publishing, 2018. p. 45–67.

CHEN, Yan-Ping; CHEN, Yen-Ming; TANG, Muoi. Solubilities of cinnamic acid, phenoxyacetic acid and 4-methoxyphenylacetic acid in supercritical carbon dioxide. **Fluid Phase Equilibria**, [*s. l.*], v. 275, n. 1, p. 33–38, 2009.

CHEN, Chen; ZHOU, Jane; JI, Chunyan. Quercetin: A potential drug to reverse multidrug resistance. **Life Sciences**, [*s. l.*], v. 87, n. 11–12, p. 333–338, 2010.

CHERUKUVADA, Suryanarayan; GURU ROW, Tayur N. Comprehending the Formation of Eutectics and Cocrystals in Terms of Design and Their Structural Interrelationships. **Crystal Growth & Design**, [*s. l.*], v. 14, n. 8, 2014.

CHIKHALIA, V. *et al.* The effect of crystal morphology and mill type on milling induced crystal disorder. **European Journal of Pharmaceutical Sciences**, [*s. l.*], v. 27, n. 1, p. 19–26, 2006.

CHIU, Hung-Yu; LEE, Ming-Jer; LIN, Ho-mu. Vapor−Liquid Phase Boundaries of Binary Mixtures of Carbon Dioxide with Ethanol and Acetone. **Journal of Chemical & Engineering Data**, [*s. l.*], v. 53, n. 10, p. 2393–2402, 2008.

CORNARD, J P; MERLIN, J C. Spectroscopic and structural study of complexes of quercetin with Al(III). **Journal of inorganic biochemistry**, [*s. l.*], v. 92, n. 1, p. 19–27, 2002.

CUADRA, Isaac A. *et al.* Pharmaceutical co-crystals of the anti-inflammatory drug diflunisal and nicotinamide obtained using supercritical CO2 as an antisolvent. **Journal of CO2 Utilization**, [*s. l.*], v. 13, p. 29–37, 2016.

CUADRA, Isaac A. *et al.* Polymorphism in the co-crystallization of the anticonvulsant drug carbamazepine and saccharin using supercritical CO2 as an anti-solvent. **The Journal of Supercritical Fluids**, [*s. l.*], v. 136, n. December 2017, p. 60–69, 2018. Disponível em: https://doi.org/10.1016/j.supflu.2018.02.004.

CUI, Wenxia *et al.* Naringenin Cocrystals Prepared by Solution Crystallization Method for Improving Bioavailability and Anti-hyperlipidemia Effects. **AAPS PharmSciTech**, [*s. l.*], v. 20, n. 3, p. 115, 2019.

DAI, Xia-Lin; CHEN, Jia-Mei; LU, Tong-Bu. Pharmaceutical cocrystallization: an effective approach to modulate the physicochemical properties of solid-state drugs. **CrystEngComm**, [*s. l.*], v. 20, n. 36, p. 5292–5316, 2018.

D'ANDREA, Gabriele. Quercetin: A flavonol with multifaceted therapeutic applications?. **Fitoterapia**, [*s. l.*], v. 106, p. 256–271, 2015. Disponível em: http://dx.doi.org/10.1016/j.fitote.2015.09.018.

DIAS, Maria Inês; FERREIRA, Isabel C. F. R.; BARREIRO, Maria Filomena. Microencapsulation of bioactives for food applications. **Food & Function**, [*s. l.*], v. 6, n. 4, p. 1035–1052, 2015.

DIAS, Jônatas Lopes; LANZA, Marcelo; FERREIRA, Sandra R.S. Cocrystallization: A tool to modulate physicochemical and biological properties of food-relevant polyphenols. **Trends in Food Science & Technology**, [*s. l.*], v. 110, p. 13–27, 2021. Disponível em: https://linkinghub.elsevier.com/retrieve/pii/S0924224421000352.

DOUROUMIS, Dennis; ROSS, Steven A.; NOKHODCHI, Ali. Advanced methodologies for cocrystal synthesis. **Advanced Drug Delivery Reviews**, [*s. l.*], v. 117, p. 178–195, 2017.

ESFANDIARI, Nadia; GHOREISHI, Seyyed M. Ampicillin Nanoparticles Production via Supercritical CO2 Gas Antisolvent Process. **AAPS PharmSciTech**, [*s. l.*], v. 16, n. 6, p. 1263–1269, 2015.

ESFANDIARI, Nadia; GHOREISHI, Seyyed M. Synthesis of 5-Fluorouracil nanoparticles via supercritical gas antisolvent process. **The Journal of Supercritical Fluids**, [*s. l.*], v. 84, p. 205–210, 2013.

FÁBIÁN, László. Cambridge Structural Database Analysis of Molecular Complementarity in Cocrystals. **Crystal Growth & Design**, [*s. l.*], v. 9, n. 3, p. 1436–1443, 2009.

FAN, Guoling *et al.* Molecular cocrystals of diphenyloxazole with tunable fluorescence, up-conversion emission and dielectric properties. **CrystEngComm**, [*s. l.*], v. 18, n. 2, p. 240–249, 2016.

FDA. **FDA Guidance for Industry. Q3C - Tables and list**. [*S. l.*]: U.S. Department of Health and Human Services Food and Drug Administration, 2018.

FDA. **FDA Guidance for industry. Q3C Impurities: Residual Solvents**. [*S. l.*]: U.S. Department of Health and Human Services Food and Drug Administration, 1997.

FILIP, Xenia *et al.* NMR crystallography methods to probe complex hydrogen bonding networks: application to structure elucidation of anhydrous quercetin. **CrystEngComm**, [*s. l.*], v. 15, n. 20, p. 4131, 2013.

FRAGA, César G. *et al.* The effects of polyphenols and other bioactives on human health. **Food & Function**, [*s. l.*], v. 10, n. 2, p. 514–528, 2019.

FRANCO, Paola *et al.* Supercritical Adsorption of Quercetin on Aerogels for Active Packaging Applications. **Industrial & Engineering Chemistry Research**, [*s. l.*], v. 57, n. 44, p. 15105–15113, 2018. Disponível em: https://pubs.acs.org/doi/10.1021/acs.iecr.8b03666.

FRISCIC, Tomas; JONES, William. Application of Mechanochemistry in the Synthesis and Discovery of New Pharmaceutical Forms: Co-crystals, Salts and Coordination Compounds. *Em*: WOUTERS, Johan; QUÉRÉ, Luc (org.). **Pharmaceutical Salts and Co-crystals**. Cambridge, UK: RSC Publishing, 2012. p. 154–187.

GAJDA, Maciej *et al.* Continuous, one-step synthesis of pharmaceutical cocrystals via hot melt extrusion from neat to matrix-assisted processing – State of the art. **International Journal of Pharmaceutics**, [*s. l.*], v. 558, n. January, p. 426–440, 2019a.

GAJDA, Maciej *et al.* Tuning the cocrystal yield in matrix-assisted cocrystallisation via hot melt extrusion: A case of theophylline-nicotinamide cocrystal. **International Journal of Pharmaceutics**, [*s. l.*], v. 569, p. 118579, 2019b.

GALLAGHER, P. M. *et al.* Gas Antisolvent Recrystallization: New Process To Recrystallize Compounds Insoluble in Supercritical Fluids. *Em*: JOHNSTON, K; PENNINGER, J (org.). **Supercritical Fluid Science and Technology**. [*S. l.*]: American Chemical Society, 1989. p. 334–354.

GALLAGHER, Paula M. *et al.* Gas anti-solvent recrystallization of RDX: Formation of ultra-fine particles of a difficult-to-comminute explosive. **The Journal of Supercritical Fluids**, [*s. l.*], v. 5, n. 2, p. 130–142, 1992.

GARCÍA-CASAS, Ignacio *et al.* Foaming of Polycaprolactone and Its Impregnation with Quercetin Using Supercritical $CO_2$. **Polymers**, [*s. l.*], v. 11, n. 9, p. 1390, 2019.

GUGLER, R.; LESCHIK, M.; DENGLER, H. J. Disposition of quercetin in man after single oral and intravenous doses. **European Journal of Clinical Pharmacology**, [*s. l.*], v. 9, n. 2–3, p. 229–234, 1975.

GUNAWARDANA, C. A.; AAKERÖY, C. B. Co-crystal synthesis: fact, fancy, and great expectations. **Chemical Communications**, [*s. l.*], v. 54, n. 100, p. 14047–14060, 2018.

HE, Hongyan *et al.* Modulating the Dissolution and Mechanical Properties of Resveratrol by Cocrystallization. **Crystal Growth & Design**, [*s. l.*], v. 17, n. 7, p. 3989–3996, 2017a.

HE, Hongyan *et al.* Structure, physicochemical properties and pharmacokinetics of resveratrol and piperine cocrystals. **CrystEngComm**, [*s. l.*], v. 19, n. 41, p. 6154–6163, 2017b.

HE, Hongyan *et al.* Zwitterionic Cocrystals of Flavonoids and Proline: Solid-State Characterization, Pharmaceutical Properties, and Pharmacokinetic Performance. **Crystal Growth & Design**, [*s. l.*], v. 16, n. 4, p. 2348–2356, 2016. Disponível em: https://pubs.acs.org/doi/10.1021/acs.cgd.6b00142.

HORIBA SCIENTIFIC. **A Guidebook to particle size analysis**. Irvine, CA: Horiba Instruments, 2010.

HUANG, Yanting *et al.* Baicalein–Nicotinamide Cocrystal with Enhanced Solubility, Dissolution, and Oral Bioavailability. **Journal of Pharmaceutical Sciences**, [*s. l.*], v. 103, n. 8, p. 2330–2337, 2014.

HUANG, Yaohui *et al.* Cocrystal Solubility Advantage Diagrams as a Means to Control Dissolution, Supersaturation, and Precipitation. **Molecular Pharmaceutics**, [*s. l.*], v. 16, n. 9, p. 3887–3895, 2019.

HUANG, Shan *et al.* Facile Tuning of the Photoluminescence and Dissolution Properties of Phloretin through Cocrystallization. **Crystal Growth & Design**, [*s. l.*], v. 19, n. 12, p. 6837–6844, 2019a.

HUANG, Shan *et al.* Simultaneously Improving the Physicochemical Properties, Dissolution Performance, and Bioavailability of Apigenin and Daidzein by Co-Crystallization With Theophylline. **Journal of Pharmaceutical Sciences**, [*s. l.*], v. 108, n. 9, p. 2982–2993, 2019b.

INTERNATIONAL ORGANIZATION FOR STANDARDIZATION. **Determination of the specific surface area of solids by gas adsorption — BET method (ISO 9277:2010)**. [*S. l.: s. n.*], 2010.

JAFARI, Dariush *et al.* Gas-Antisolvent (GAS) Crystallization of Aspirin Using Supercritical Carbon Dioxide: Experimental Study and Characterization. **Industrial & Engineering Chemistry Research**, [*s. l.*], v. 54, n. 14, p. 3685–3696, 2015. Disponível em: https://pubs.acs.org/doi/10.1021/ie5046445.

JESSOP, Philip G.; SUBRAMANIAM, Bala. Gas-Expanded Liquids. **Chemical Reviews**, [*s. l.*], v. 107, n. 6, p. 2666–2694, 2007. Disponível em: https://pubs.acs.org/doi/10.1021/cr040199o.

JOHANNSEN, Monika; BRUNNER, Gerd. Solubilities of the xanthines caffeine, theophylline and theobromine in supercritical carbon dioxide. **Fluid Phase Equilibria**, [*s. l.*], v. 95, p. 215–226, 1994.

KALE, Dnyaneshwar P.; ZODE, Sandeep S.; BANSAL, Arvind K. Challenges in Translational Development of Pharmaceutical Cocrystals. **Journal of Pharmaceutical Sciences**, [*s. l.*], v. 106, n. 2, p. 457–470, 2017.

KARAGIANNI, Anna; MALAMATARI, Maria; KACHRIMANIS, Kyriakos. Pharmaceutical cocrystals: New solid phase modification approaches for the formulation of APIs. **Pharmaceutics**, [*s. l.*], v. 10, n. 1, p. 1–30, 2018.

KARIMI-JAFARI, Maryam *et al.* Creating cocrystals: A review of pharmaceutical cocrystal preparation routes and applications. review-article. **Crystal Growth and Design**, [*s. l.*], v. 18, n. 10, p. 6370–6387, 2018a.

KARIMI-JAFARI, Maryam *et al.* Creating Cocrystals: A Review of Pharmaceutical Cocrystal Preparation Routes and Applications. review-article. **Crystal Growth and Design**,

[*s. l.*], v. 18, n. 10, p. 6370–6387, 2018b. Disponível em: https://pubs.acs.org/doi/10.1021/acs.cgd.8b00933.

KETKAR, Sameer *et al.* Tracing the Architecture of Caffeic Acid Phenethyl Ester Cocrystals: Studies on Crystal Structure, Solubility, and Bioavailability Implications. **Crystal Growth & Design**, [*s. l.*], v. 16, n. 10, p. 5710–5716, 2016.

KIM, Hee-Jeong; YEO, Sang-Do. Liquid antisolvent crystallization of griseofulvin from organic solutions. **Chemical Engineering Research and Design**, [*s. l.*], v. 97, p. 68–76, 2015.

KLITOU, Panayiotis *et al.* Solid-State Characterization and Role of Solvent Molecules on the Crystal Structure, Packing, and Physiochemical Properties of Different Quercetin Solvates. **Crystal Growth & Design**, [*s. l.*], v. 20, n. 10, p. 6573–6584, 2020.

KLITOU, Panayiotis; ROSBOTTOM, Ian; SIMONE, Elena. Synthonic Modeling of Quercetin and Its Hydrates: Explaining Crystallization Behavior in Terms of Molecular Conformation and Crystal Packing. **Crystal Growth & Design**, [*s. l.*], v. 19, n. 8, p. 4774–4783, 2019.

KOTBANTAO, Gunaree; CHAROENCHAITRAKOOL, Manop. Processing of ketoconazole–4-aminobenzoic acid cocrystals using dense CO 2 as an antisolvent. **Journal of CO2 Utilization**, [*s. l.*], v. 17, p. 213–219, 2017. Disponível em: http://dx.doi.org/10.1016/j.jcou.2016.12.007.

KOTNIK, Petra; ŠKERGET, Mojca; KNEZ, Željko. Solubility of Nicotinic Acid and Nicotinamide in Carbon Dioxide at T = (313.15 to 373.15) K and p = (5 to 30) MPa: Experimental Data and Correlation. **Journal of Chemical & Engineering Data**, [*s. l.*], v. 56, n. 2, p. 338–343, 2011. Disponível em: https://pubs.acs.org/doi/10.1021/je100697a.

KRAWCZUK, Anna; GRYL, Marlena. Qualitative and quantitative crystal engineering of multi-functional co-crystals. *Em*: TIEKINK, Edward R. T.; ZUKERMAN-SCHPECTOR, Julio (org.). **Multi-Component Crystals**. Berlim, DE: De Gruyter, 2018. p. 365.

KURNIAWANSYAH, Firman; MAMMUCARI, Raffaella; FOSTER, Neil R. Polymorphism of curcumin from dense gas antisolvent precipitation. **Powder Technology**, [*s. l.*], v. 305, p. 748–756, 2017.

LESJAK, Marija *et al.* Antioxidant and anti-inflammatory activities of quercetin and its derivatives. **Journal of Functional Foods**, [*s. l.*], v. 40, n. November 2016, p. 68–75, 2018. Disponível em: http://linkinghub.elsevier.com/retrieve/pii/S1756464617306588.

LI, Wen *et al.* A strategy to improve the oral availability of baicalein: The baicalein-theophylline cocrystal. **Fitoterapia**, [*s. l.*], v. 129, p. 85–93, 2018.

LI, Xizhen *et al.* Rich polymorphism in nicotinamide revealed by melt crystallization and crystal structure prediction. **Communications Chemistry**, [*s. l.*], v. 3, n. 1, 2020.

LI, Jing-Wen *et al.* The effect of crystal-solvent interaction on crystal growth and morphology. **Journal of Crystal Growth**, [*s. l.*], v. 507, p. 260–269, 2019.

LI, Peizhe *et al.* Two Cocrystals of Berberine Chloride with Myricetin and Dihydromyricetin: Crystal Structures, Characterization, and Antitumor Activities. **Crystal Growth & Design**, [*s. l.*], v. 20, n. 1, p. 157–166, 2020.

LIGHTSOURCES.ORG. **Light sources of the world**. [*S. l.*], 2022.

LITWACK, Gerald. Vitamins and Nutrition. *Em*: LITWACK, Gerald (org.). **Human Biochemistry**. Los Angeles, USA: Elsevier, 2018. p. 645–680.

LIU, Fang *et al.* A new cocrystal of isoniazid-quercetin with hepatoprotective effect: The design, structure, and in vitro/in vivo performance evaluation. **European Journal of Pharmaceutical Sciences**, [*s. l.*], v. 144, p. 105216, 2020.

LIU, Mingyu *et al.* Development of a pharmaceutical cocrystal with solution crystallization technology: Preparation, characterization, and evaluation of myricetin-proline cocrystals. **European Journal of Pharmaceutics and Biopharmaceutics**, [*s. l.*], v. 107, p. 151–159, 2016a.

LIU, Mingyu *et al.* The generation of myricetin–nicotinamide nanococrystals by top down and bottom up technologies. **Nanotechnology**, [*s. l.*], v. 27, n. 39, p. 395601, 2016b.

LIU, Guijin; LI, Junjian; DENG, Shiming. Applications of Supercritical Anti-Solvent Process in Preparation of Solid Multicomponent Systems. **Pharmaceutics**, [*s. l.*], v. 13, n. 4, 2021.

LONG, Barry *et al.* Generation and physicochemical characterization of posaconazole cocrystals using Gas Antisolvent (GAS) and Supercritical Solvent (CSS) methods. **The Journal of Supercritical Fluids**, [*s. l.*], v. 170, p. 105134, 2021.

LOSCHEN, Christoph; KLAMT, Andreas. Solubility prediction, solvate and cocrystal screening as tools for rational crystal engineering. **Journal of Pharmacy and Pharmacology**, [*s. l.*], v. 67, n. 6, p. 803–811, 2015.

LUO, Yumiao *et al.* Luteolin cocrystals: Characterization, evaluation of solubility, oral bioavailability and theoretical calculation. **Journal of Drug Delivery Science and Technology**, [*s. l.*], v. 50, n. September 2018, p. 248–254, 2019a.

LUO, Yumiao *et al.* Luteolin cocrystals: Characterization, evaluation of solubility, oral bioavailability and theoretical calculation. **Journal of Drug Delivery Science and Technology**, [*s. l.*], v. 50, n. September 2018, p. 248–254, 2019b.

LUO, Chun *et al.* Pharmaceutical cocrystals of naringenin with improved dissolution performance. **CrystEngComm**, [*s. l.*], v. 20, n. 22, p. 3025–3033, 2018. Disponível em: http://xlink.rsc.org/?DOI=C8CE00341F.

MACEACHERN, Lauren; KERMANSHAHI-POUR, Azadeh; MIRMEHRABI, Mahmoud. Supercritical Carbon Dioxide for Pharmaceutical Co-Crystal Production. **Crystal Growth & Design**, [*s. l.*], v. 20, n. 9, p. 6226–6244, 2020.

MACHADO, Tatiane Cogo *et al.* The role of pH and dose/solubility ratio on cocrystal dissolution, drug supersaturation and precipitation. **European Journal of Pharmaceutical Sciences**, [*s. l.*], v. 152, p. 105422, 2020.

MACRAE, Clare F. *et al.* Mercury 4.0 : from visualization to analysis, design and prediction. **Journal of Applied Crystallography**, [*s. l.*], v. 53, n. 1, p. 226–235, 2020.

MALAMATARI, Maria *et al.* Experimental cocrystal screening and solution based scale-up cocrystallization methods. **Advanced Drug Delivery Reviews**, [*s. l.*], v. 117, p. 162–177, 2017. Disponível em: https://doi.org/10.1016/j.addr.2017.08.006.

MARTINS, Artur J. *et al.* Edible oleogels: an opportunity for fat replacement in foods. **Food & Function**, [*s. l.*], v. 9, n. 2, p. 758–773, 2018.

MCCLEMENTS, David Julian; LI, Fang; XIAO, Hang. The Nutraceutical Bioavailability Classification Scheme: Classifying Nutraceuticals According to Factors Limiting their Oral Bioavailability. **Annual Review of Food Science and Technology**, [*s. l.*], v. 6, n. 1, p. 299–327, 2015.

MILINČIĆ, Danijel D. *et al.* Application of polyphenol-loaded nanoparticles in food industry. **Nanomaterials**, [*s. l.*], v. 9, n. 11, 2019.

MOHITE, Rohini *et al.* Synthesis of fisetin co-crystals with caffeine and nicotinamide using the cooling crystallization technique: biopharmaceutical studies. **New Journal of Chemistry**, [*s. l.*], v. 43, n. 34, p. 13471–13479, 2019.

MUKHOPADHYAY, Piyasi; PRAJAPATI, A. K. Quercetin in anti-diabetic research and strategies for improved quercetin bioavailability using polymer-based carriers – a review. **RSC Advances**, [*s. l.*], v. 5, n. 118, p. 97547–97562, 2015.

MÜLLERS, Katrin C.; PAISANA, Maria; WAHL, Martin A. Simultaneous Formation and Micronization of Pharmaceutical Cocrystals by Rapid Expansion of Supercritical Solutions (RESS). **Pharmaceutical Research**, [*s. l.*], v. 32, n. 2, p. 702–713, 2015.

MUNTÓ, Maria *et al.* Solubility behaviors of ibuprofen and naproxen drugs in liquid "CO2–organic solvent" mixtures. **The Journal of Supercritical Fluids**, [*s. l.*], v. 47, n. 2, p. 147–153, 2008.

MUSUMECI, Daniele *et al.* Virtual cocrystal screening. **Chemical Science**, [*s. l.*], v. 2, n. 5, p. 883, 2011.

NABAVI, Seyed Fazel *et al.* Role of quercetin as an alternative for obesity treatment: You are what you eat!. **Food Chemistry**, [*s. l.*], v. 179, p. 305–310, 2015.

NEUROHR, C. *et al.* Naproxen-nicotinamide cocrystals produced by CO2 antisolvent. **Journal of Supercritical Fluids**, [*s. l.*], v. 83, p. 78–85, 2013.

NIKAS, Ilias P.; PASCHOU, Stavroula A.; RYU, Han Suk. The Role of Nicotinamide in Cancer Chemoprevention and Therapy. **Biomolecules**, [*s. l.*], v. 10, n. 3, p. 477, 2020.

NOOMHORM, Athapol; AHMAD, Imran; ANAL, Anil Kumar. **Functional Foods and Dietary Supplements: Processing Effects and Health Benefits**. Chichester, UK: John Wiley & Sons, Ltd, 2014.

NUGRAHANI, Ilma; JESSICA, Maria Anabella. Amino Acids as the Potential Co-Former for Co-Crystal Development: A Review. **Molecules**, [*s. l.*], v. 26, n. 11, p. 3279, 2021.

OBER, Courtney A; GUPTA, Ram B. Formation of Itraconazole–Succinic Acid Cocrystals by Gas Antisolvent Cocrystallization. **AAPS PharmSciTech**, [*s. l.*], v. 13, n. 4, p. 1396–1406, 2012.

OBER, Courtney A.; MONTGOMERY, Stephen E.; GUPTA, Ram B. Formation of itraconazole/L-malic acid cocrystals by gas antisolvent cocrystallization. **Powder Technology**, [*s. l.*], v. 236, p. 122–131, 2013.

OÑATIBIA-ASTIBIA, Ainhoa; FRANCO, Rafael; MARTÍNEZ-PINILLA, Eva. Health benefits of methylxanthines in neurodegenerative diseases. **Molecular Nutrition & Food Research**, [*s. l.*], v. 61, n. 6, p. 1600670, 2017.

OUYANG, Jinbo *et al.* Solubility Determination of Nicotinamide and Its Application for the Cocrystallization with Benzoic Acid. **Journal of Chemical & Engineering Data**, [*s. l.*], v. 63, n. 11, p. 4157–4165, 2018. Disponível em: https://pubs.acs.org/doi/10.1021/acs.jced.8b00560.

PADRELA, Luis *et al.* Formation of indomethacin–saccharin cocrystals using supercritical fluid technology. **European Journal of Pharmaceutical Sciences**, [*s. l.*], v. 38, n. 1, p. 9–17, 2009.

PADRELA, Luis *et al.* Insight into the Mechanisms of Cocrystallization of Pharmaceuticals in Supercritical Solvents. **Crystal Growth and Design**, [*s. l.*], v. 15, n. 7, p. 3175–3181, 2015.

PADRELA, Luis *et al.* Tuning physicochemical properties of theophylline by cocrystallization using the supercritical fluid enhanced atomization technique. **The Journal of Supercritical Fluids**, [*s. l.*], v. 86, p. 129–136, 2014.

PANDO, Concepción; CABAÑAS, Albertina; CUADRA, Isaac A. Preparation of pharmaceutical co-crystals through sustainable processes using supercritical carbon dioxide: A review. **RSC Advances**, [*s. l.*], v. 6, n. 75, p. 71134–71150, 2016. Disponível em: https://pubs.rsc.org/en/content/articlepdf/2016/ra/c6ra10917a.

PARK, Su-Jin; YEO, Sang-Do. Recrystallization of caffeine using gas antisolvent process. **The Journal of Supercritical Fluids**, [*s. l.*], v. 47, n. 1, p. 85–92, 2008.

PATIL, Sharvil; CHAUDHARI, Khushbu; KAMBLE, Ravindra. Electrospray technique for cocrystallization of phytomolecules. **Journal of King Saud University - Science**, [*s. l.*], v. 30, n. 1, p. 138–141, 2018. Disponível em: https://linkinghub.elsevier.com/retrieve/pii/S1018364716307133.

PESSOA, Alcidênio S. *et al.* Precipitation of resveratrol-isoniazid and resveratrol-nicotinamide cocrystals by gas antisolvent. **The Journal of Supercritical Fluids**, [*s. l.*], v. 145, n. August 2018, p. 93–102, 2019. Disponível em: https://linkinghub.elsevier.com/retrieve/pii/S0896844618305266.

PHILLIPS, Melissa M.; RIMMER, Catherine A. Functional foods and dietary supplements. **Analytical and Bioanalytical Chemistry**, [*s. l.*], v. 405, n. 13, p. 4323–4324, 2013.

PHOTHIPANYAKUN, Sasiwimon; SUTTIKORNCHAI, Siwaporn; CHAROENCHAITRAKOOL, Manop. Dissolution rate enhancement of sulfamethoxazole using the gas anti-solvent (GAS) process. **Powder Technology**, [*s. l.*], v. 250, p. 84–90, 2013. Disponível em: http://dx.doi.org/10.1016/j.powtec.2013.10.019.

PI, Jiaxin *et al.* A nano-cocrystal strategy to improve the dissolution rate and oral bioavailability of baicalein. **Asian Journal of Pharmaceutical Sciences**, [*s. l.*], v. 14, n. 2, p. 154–164, 2019a.

PI, Jiaxin *et al.* A nano-cocrystal strategy to improve the dissolution rate and oral bioavailability of baicalein. **Asian Journal of Pharmaceutical Sciences**, [*s. l.*], v. 14, n. 2, p. 154–164, 2019b.

PIMENTEL-MORAL, S. *et al.* Lipid nanocarriers for the loading of polyphenols – A comprehensive review. **Advances in Colloid and Interface Science**, [*s. l.*], v. 260, p. 85–94, 2018.

PINDELSKA, Edyta; SOKAL, Agnieszka; KOLODZIEJSKI, Waclaw. Pharmaceutical cocrystals, salts and polymorphs: Advanced characterization techniques. **Advanced Drug Delivery Reviews**, [*s. l.*], v. 117, p. 111–146, 2017. Disponível em: https://linkinghub.elsevier.com/retrieve/pii/S0169409X17301953.

POKORNÝ, Václav *et al.* Heat Capacities of l-Histidine, l-Phenylalanine, l-Proline, l-Tryptophan and l-Tyrosine. **Molecules**, [*s. l.*], v. 26, n. 14, p. 4298, 2021.

PRAT, Denis *et al.* CHEM21 selection guide of classical- and less classical-solvents. **Green Chemistry**, [*s. l.*], v. 18, n. 1, p. 288–296, 2016.

RAJBONGSHI, Trishna *et al.* Preparation of Pyrazinamide Eutectics versus Cocrystals Based on Supramolecular Synthon Variations. **Crystal Growth & Design**, [*s. l.*], v. 18, n. 11, 2018.

RAJESH KUMAR, S. *et al.* Quercetin conjugated superparamagnetic magnetite nanoparticles for in-vitro analysis of breast cancer cell lines for chemotherapy applications. **Journal of Colloid and Interface Science**, [*s. l.*], v. 436, p. 234–242, 2014.

RAZMARA, Reza S.; DANESHFAR, Ali; SAHRAEI, Reza. Solubility of quercetin in water + methanol and water + ethanol from (292.8 to 333.8) K. **Journal of Chemical and Engineering Data**, [*s. l.*], v. 55, n. 9, p. 3934–3936, 2010.

REUTZEL-EDENS, Susan M. Analytical Techniques and Strategies for Salt/Co-crystal Characterization. *Em*: WOUTERS, Johan; QUÉRÉ, Luc (org.). **Pharmaceutical Salts and Co-crystals**. Cambridge, UK: RSC Publishing, 2012. p. 212–246.

REVELLI, Anne Laure *et al.* High-pressure solubility of naproxen, nicotinamide and their mixture in acetone with supercritical CO2 as an anti-solvent. **Fluid Phase Equilibria**, [*s. l.*], v. 373, p. 29–33, 2014.

RIBAS, Marcela M. *et al.* Curcumin-nicotinamide cocrystallization with supercritical solvent (CSS): Synthesis, characterization and in vivo antinociceptive and anti-inflammatory activities. **Industrial Crops and Products**, [*s. l.*], v. 139, p. 111537, 2019.

RODRIGUES, Marisa *et al.* Pharmaceutical cocrystallization techniques. Advances and challenges. **International Journal of Pharmaceutics**, [*s. l.*], v. 547, n. 1–2, p. 404–420, 2018. Disponível em: https://doi.org/10.1016/j.ijpharm.2018.06.024.

RODRIGUES, Miguel A. *et al.* Polymorphism in Pharmaceutical Drugs by Supercritical CO 2 Processing: Clarifying the Role of the Antisolvent Effect and Atomization Enhancement. **Crystal Growth & Design**, [*s. l.*], v. 16, n. 11, 2016.

RODRÍGUEZ-RUIZ, Christian *et al.* Tailoring Chlorthalidone Aqueous Solubility by Cocrystallization: Stability and Dissolution Behavior of a Novel Chlorthalidone-Caffeine Cocrystal. **Pharmaceutics**, [*s. l.*], v. 14, n. 2, p. 334, 2022.

ROJAS-ÁVILA, Adrián *et al.* Solubility of Binary and Ternary Systems Containing Vanillin and Vanillic Acid in Supercritical Carbon Dioxide. **Journal of Chemical & Engineering Data**, [*s. l.*], v. 61, n. 9, p. 3225–3232, 2016.

ROY, Christelle *et al.* Effect of CO2-antisolvent techniques on size distribution and crystal lattice of theophylline. **The Journal of Supercritical Fluids**, [*s. l.*], v. 57, n. 3, p. 267–277, 2011.

SAIKIA, Basanta; PATHAK, Debabrat; SARMA, Bipul. Variable stoichiometry cocrystals: occurrence and significance. **CrystEngComm**, [*s. l.*], v. 23, n. 26, p. 4583–4606, 2021.

SALAS-ZÚÑIGA, Reynaldo *et al.* Dissolution Advantage of Nitazoxanide Cocrystals in the Presence of Cellulosic Polymers. **Pharmaceutics**, [*s. l.*], v. 12, n. 1, p. 23, 2019.

SALZILLO, Tommaso *et al.* Structure, Stoichiometry, and Charge Transfer in Cocrystals of Perylene with TCNQ-F $_x$. **Crystal Growth & Design**, [*s. l.*], v. 16, n. 5, p. 3028–3036, 2016.

SAMIPILLAI, Marivel; ROHANI, Sohrab. The role of higher coformer stoichiometry ratio in pharmaceutical cocrystals for improving their solid-state properties: The cocrystals of progesterone and 4-hydroxybenzoic acid. **Journal of Crystal Growth**, [*s. l.*], v. 507, 2019.

SARKAR, Nandini; AAKERÖY, Christer B. Evaluating hydrogen-bond propensity, hydrogen-bond coordination and hydrogen-bond energy as tools for predicting the outcome of attempted co-crystallisations. **Supramolecular Chemistry**, [*s. l.*], v. 32, n. 2, p. 81–90, 2020.

SATHISARAN, Indumathi; DALVI, Sameer Vishvanath. Engineering cocrystals of poorlywater-soluble drugs to enhance dissolution in aqueous medium. **Pharmaceutics**, [*s. l.*], v. 10, n. 3, 2018.

SCHNEIDER, Caroline A; RASBAND, Wayne S; ELICEIRI, Kevin W. NIH Image to ImageJ: 25 years of image analysis. **Nature Methods**, [*s. l.*], v. 9, n. 7, p. 671–675, 2012.

SCHULTHEISS, Nate; BETHUNE, Sarah; HENCK, Jan-Olav. Nutraceutical cocrystals: utilizing pterostilbene as a cocrystal former. **CrystEngComm**, [*s. l.*], v. 12, n. 8, p. 2436, 2010.

SERRANO, Dolores R *et al.* Cocrystal habit engineering to improve drug dissolution and alter derived powder properties. **Journal of Pharmacy and Pharmacology**, [*s. l.*], v. 68, n. 5, p. 665–677, 2016.

SHIMPI, Manishkumar R. *et al.* New cocrystals of ezetimibe with <scp>l</scp> -proline and imidazole. **CrystEngComm**, [*s. l.*], v. 16, n. 38, p. 8984–8993, 2014.

SINHA, Abhijeet S.; MAGUIRE, Anita R.; LAWRENCE, Simon E. Cocrystallization of Nutraceuticals. **Crystal Growth & Design**, [*s. l.*], v. 15, n. 2, p. 984–1009, 2015.

SMITH, Adam J. *et al.* Cocrystals of quercetin with improved solubility and oral bioavailability. **Molecular Pharmaceutics**, [*s. l.*], v. 8, n. 5, p. 1867–1876, 2011.

SMITH, Adam J. *et al.* Crystal Engineering of Green Tea Epigallocatechin-3-gallate (EGCg) Cocrystals and Pharmacokinetic Modulation in Rats. **Molecular Pharmaceutics**, [*s. l.*], v. 10, n. 8, p. 2948–2961, 2013.

SOWA, Michał; ŚLEPOKURA, Katarzyna; MATCZAK-JON, Ewa. Cocrystals of fisetin, luteolin and genistein with pyridinecarboxamide coformers: Crystal structures, analysis

of intermolecular interactions, spectral and thermal characterization. **CrystEngComm**, [*s. l.*], v. 15, n. 38, p. 7696–7708, 2013.

SOWA, Michał; ŚLEPOKURA, Katarzyna; MATCZAK-JON, Ewa. Improving solubility of fisetin by cocrystallization. **CrystEngComm**, [*s. l.*], v. 16, n. 46, p. 10592–10601, 2014a.

SOWA, Michał; ŚLEPOKURA, Katarzyna; MATCZAK-JON, Ewa. Solid-state characterization and solubility of a genistein–caffeine cocrystal. **Journal of Molecular Structure**, [*s. l.*], v. 1076, p. 80–88, 2014b.

SPIZZIRRI, U.G. *et al.* Synthesis and characterization of a (+)-catechin and L-(+)-ascorbic acid cocrystal as a new functional ingredient for tea drinks. **Heliyon**, [*s. l.*], v. 5, n. 8, p. e02291, 2019.

STAHL, Egon *et al.* A Quick Method for the Microanalytical Evaluation of the Dissolving Power of Supercritical Gases. **Angewandte Chemie International Edition in English**, [*s. l.*], v. 17, n. 10, p. 731–738, 1978.

STEED, Jonathan W. The role of co-crystals in pharmaceutical design. **Trends in Pharmacological Sciences**, [*s. l.*], v. 34, n. 3, p. 186–194, 2013.

SU, Chie-Shaan. Prediction of volumetric properties of carbon dioxide-expanded organic solvents using the Predictive Soave–Redlich–Kwong (PSRK) equation of state. **The Journal of Supercritical Fluids**, [*s. l.*], v. 72, p. 223–231, 2012.

SUBRA-PATERNAULT, P. *et al.* Solvent effect on tolbutamide crystallization induced by compressed CO2 as antisolvent. **Journal of Crystal Growth**, [*s. l.*], v. 309, n. 1, p. 76–85, 2007. Disponível em: https://linkinghub.elsevier.com/retrieve/pii/S0022024807007646.

SUN, Chongde *et al.* Dietary polyphenols as antidiabetic agents: Advances and opportunities. **Food Frontiers**, [*s. l.*], v. 1, n. 1, p. 18–44, 2020.

SUN, Changquan Calvin; HOU, Hao. Improving Mechanical Properties of Caffeine and Methyl Gallate Crystals by Cocrystallization. **Crystal Growth & Design**, [*s. l.*], v. 8, n. 5, p. 1575–1579, 2008.

SUZUKI, Yumena *et al.* Exploring Novel Cocrystalline Forms of Oxyresveratrol to Enhance Aqueous Solubility and Permeability across a Cell Monolayer. **Biological and Pharmaceutical Bulletin**, [*s. l.*], v. 42, n. 6, p. 1004–1012, 2019.

THAKURIA, Ranjit *et al.* Cocrystal Dissociation under Controlled Humidity: A Case Study of Caffeine–Glutaric Acid Cocrystal Polymorphs. **Organic Process Research & Development**, [*s. l.*], v. 23, n. 5, p. 845–851, 2019.

TOTHADI, Srinu; PHADKULE, Amala. Does stoichiometry matter? Cocrystals of aliphatic dicarboxylic acids with isonicotinamide: odd–even alternation in melting points. **CrystEngComm**, [*s. l.*], v. 21, n. 15, p. 2481–2484, 2019.

TRANG, T.T.T. *et al.* Drug Release Profile Study of Gentamicin Encapsulated Poly(lactic Acid) Microspheres for Drug Delivery. **Materials Today: Proceedings**, [*s. l.*], v. 17, p. 836–845, 2019.

TUMANOVA, Natalia *et al.* Exploring polymorphism and stoichiometric diversity in naproxen/proline cocrystals. **CrystEngComm**, [*s. l.*], v. 20, n. 45, 2018.

VAKSLER, Ye.A. *et al.* Spectroscopic characterization of single co-crystal of mefenamic acid and nicotinamide using supercritical CO2. **Journal of Molecular Liquids**, [*s. l.*], v. 334, p. 116117, 2021.

VASISHT, Karan *et al.* Enhancing biopharmaceutical parameters of bioflavonoid quercetin by cocrystallization. **CrystEngComm**, [*s. l.*], v. 18, n. 8, p. 1403–1415, 2016. Disponível em: http://xlink.rsc.org/?DOI=C5CE01899D.

VEVERKA, Miroslav *et al.* Cocrystals of quercetin: Synthesis, characterization, and screening of biological activity. **Monatshefte fur Chemie**, [*s. l.*], v. 146, n. 1, p. 99–109, 2015.

WANG, Weiyou *et al.* The biological activities, chemical stability, metabolism and delivery systems of quercetin: A review. **Trends in Food Science & Technology**, [*s. l.*], v. 56, p. 21–38, 2016.

WANG, Yuan; LIANG, Zuozhong. Solvent effects on the crystal growth structure and morphology of the pharmaceutical dirithromycin. **Journal of Crystal Growth**, [*s. l.*], v. 480, p. 18–27, 2017.

WEI, Yuanfeng *et al.* Mechanistic Study on Complexation-Induced Spring and Hover Dissolution Behavior of Ibuprofen-Nicotinamide Cocrystal. **Crystal Growth & Design**, [*s. l.*], v. 18, n. 12, p. 7343–7355, 2018.

WICHIANPHONG, Napada; CHAROENCHAITRAKOOL, Manop. Application of Box-Behnken design for processing of mefenamic acid-paracetamol cocrystals using gas anti-solvent (GAS) process. **Journal of CO2 Utilization**, [*s. l.*], v. 26, n. February, p. 212–220, 2018a. Disponível em: https://doi.org/10.1016/j.jcou.2018.05.011.

WICHIANPHONG, Napada; CHAROENCHAITRAKOOL, Manop. Statistical optimization for production of mefenamic acid–nicotinamide cocrystals using gas anti-solvent (GAS) process. **Journal of Industrial and Engineering Chemistry**, [*s. l.*], v. 62, p. 375–382, 2018b. Disponível em: https://doi.org/10.1016/j.jiec.2018.01.017.

WISCONS, Ren A.; MATZGER, Adam J. Evaluation of the Appropriate Use of Characterization Methods for Differentiation between Cocrystals and Physical Mixtures in the Context of Energetic Materials. **Crystal Growth & Design**, [*s. l.*], v. 17, n. 2, p. 901–906, 2017.

WONG, Si Nga *et al.* Cocrystallization of Curcumin with Benzenediols and Benzenetriols via Rapid Solvent Removal. **Crystal Growth & Design**, [*s. l.*], v. 18, n. 9, p. 5534–5546, 2018.

WU, Na *et al.* Preparation of quercetin–nicotinamide cocrystals and their evaluation under *in vivo* and *in vitro* conditions. **RSC Advances**, [*s. l.*], v. 10, n. 37, 2020.

XU, Jia *et al.* Cocrystals of isoliquiritigenin with enhanced pharmacokinetic performance. **CrystEngComm**, [*s. l.*], v. 18, n. 45, p. 8776–8786, 2016.

XU, Zhonglin. Particle and Size Distribution. *Em*: FUNDAMENTALS OF AIR CLEANING TECHNOLOGY AND ITS APPLICATION IN CLEANROOMS. Berlin, Heidelberg: Springer Berlin Heidelberg, 2014. p. 1–46.

XUE, Na *et al.* The mechanism of binding with the α-glucosidase in vitro and the evaluation on hypoglycemic effect in vivo: Cocrystals involving synergism of gallic acid and conformer. **European Journal of Pharmaceutics and Biopharmaceutics**, [*s. l.*], v. 156, p. 64–74, 2020.

YAMAMOTO, Katsuhiko; TSUTSUMI, Shunichirou; IKEDA, Yukihiro. Establishment of cocrystal cocktail grinding method for rational screening of pharmaceutical cocrystals. **International Journal of Pharmaceutics**, [*s. l.*], v. 437, n. 1–2, p. 162–171, 2012.

YEO, Sang-Do; LEE, Jong-Chan. Crystallization of sulfamethizole using the supercritical and liquid antisolvent processes. **The Journal of Supercritical Fluids**, [*s. l.*], v. 30, n. 3, p. 315–323, 2004.

ZHAN, Shiping *et al.* Measurement and Correlation of Curcumin Solubility in Supercritical Carbon Dioxide. **Journal of Chemical & Engineering Data**, [*s. l.*], v. 62, n. 4, p. 1257–1263, 2017.

ZHANG, Zhijie *et al.* Cocrystals of Natural Products: Improving the Dissolution Performance of Flavonoids Using Betaine. **Crystal Growth & Design**, [*s. l.*], v. 19, n. 7, p. 3851–3859, 2019. Disponível em: https://pubs.acs.org/doi/10.1021/acs.cgd.9b00294.

ZHANG, Geoff G.Z. *et al.* Efficient Co-crystal Screening Using Solution-Mediated Phase Transformation. **Journal of Pharmaceutical Sciences**, [*s. l.*], v. 96, n. 5, p. 990–995, 2007.

ZHENG, Kai *et al.* Effect of Particle Size and Polymer Loading on Dissolution Behavior of Amorphous Griseofulvin Powder. **Journal of Pharmaceutical Sciences**, [*s. l.*], v. 108, n. 1, p. 234–242, 2019.

ZHU, Bingqing *et al.* Cocrystals of Baicalein with Higher Solubility and Enhanced Bioavailability. **Crystal Growth & Design**, [*s. l.*], v. 17, n. 4, p. 1893–1901, 2017.

ZIELINSKI, Acácio Antonio Ferreira *et al.* High-pressure fluid technologies: Recent approaches to the production of natural pigments for food and pharmaceutical applications. **Trends in Food Science & Technology**, [*s. l.*], v. 118, p. 850–869, 2021.

ZINOVIADOU, K.G.; GOUGOULI, M.; BILIADERIS, C.G. Innovative Biobased Materials for Packaging Sustainability. *Em*: GALANAKIS, Charis M. (org.). **Innovation Strategies in the Food Industry**. Amsterdam, NL: Elsevier, 2016. p. 167–189.

# APPENDIX A. - SUPPLEMENTARY DATA OF CHAPTER 3
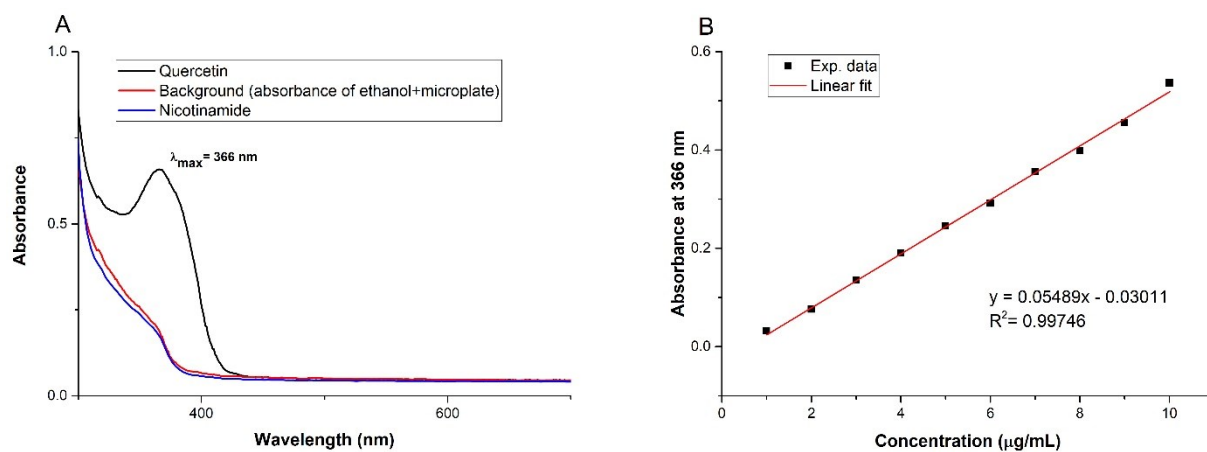


**Figure A.1**- (A) The UV–visible absorption spectra of quercetin in ethanol. (B) Quercetin standard curve spectrophotometrically assayed at 366 nm.

Name                    : Nicotinamide
Quantitative Method     : External Standard
Function                : f(x)=9606,00*x-27413,5
    Rr1=0,9991802  Rr2=0,9983611  RSS=9,282068e+008
    MeanRF: 8,895391e+003  RFSD: 5,433610e+002  RFRSD: 6,108343
FitType                 : Linear
Detector Name           : PDA
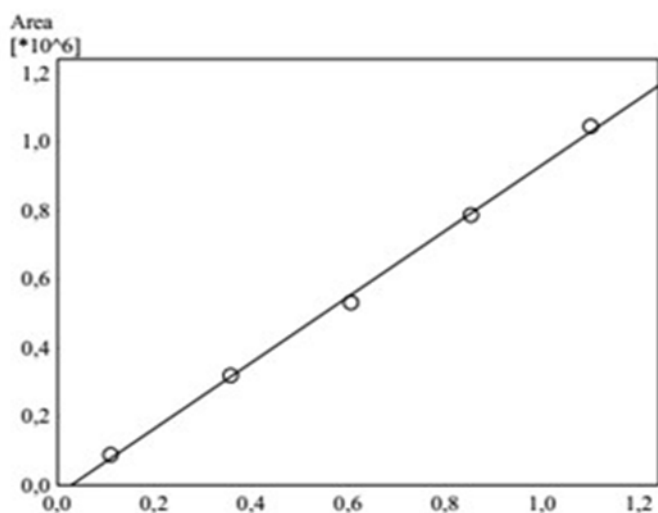
| # | Conc.(Ratio) | MeanArea | Area |
|---|---|---|---|
| 1 | 11 | 88641 | 88641 |
| 2 | 35,728 | 319415 | 319415 |
| 3 | 60,544 | 530818 | 530818 |
| 4 | 85,272 | 785937 | 785937 |
| 5 | 110 | 1044359 | 1044359 |

Name                    : Quercetin dihydrate
Quantitative Method     : External Standard
Function                : f(x)=20797,2*x+10283,7
    Rr1=0,9924853  Rr2=0,9850271  RSS=3,461066e+010
    MeanRF: 2,099906e+004  RFSD: 1,338887e+003  RFRSD: 6,375937
FitType                 : Linear
Detector Name           : PDA
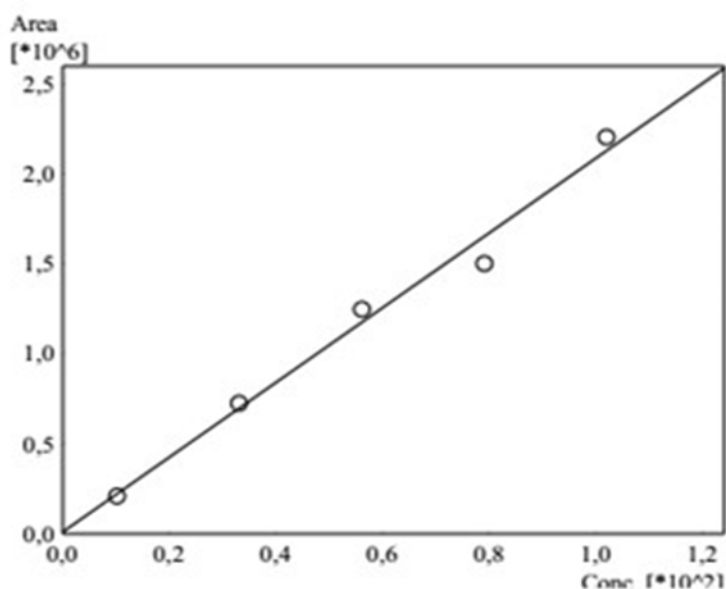
| # | Conc.(Ratio) | MeanArea | Area |
|---|---|---|---|
| 1 | 10,25 | 207997 | 207997 |
| 2 | 33,1296 | 724731 | 724731 |
| 3 | 56,1408 | 1247158 | 1247158 |
| 4 | 79,0704 | 1501553 | 1501553 |
| 5 | 102 | 2205485 | 2205485 |

**Figure A.2** - Calibration curves for nicotinamide and quercetin at 245 nm.
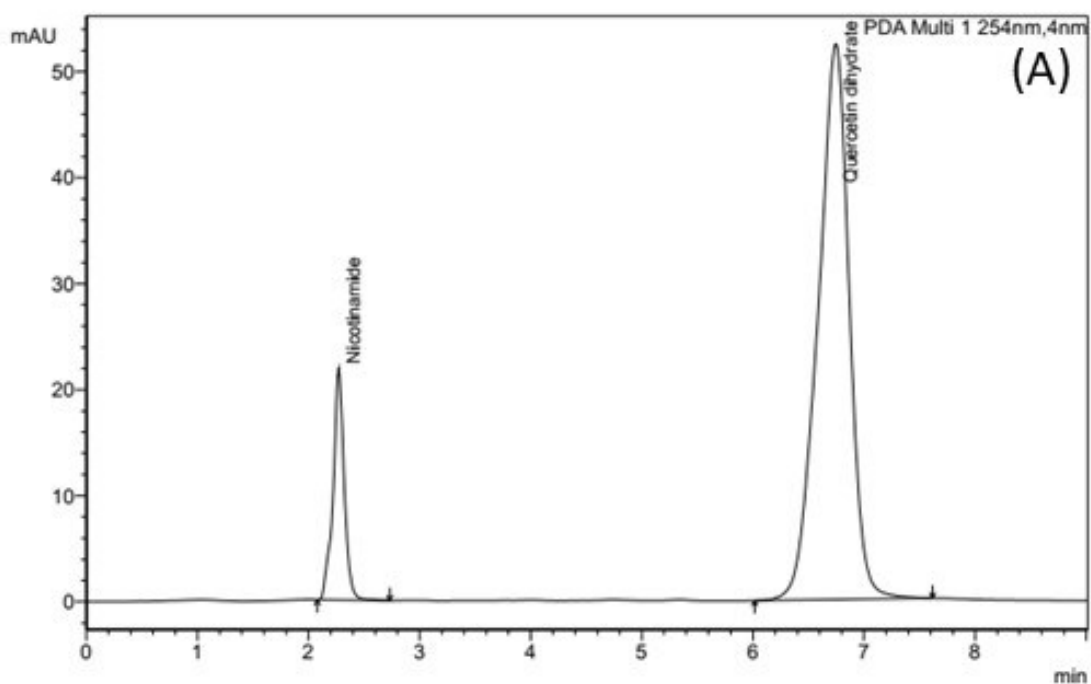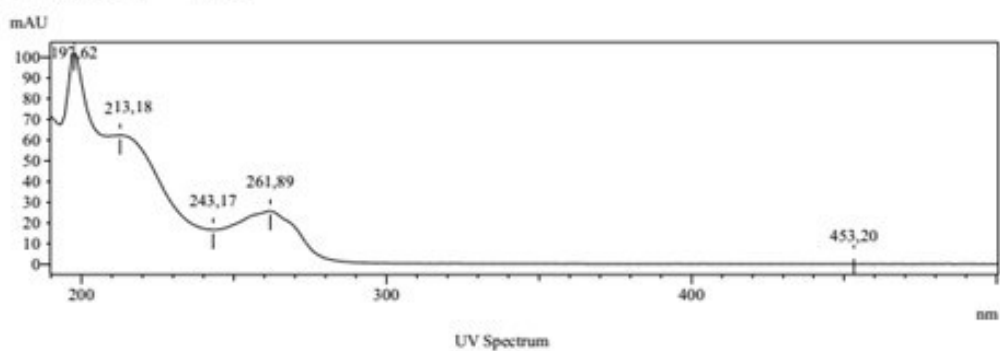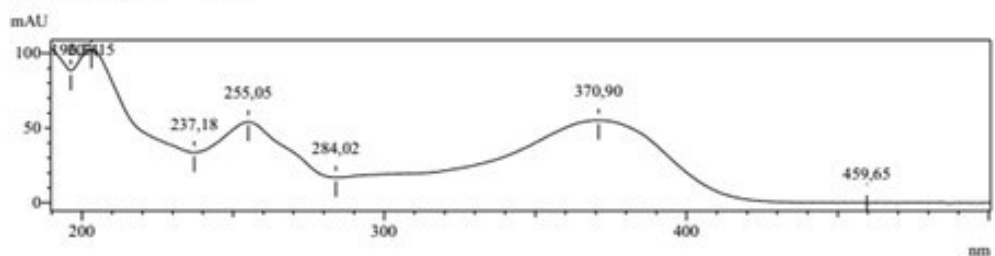
**Figure A.3** - (A) Chromatogram and (B) the UV spectrum of nicotinamide and quercetin.
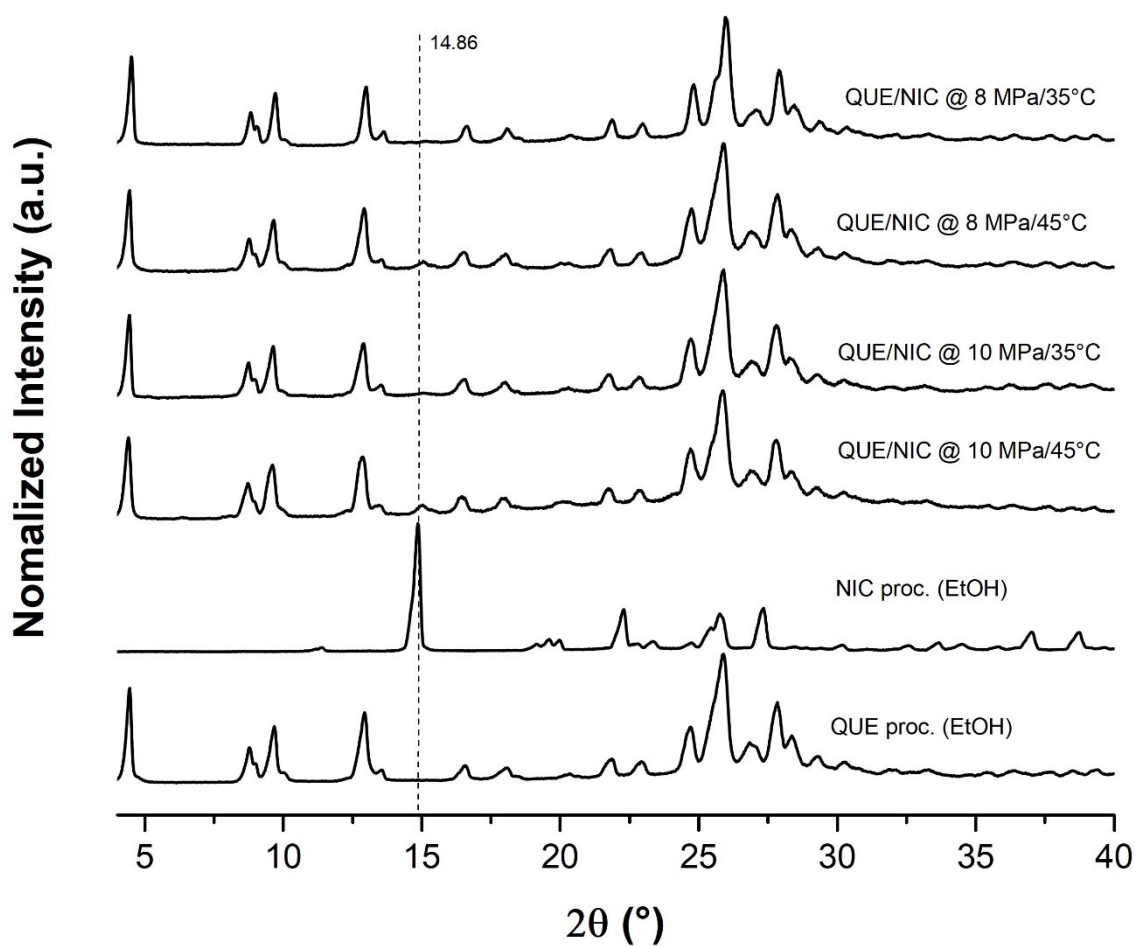
**Figure A.4** - PXRD diffractograms of GAS-processed QUE/NIC cocrystal samples using ethanol; NIC sample GAS-processed with ethanol; QUE sample GAS-processed using ethanol.
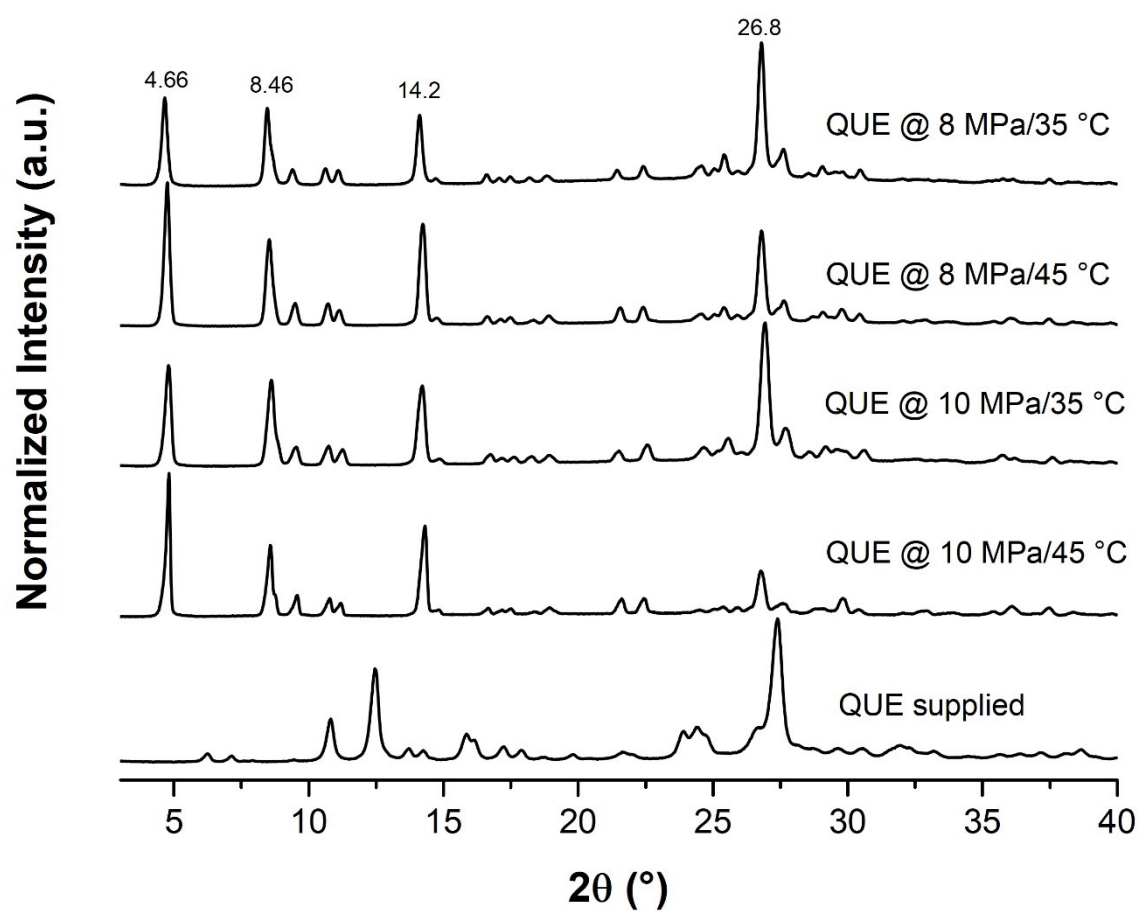
**Figure A.5** - PXRD diffractograms of GAS-processed QUE samples using acetone and QUE sample commercially supplied.
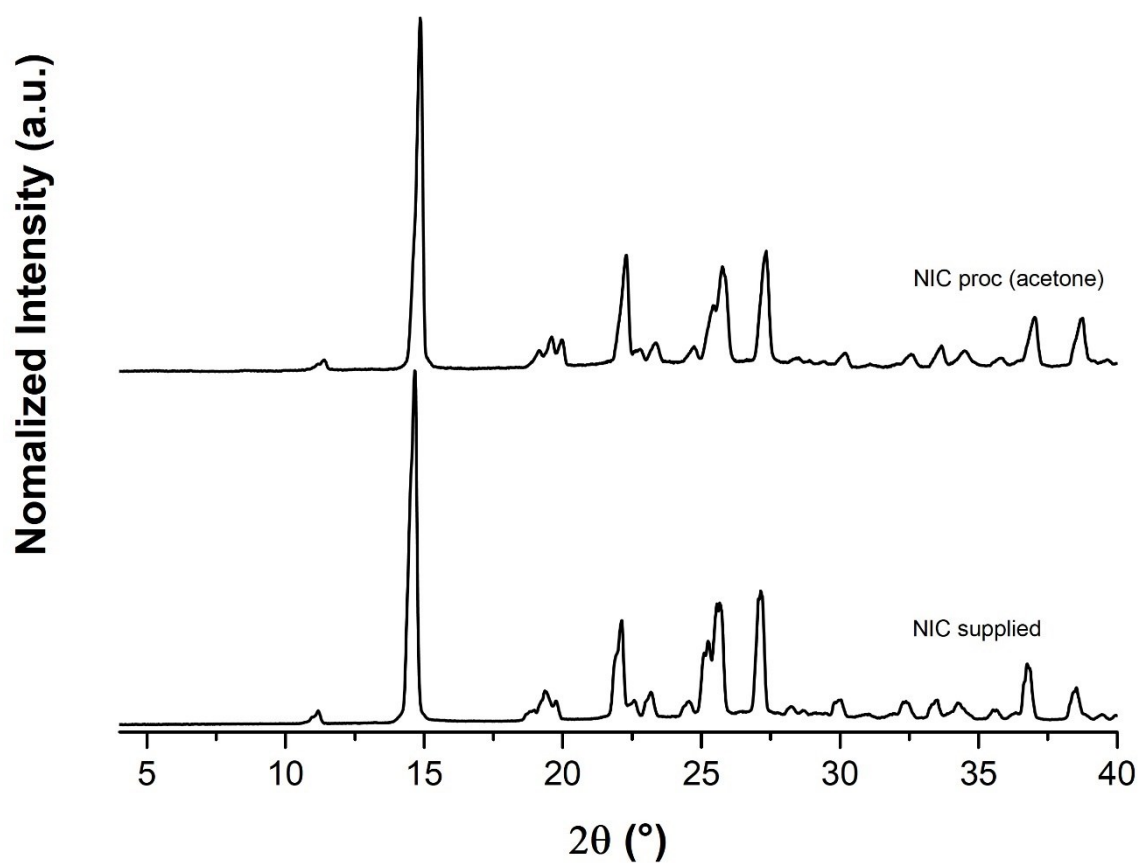
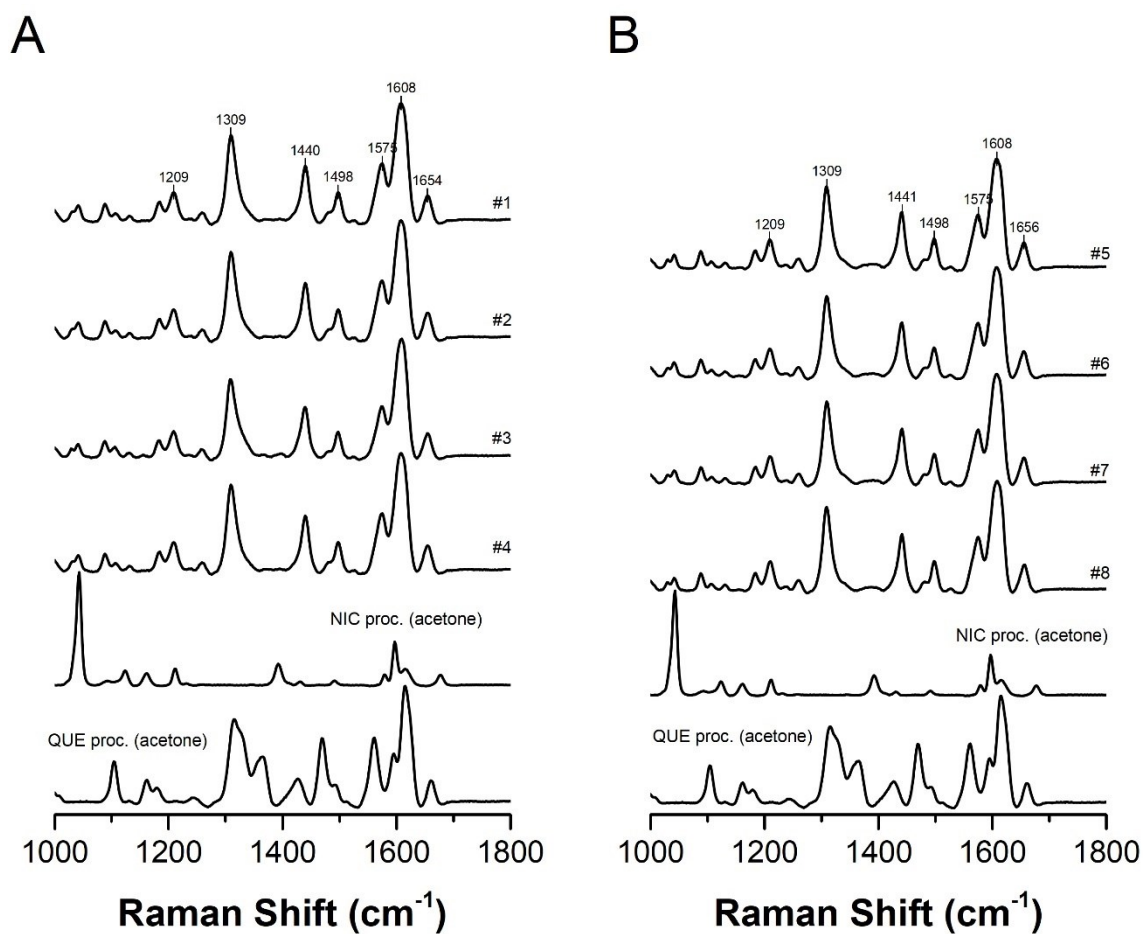**Figure A.6** - PXRD diffractograms of GAS-processed NIC sample using acetone (@10 MPa/45°C) and NIC sample commercially supplied.

**Figure A.7** - Raman spectra of GAS-processed QUE and NIC samples and the formed cocrystals. (A) Samples processed with 1:1 QUE-to-NIC molar ratio (runs #1 - #4); (B) Samples processed with 1:2 QUE-to-NIC molar ratio (runs #5 - #8).
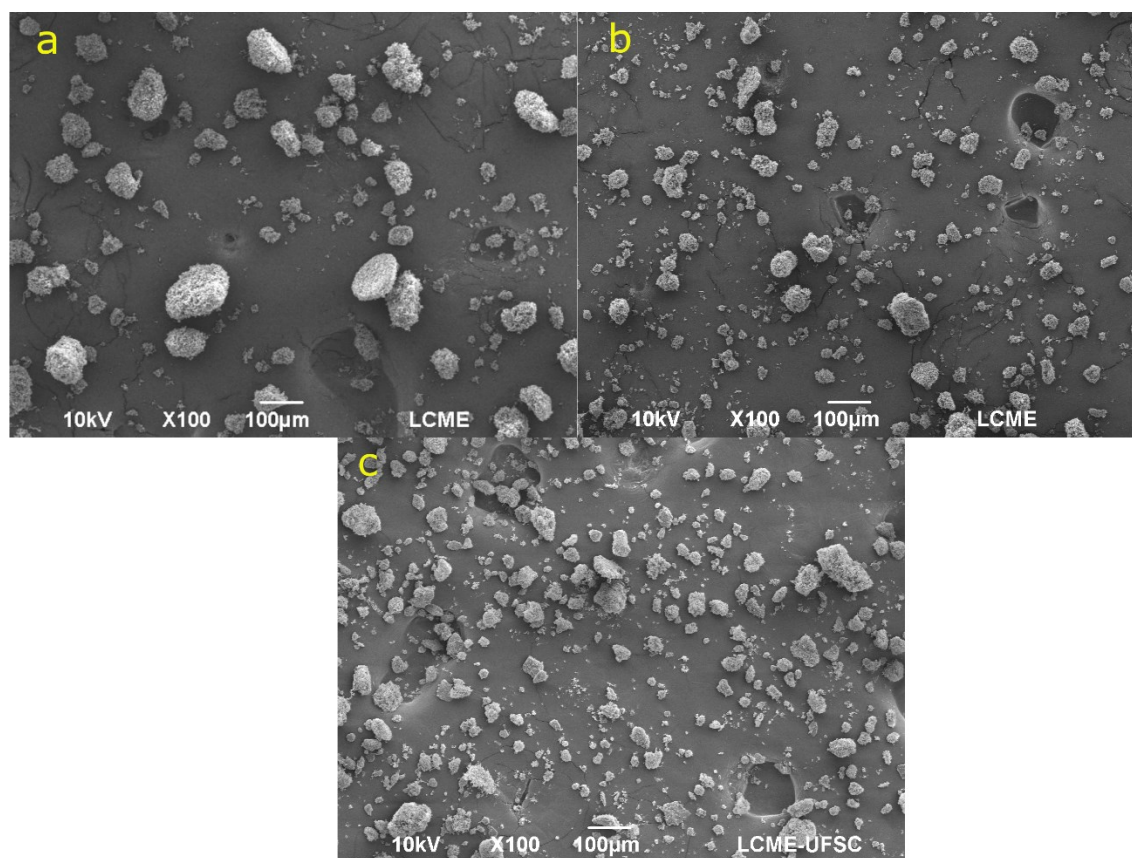
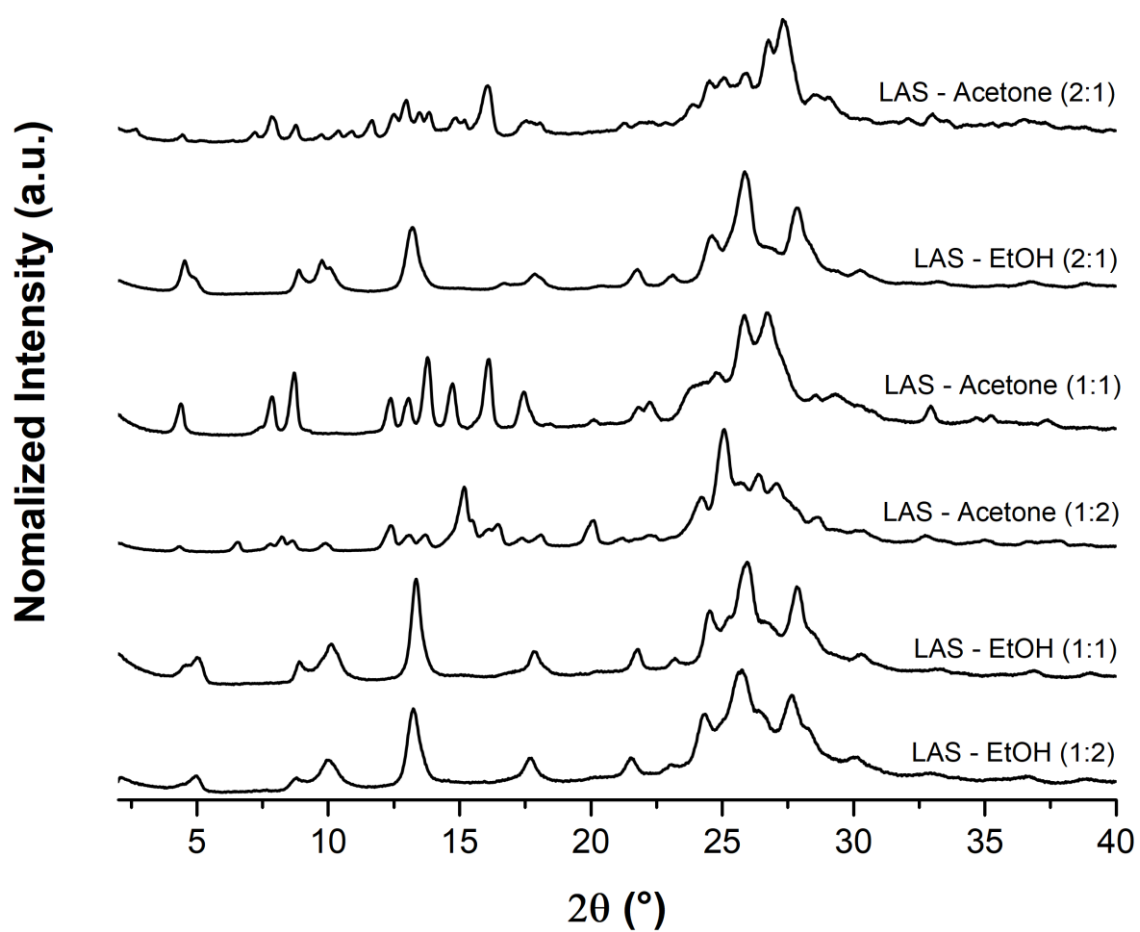**Figure A.8** - SEM images at 100× magnification of cocrystal samples: (a) #1, (b) #4, and (c) #5.

**Figure A.9** - PXRD diffractograms of LAS-processed QUE/NIC samples at different QUE-to-NIC ratios and solvents.
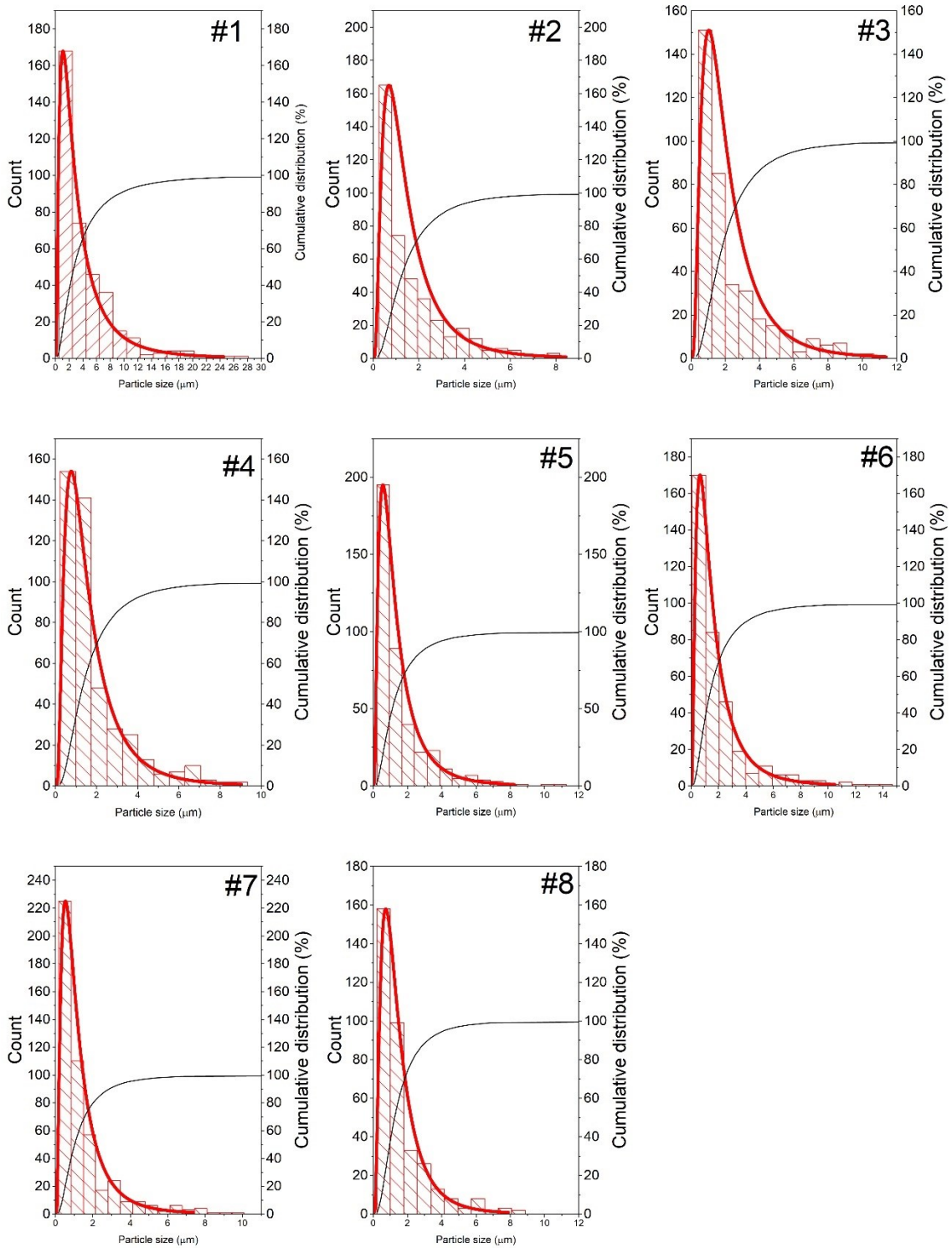
**Figure A.10** - Particle size distribution of GAS-processed samples. Log-normal fit (red curve), cumulative Log-normal fit (black curve).

**Table A.1**- Amount of quercetin and nicotinamide assayed by HPLC.

| Assay | Peak area | | Number of mols (µmol) | | Ratio (mol/mol) |
|---|---|---|---|---|---|
| | *NIC* | *QUE* | *NIC* | *QUE* | |
| #1 | 123183 | 975639 | 32.094 | 34.305 | 1.068890785 |
| #2 | 165123 | 1041972 | 41.032 | 36.662 | 0.893503913 |
| #3 | 148245 | 1008604 | 37.435 | 35.477 | 0.947680094 |
| #4 | 153055 | 1023428 | 38.460 | 36.003 | 0.936118705 |
| #5 | 152036 | 1102924 | 38.243 | 38.828 | 1.015303745 |
| #6 | 148736 | 1063804 | 37.540 | 37.438 | 0.997292424 |
| #7 | 160894 | 1192668 | 40.131 | 42.018 | 1.047012973 |
| #8 | 143862 | 1000628 | 36,501 | 35,193 | 0.96416639 |

**Table A.2** - Summary of the results of cocrystallization trials by liquid antisolvent method (LAS).

| Method | Solvent | QUE-toNIC ratio (mo:/mol) | Result[1] |
|--------|---------|---------------------------|-----------|
| **LAS** | acetone | 1:1 | 1:1 QUE/NIC cocrystal reported by Vasisht *et al.* (VASISHT *et al.*, 2016). Characteristic peaks at 4.5°,8.8°, 13.91° and 16.25° 2θ. |
| | | 1:2 | 1:2 QUE/NIC reported by Wu *et al.* (WU *et al.*, 2020) |
| | | 2:1 | unkown phase |
| | ethanol | 1:1 | QUE (PXRD pattern reported by Borghetti *et al.* (BORGHETTI *et al.*, 2012) |
| | | 1:2 | |
| | | 2:1 | |

[1] Phase attribution by PXRD (**Figure A.9**).

# APPENDIX B. - SUPPLEMENTARY DATA OF CHAPTER 4
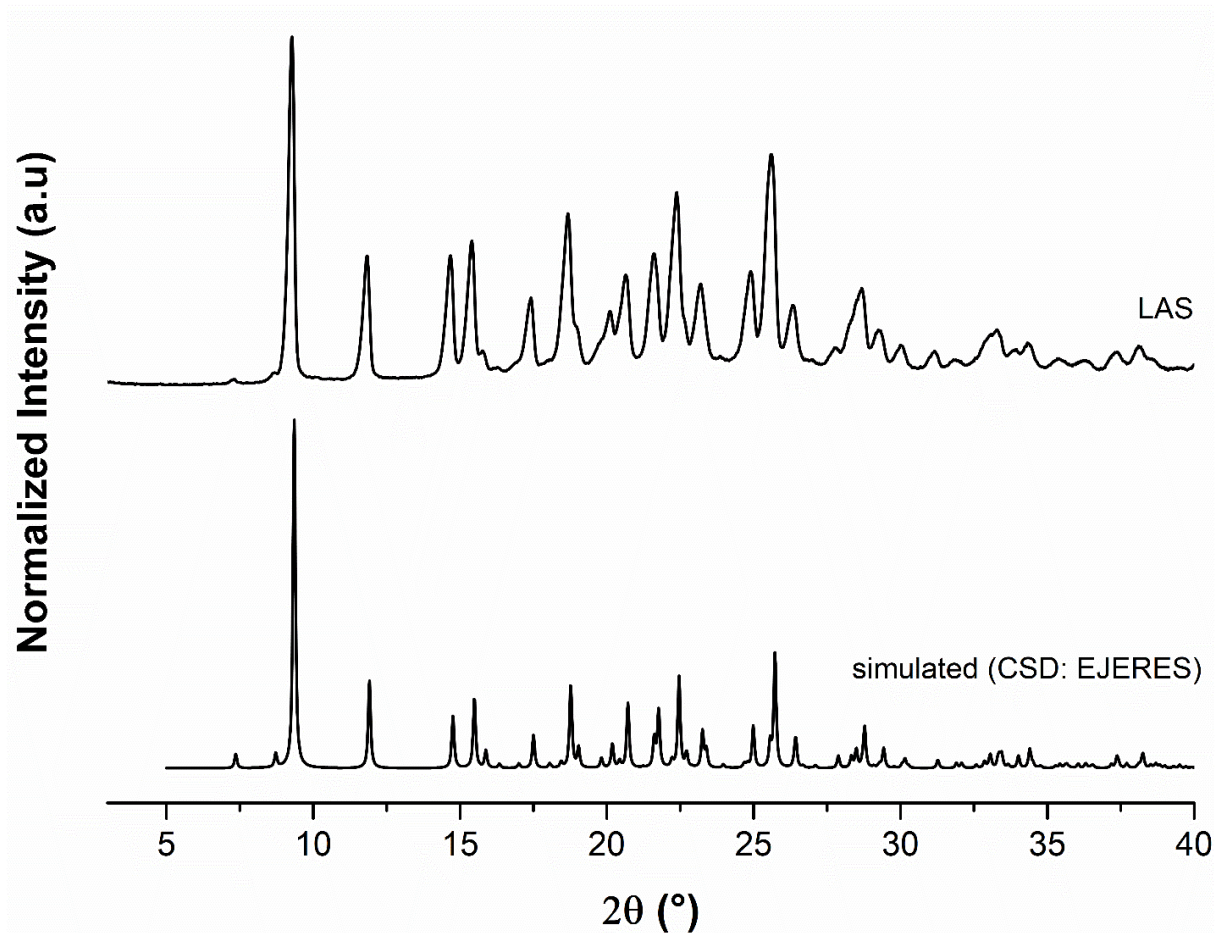


**Figure B.1** - PXRD diffractograms of GAS-processed QUE samples using acetone and QUE sample commercially supplied.
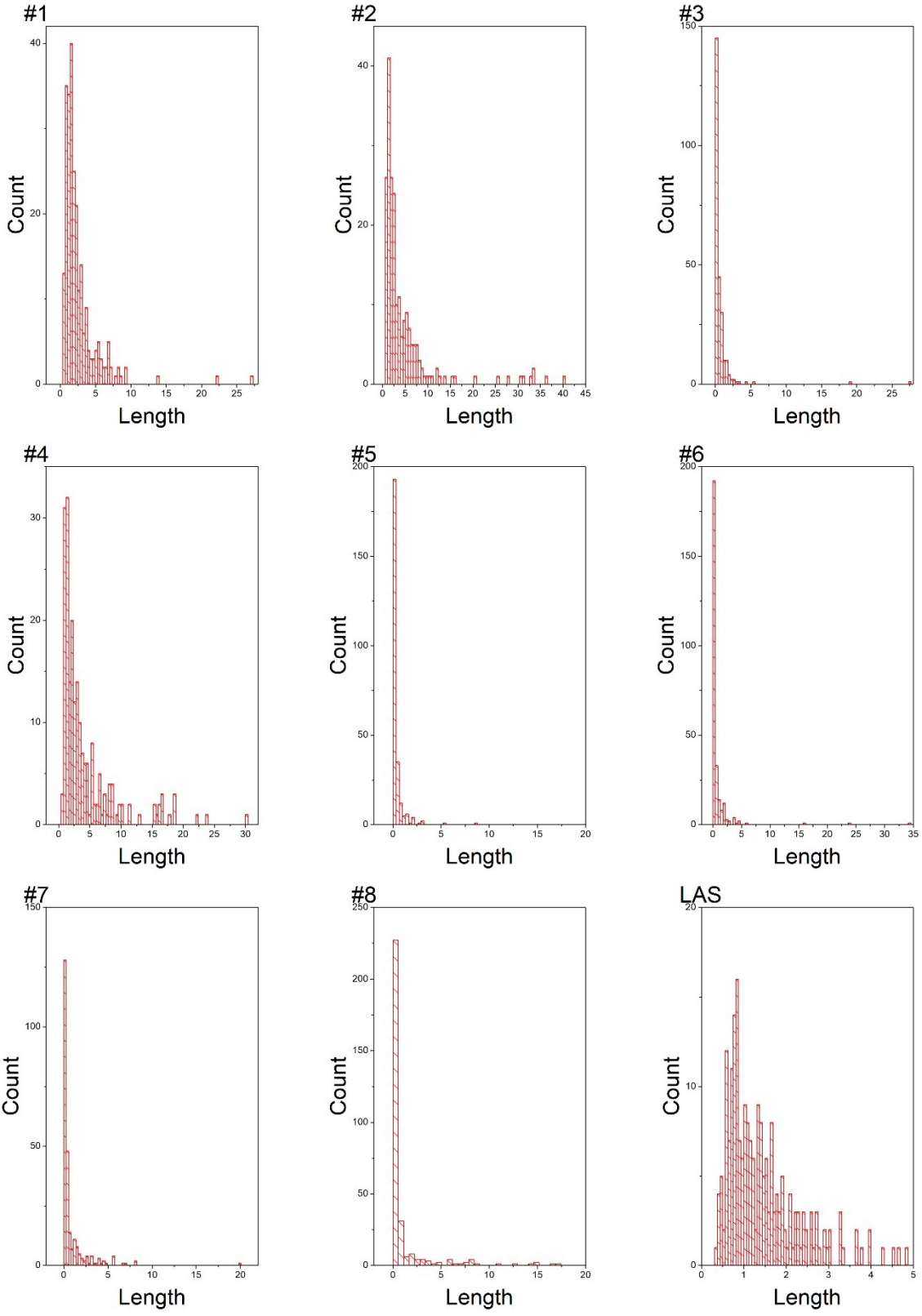
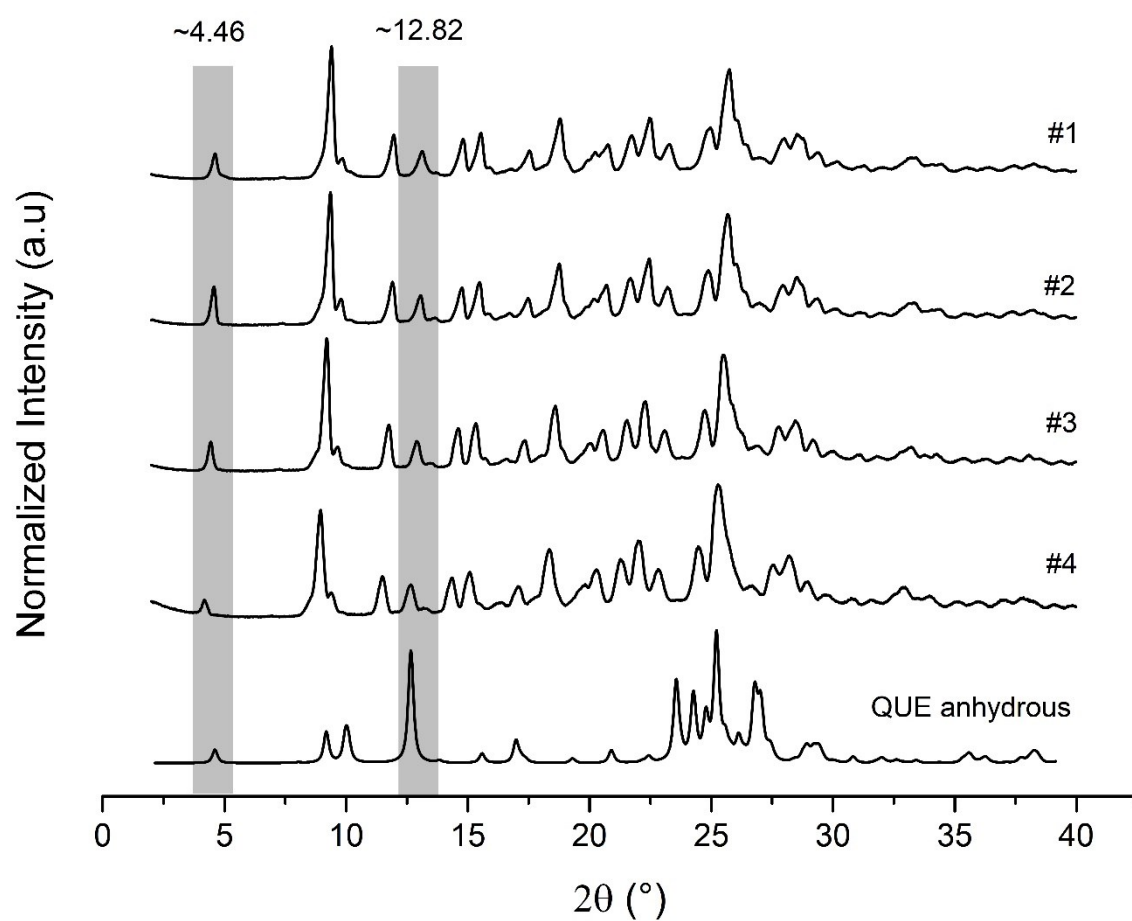**Figure B.2** - Particle size distribution of GAS- and LAS-processed samples.

**Figure B.3** - PXRD diffractograms of GAS-processed cocrystal samples (#1 - #4) and simulated PXRD of QUE anhydrous (FILIP *et al.*, 2013).